Electronic Supplementary Information

Multiple Control of Azoquinoline Based Molecular Photoswitches

Youming Lv,[a,b] Hebo Ye,[a] and Lei You[a,b,c*]

[a]State Key Laboratory of Structural Chemistry, Fujian Institute of Research on the Structure of Matter, Chinese Academy of Sciences, Fuzhou 350002, China.

[b]University of Chinese Academy of Sciences, Beijing 100049, China.

[c]Fujian Science & Technology Innovation Laboratory for Optoelectronic Information of China, Fuzhou 350108, China.

TABLE OF CONTENTS

1. General Methods……S3

2. Synthesis and Characterization……S4-S23

^{1}H NMR and ^{13}C NMR Spectra……S10-S21

X-ray Crystallography……S22-S23

3. Photoswitching Behaviors……S24-S27

4. pH Effects……S28-S37

5. Coordination Effects……S38-S42

6. Dynamic Covalent Chemistry……S43-S58

7. Photoisomerisation quantum yields……S59-S61

8. References……S62

1. General Methods

^{1}H NMR and ^{13}C NMR spectra were recorded on a 400 MHz Bruker Biospin avance III spectrometer or 400 MHz Bruker Biospin avance III HD spectrometer. Deuterated reagents for characterization and *in situ* reactions were purchased from Sigma-Aldrich Chemical Co. and Cambridge Isotope Laboratories, Inc. (purity ≥ 99.9%). The chemical shifts (δ) for ^{1}H NMR spectra, given in ppm, are referenced to the residual proton signal of the deuterated solvent. Mass spectra were recorded on a Bruker IMPACT-II or Thermo Scientific LCQ Fleet spectrometer. The UV-Vis spectra were recorded on a Shimadzu UV-1700i spectrometer. All other reagents were obtained from commercial sources and used without further purification, unless indicated otherwise.

Irradiation experiments. The UV and Visible light irradiation experiments were carried out on a UV LED strip light (wavelength = 365 nm, power = 20 W) and a blue LED strip light (wavelength = 425 nm, power = 20 W), respectively.

Determination of thermal half-lives. Each azoarene (at a concentration of 10 mM) in DMSO-d_6 was irradiated with 365 nm LEDs for at least 1.5 h to produce Z isomer, and then placed in a dark environment at a constant temperature (25 ºC). ^{1}H NMR spectra were used to monitor the thermal conversion of azoarene from *Z* to *E* isomer. Rate constants (*k*) for the first order thermal isomerization were determined from exponential fit of a graph of percent of *Z* isomer vs. time, where $t_{½} = \ln(2)/k$.

pH and Coordination experiments. Protonation/deprotonation and metal ions complexation/de-complexation of molecular switches were performed *in situ* in DMSO-d_6 at room temperature, and the mixture was characterized by ^{1}H NMR. See specific conditions in figure captions of the main text or supplementary information if necessary.

Dynamic covalent reactions in solution.
Dynamic Covalent Reactions (DCRs) were performed *in situ* in DMSO-d_6 at room temperature without isolation and purification, and the mixture was characterized by ^{1}H NMR. See specific conditions in figure captions of the main text or supplementary information if necessary.

2. Synthesis and Characterization

Scheme S1. Synthesis of *E*-**1**.[S1]

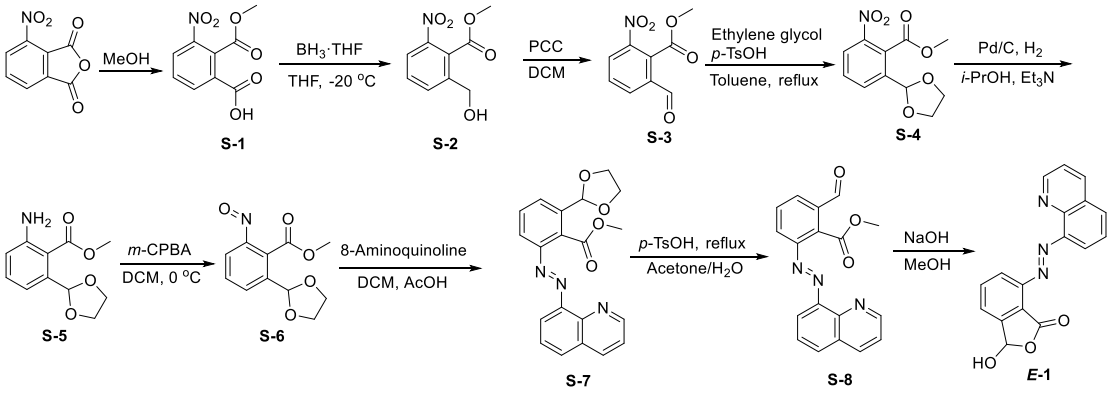

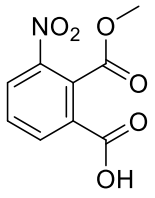

S-1

S-1 was synthesized according to the literature method. [S1]

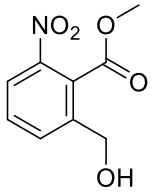

S-2

S-1 (10 g, 44 mmol) was added into a 250 mL two-necked round-bottom flask equipped with a reflux condenser and an addition funnel and dissolved in THF (40 mL), and then the solution was cooled to -20 °C under nitrogen atmosphere. 1 M Borane-tetrahydrofuran solution (90 mL, 90 mmol) was added dropwise over 10 min, and the reaction was slowly warmed to room temperature and then heated to reflux for 3 h. After being cooled to room temperature the reaction was quenched with 1 M HCl and extracted with EtOAc. The combined organic extracts were washed with water, dried over Na_2SO_4, and evaporated under reduced pressure. The crude was then purified via flash column chromatography (silica gel, 30% EtOAc in petroleum ether) to give **S-2** (5.9 g, 63%) as a white solid. ^{1}H NMR (400 MHz, DMSO-d_6): δ 8.08 (d, J = 8.1 Hz, 1H), 7.94 (d, J = 7.7 Hz, 1H), 7.75 (t, J = 8.0 Hz, 1H), 5.62 (t, J = 5.6 Hz, 1H), 4.57 (d, J = 5.6 Hz, 2H), 3.84 (s, 3H). ^{13}C NMR (101 MHz, DMSO-d_6) δ 166.1, 150.6, 146.7, 142.6, 136.0, 133.7, 131.4, 127.9, 126.7, 123.8, 123.4, 117.2, 70.1, 60.4, 53.6. ESI-HRMS: *m/z* calculated for $C_9H_9NO_5Na$ $[M + Na]^+$: 234.0373; found: 234.0378.

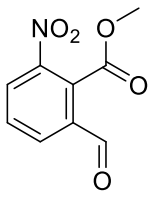

S-3

To a solution of **S-2** (5.0 g, 24 mmol) in dry DCM (50 mL) was added Pyridinium chlorochromate (7.7 g, 36 mmol) and 3 Å molecular sieves. The reaction was stirred for 24 h under nitrogen atmosphere and then filtered through a Celite pad. The filtrate was washed with water and extracted with DCM, and the combined organic extracts were dried over Na_2SO_4 and evaporated under reduced pressure. The crude was then purified via flash column chromatography (silica gel, 15% EtOAc in petroleum ether) to give **S-3** (3.5 g, 71%) as a white solid. ^{1}H NMR (400 MHz, DMSO-d_6): δ 10.07 (s, 1H), 8.52 (d, J = 8.3 Hz, 1H), 8.44 (d, J = 7.7 Hz, 1H), 8.02 (t, J = 8.0 Hz, 1H), 3.92 (s, 3H). ^{13}C NMR (101 MHz, $CDCl_3$) δ 188.1, 165.1, 146.4, 135.4, 134.5, 131.0, 130.6, 129.4, 53.9. ESI-HRMS: *m/z* calculated for $C_9H_7NO_5Na$ $[M + Na]^+$: 232.0216; found: 232.0215.

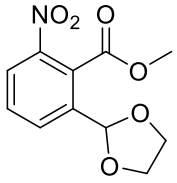

S-4

To a solution of **S-3** (3.0 g, 14 mmol) in toluene (35 mL) was added ethylene glycol (8.9 g, 143 mmol) and *p*-toluenesulfonic acid (0.27 g, 1.4 mmol). The reaction was heated under reflux for 7 h, while water was removed by using a Dean-Stark trap. After being cooled to room temperature the reaction mixture was washed successively with saturated Na_2CO_3 solution and brine, dried over Na_2SO_4, and evaporated under reduced pressure. The crude was purified by flash chromatography (neutral aluminum oxide, 15% EtOAc in petroleum ether) to give **S-4** (3.1 g, 85%) as a colourless liquid. ^{1}H NMR (400 MHz, DMSO-d_6): δ 8.23 (d, J = 8.2 Hz, 1H), 7.98 (d, J = 7.8 Hz, 1H), 7.81 (t, J = 8.0 Hz, 1H), 5.95 (s, 1H), 3.97 (s, 4H), 3.85 (s, 3H). ^{13}C NMR (101 MHz, DMSO-d_6) δ 165.6, 146.8, 138.3, 133.2, 131.7, 127.8, 125.7, 100.1, 65.5, 53.7. ESI-HRMS: *m/z* calculated for $C_{11}H_{11}NO_6Na$ $[M + Na]^+$: 276.0479; found: 276.0481.

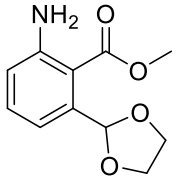

S-5

To a solution of **S-4** (2.9 g, 11 mmol) in isopropanol (30 mL) was added triethylamine (2.3 g, 23 mmol) and 5% Pd/C (0.12 g, 1.1 mmol). The reaction was stirred for 5 h

under hydrogen atmosphere and then filtered through a Celite pad, and the filtrate was evaporated under reduced pressure. The crude was purified by flash chromatography (neutral aluminum oxide, 15% EtOAc in petroleum ether) to give **S-5** (1.8 g, 70%) as a white solid. ^{1}H NMR (400 MHz, DMSO-d_6): δ 7.14 (t, J = 7.9 Hz, 1H), 6.75 (dd, J = 7.7, 5.0 Hz, 2H), 6.08 (s, 1H), 5.63 (s, 2H), 3.92 – 3.81 (m, 4H), 3.77 (s, 3H). ^{13}C NMR (101 MHz, $CDCl_3$) δ 169.3, 147.9, 139.7, 131.6, 117.3, 115.4, 113.6, 101.9, 64.8, 60.0. ESI-HRMS: *m/z* calculated for $C_{11}H_{13}NO_4Na$ $[M + Na]^+$: 246.0737; found: 246.0738.

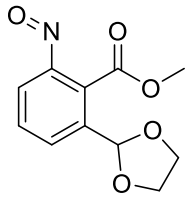

S-6

To a solution of **S-5** (1.4 g, 5.6 mmol) in DCM (30 mL) at 0 °C was added dropwise a solution of *m*-Chloroperoxybenzoic acid (2.4 g, 14 mmol) in DCM (15 mL). The reaction was slowly warmed to room temperature and stirred for 5 h. The reaction mixture was diluted with DCM, washed consecutively with $Na_2S_2O_3$ solution, saturated $NaHCO_3$ solution, and then brine, dried over Na_2SO_4, and evaporated under reduced pressure. The crude was purified via flash column chromatography (silica gel, 15% EtOAc in petroleum ether) to give **S-6** (1.2 g, 81%) as a white solid. ^{1}H NMR (400 MHz, $CDCl_3$): δ 7.97 (d, J = 7.7 Hz, 1H), 7.58 (t, J = 7.8 Hz, 1H), 7.03 (d, J = 8.0 Hz, 1H), 6.20 (d, J = 9.0 Hz, 1H), 4.12 (s, 4H), 4.08 (s, 3H). ^{13}C NMR (101 MHz, $CDCl_3$) δ 168.0, 161.5, 137.8, 133.5, 132.6, 129.8, 113.1, 100.9, 65.5, 53.0. ESI-HRMS: *m/z* calculated for $C_{11}H_{11}NO_5Na$ $[M + Na]^+$: 260.0529; found: 260.0529.

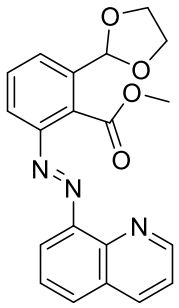

S-7

To a solution of **S-6** (0.92 g, 3.9 mmol) in DCM (30 mL) was added 8-aminoquinoline (0.67 g, 4.6 mmol) and acetic acid (4.9 g, 82 mmol). The reaction was stirred for 12 h under nitrogen atmosphere, washed successively with saturated $NaHCO_3$ solution and then brine, dried over Na_2SO_4, and evaporated under reduced pressure. The crude was purified via flash column chromatography (silica gel, 50% EtOAc in petroleum ether) to give **S-7** (0.92 g, 65%) as a red solid. ^{1}H NMR (400 MHz, $CDCl_3$): δ 9.15 (d, J = 5.7 Hz, 1H), 8.25 (d, J = 9.8 Hz, 1H), 8.04 (d, J = 8.0 Hz, 1H), 7.98 (d, J = 7.9 Hz, 1H), 7.81 (d, J = 7.4 Hz, 1H), 7.72 (d, J = 7.6 Hz, 1H), 7.63 (t, J = 7.8 Hz, 1H), 7.60-7.49 (m, 2H), 6.17 (s, 1H), 4.12-4.02 (m, 4H), 3.97 (s, 3H). ^{13}C NMR (101 MHz, $CDCl_3$) δ

168.7, 151.6, 150.1, 148.9, 144.7, 136.8, 136.3, 132.9, 131.5, 130.1, 129.3, 129.2, 126.6, 121.9, 118.2, 116.5, 101.5, 65.3, 52.5. ESI-HRMS: *m/z* calculated for $C_{20}H_{17}N_3O_4Na$ $[M + Na]^+$: 386.1111; found: 386.1111.

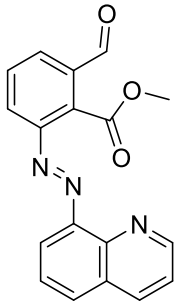

S-8

To a solution of **S-7** (0.80 g, 2.2 mmol) in acetone (20 mL) was added *p*-toluenesulfonic acid monohydrate (0.14 g, 2.2 mmol) and 10 mL water. The reaction was heated under reflux for 30 h and then cooled to room temperature. The reaction mixture was extracted with EtOAc, washed successively with saturated $NaHCO_3$ solution and then brine, dried over Na_2SO_4, and evaporated under reduced pressure. The crude was purified via flash column chromatography (silica gel, 50% EtOAc in petroleum ether) to give **S-8** (0.49 g, 70%) as a red solid. ^{1}H NMR (400 MHz, DMSO-d_6): δ 10.13 (s, 1H), 9.11 (d, J = 5.7 Hz, 1H), 8.54 (d, J = 9.8 Hz, 1H), 8.31 – 8.22 (m, 2H), 8.18 (d, J = 8.9 Hz, 1H), 7.96 (t, J = 7.8 Hz, 1H), 7.78 (t, J = 7.8 Hz, 1H), 7.75 – 7.66 (m, J = 8.6, 7.9, 2.6 Hz, 2H), 3.94 (s, 3H). ^{13}C NMR (101 MHz, $CDCl_3$) δ 189.8, 167.7, 151.6, 149.9, 148.6, 144.7, 136.3, 134.2, 133.4, 133.2, 132.1, 130.5, 129.2, 126.5, 123.5, 121.9, 116.5, 52.9. ESI-HRMS: *m/z* calculated for $C_{18}H_{14}N_3O_3$ $[M + H]^+$: 320.1030; found: 320.1031.

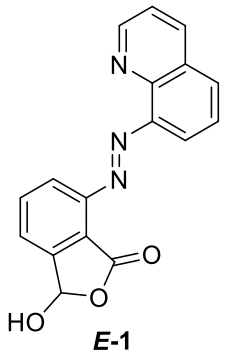

***E*-1**

To a solution of **S-8** (0.40 g, 1.2 mmol) in methanol (20 mL) was added 1 M aqueous NaOH solution (5 mL), The reaction was stirred for 5 h, and then acidified to pH 4.5 by using 1 M HCl. The mixture was extracted with EtOAc, and the combined organic extracts were washed with water and then brine, dried over Na_2SO_4, and evaporated under reduced pressure. The crude was purified via flash column chromatography (silica gel, 5% MeOH in EtOAc) to give *E*-**1** (0.25 g, 65%) as a red solid. ^{1}H NMR (400 MHz, DMSO-d_6): δ 9.10 (d, J = 5.3 Hz, 1H), 8.55 (d, J = 8.3 Hz, 1H), 8.42 – 8.16 (m, J = 12.1, 8.8 Hz, 2H), 8.11 – 7.85 (m, 2H), 7.85 – 7.57 (m, 4H), 6.77 (br, 1H). ^{13}C NMR (101 MHz, DMSO-d_6) δ 151.7, 149.6, 148.8, 143.6, 136.5, 132.30, 128.8, 126.6, 122.5,

116.3. ESI-HRMS: *m/z* calculated for $C_{17}H_{12}N_3O_3$ $[M + H]^+$: 306.0873; found: 306.0878.

Scheme S2. Synthesis of *E*-**2**.[S2]

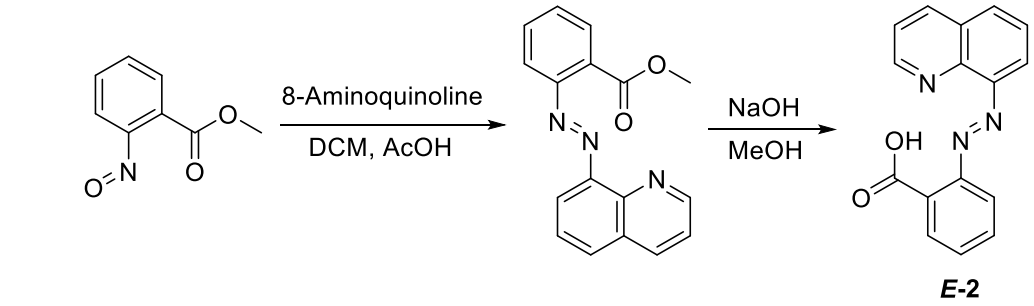

***E*-2**

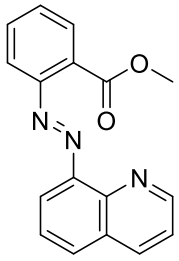

S-9

2-Carbomethoxy-nitrosobenzene was synthesized according to the literature method.[S2] To a solution of 8-aminoquinoline (0.11 g, 0.76 mmol) in DCM (15 mL) was added 2-carbomethoxy-nitrosobenzene (0.20 g, 1.2 mmol) and acetic acid (0.9 mL, 16 mmol). The reaction was stirred for 12 h under nitrogen atmosphere, acidified to pH 3.0 by using 1 M HCl, and organic phase was decanted. The aqueous phase was extracted with EtOAc, washed with saturated $NaHCO_3$ solution and then brine, dried over Na_2SO_4, and evaporated under reduced pressure. The crude product **S-9** was carried on to the following reaction without purification.

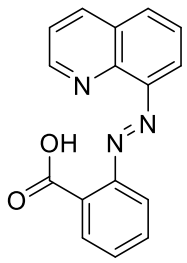

***E*-2**

To a solution of **S-9** (70 mg, 0.24 mmol) in methanol (12 mL) was added 1 M aqueous NaOH solution (3 mL). The reaction was stirred for 5 h, acidified to pH 5.0 by using 1 M HCl, and extracted with EtOAc. The combined organic extracts were washed with water, dried over Na_2SO_4, and evaporated under reduced pressure. The crude was purified via flash column chromatography (silica gel, 3% MeOH in EtOAc) to give *E*-**2** (60 mg, 28% for two steps) as a red solid. ^{1}H NMR (400 MHz, DMSO-d_6): δ 13.25 (s, 1H), 9.09 (s, 1H), 8.54 (d, J = 8.3 Hz, 1H), 8.23 (d, J = 7.9 Hz, 1H), 7.88 (d, J = 7.4

Hz, 1H), 7.75 (m, 4H), 7.65 (t, J = 7.6 Hz, 2H). ^{13}C NMR (101 MHz, DMSO-d_6) δ 168.5, 152.0, 152.0, 149.3, 143.7, 136.9, 132.4, 132.0, 131.0, 131.0, 129.9, 129.2, 127.0, 122.8, 118.3, 117.5. ESI-HRMS: *m/z* calculated for $C_{16}H_{12}N_3O_2$ $[M + H]^+$: 278.0930; found: 278.0922.

Scheme S3. Synthesis of *E*-**1**-H$^+$.

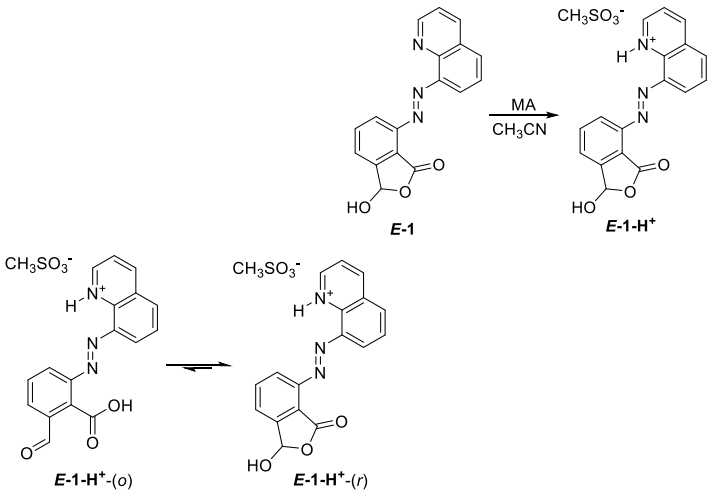

To a solution of ***E*-1** (104 mg, 0.34 mmol) in DMSO (5 mL) was added methanesulfonic acid (22 μL, 0.34 mmol). After stirring at room temperature for 10 min, acetonitrile was added. The solids precipitated out and were filtered and then dried *in vacuo* to give *E*-**1**-H$^+$ (120 mg, 88%). ^{1}H NMR (400 MHz, DMSO-d_6, the ratio of ring-chain tautomers around 1:0.21): δ 10.17 (s, 0.21H, *E*-**1**-H$^+$-(*o*)), 9.29 (d, *J* = 4.5 Hz, 1H, *E*-**1**-H$^+$-(*r*)), 9.27-9.23 (m, 0.21H, *E*-**1**-H$^+$-(*o*)), 8.99 (d, *J* = 8.5 Hz, 1H, *E*-**1**-H$^+$-(*r*)), 8.90 (s, 0.21H, *E*-**1**-H$^+$-(*o*)), 8.48 (d, *J* = 8.0 Hz, 1H, *E*-**1**-H$^+$-(*r*)), 8.43 (d, *J* = 7.7 Hz, 0.21H, *E*-**1**-H$^+$-(*o*)), 8.32 (d, *J* = 8.3 Hz, 0.21H, *E*-**1**-H$^+$-(*o*)), 8.26 (d, *J* = 7.4 Hz, 0.21H, *E*-**1**-H$^+$-(*o*)), 8.20 (d, *J* = 7.3 Hz, 1H, *E*-**1**-H$^+$-(*r*)), 8.09-7.99 (m, 3H, *E*-**1**-H$^+$-(*r*)), 7.99-7.71 (m, 2.84H, *E*-**1**-H$^+$-(*r*), 2H, *E*-**1**-H$^+$-(*o*), 0.84H), 6.81 (s, 1H, *E*-**1**-H$^+$-(*r*)), 2.32 (s, 3.63H, *E*-**1**-H$^+$-(*r*), 3H, *E*-**1**-H$^+$-(*o*), 0.63H). ^{13}C NMR (101 MHz, DMSO-d_6): δ 167.0, 149.8, 148.8, 148.6, 145.8, 142.6, 136.2, 136.1, 134.1, 129.9, 129.7, 127.8, 123.9, 123.9, 123.1, 117.6, 98.2. ESI-HRMS: *m/z* calculated for $C_{17}H_{12}N_3O_3$ $[M - CH_3SO_3^-]^+$: 306.0873; found: 306.0874.

^{1}H NMR and ^{13}C NMR Spectra

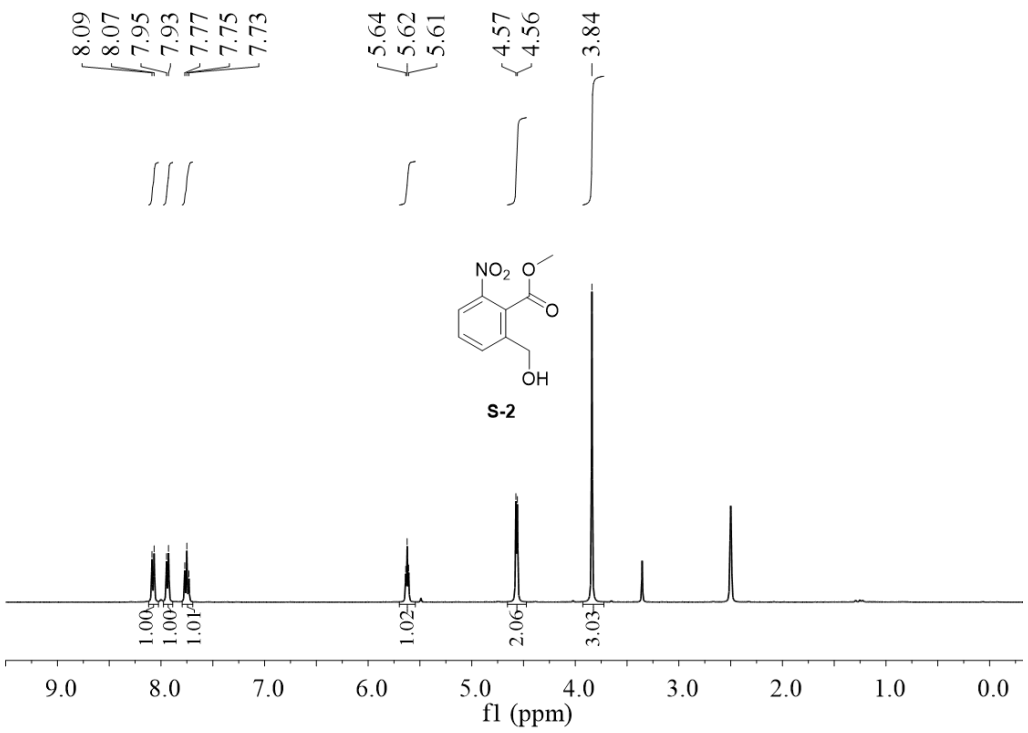

Figure S1. ^{1}H NMR spectrum (400 MHz) of **S-2** in DMSO-d_6.

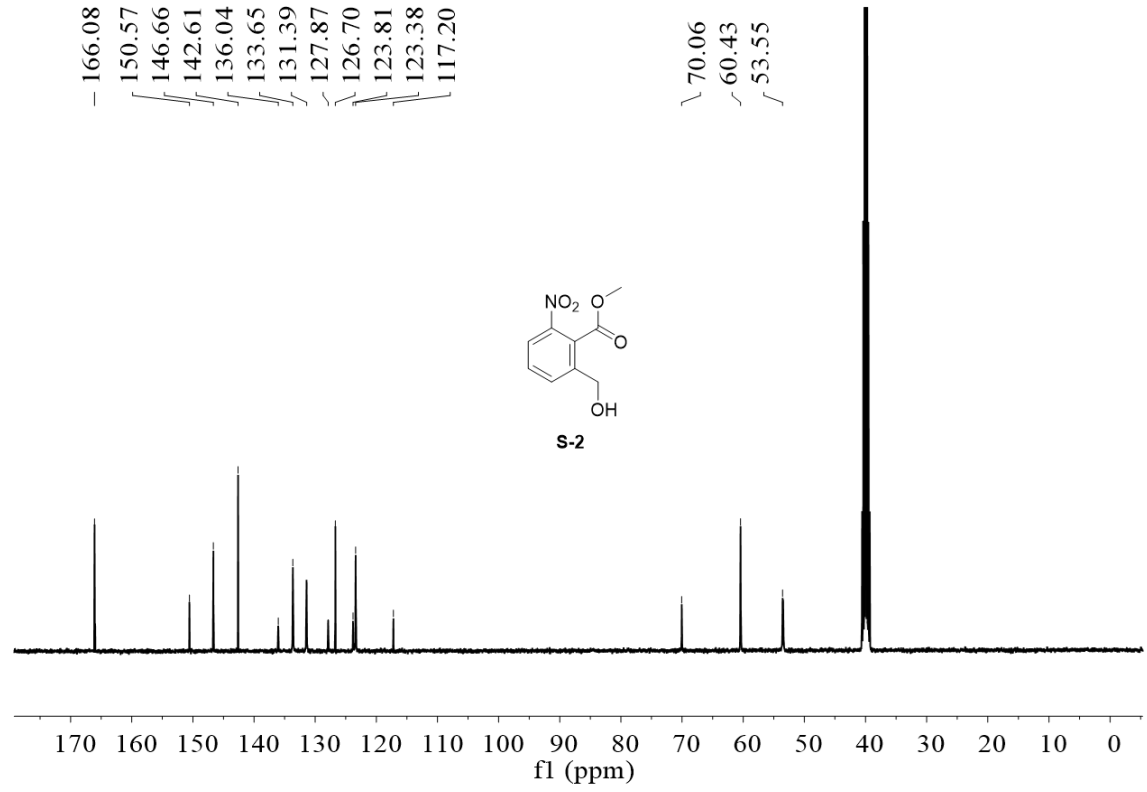

Figure S2. ^{13}C NMR spectrum (101 MHz) of S-**2** in DMSO-d_6.

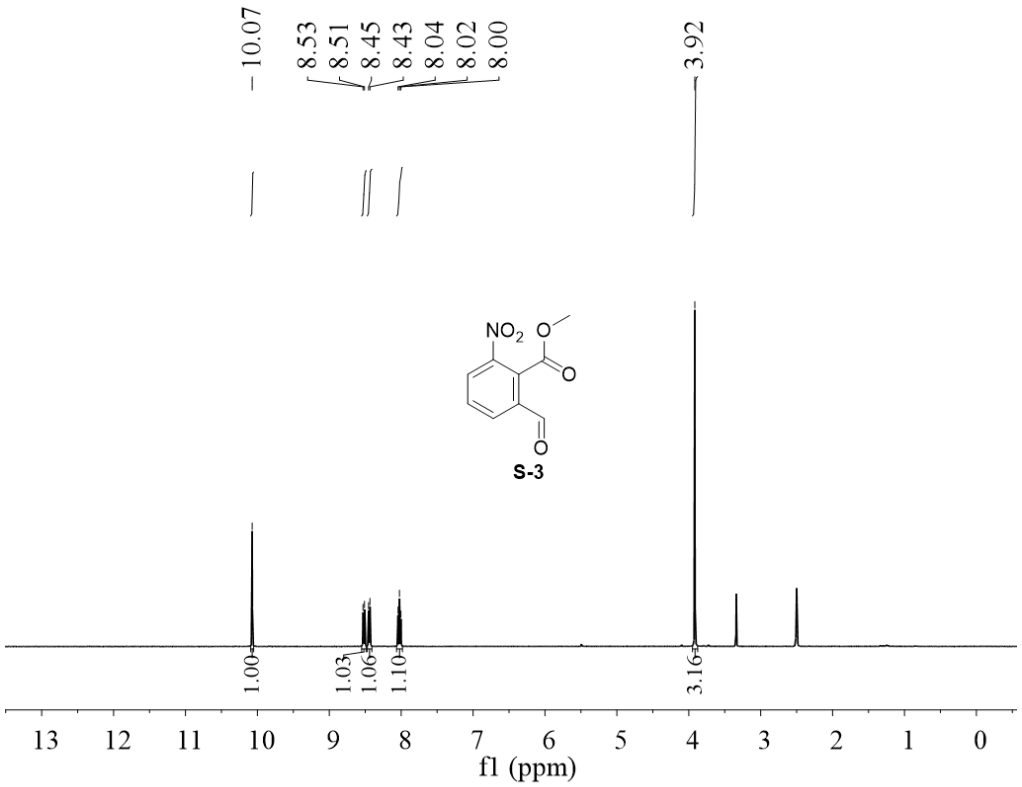

Figure S3. ^{1}H NMR spectrum (400 MHz) of **S-3** in DMSO-d_6.

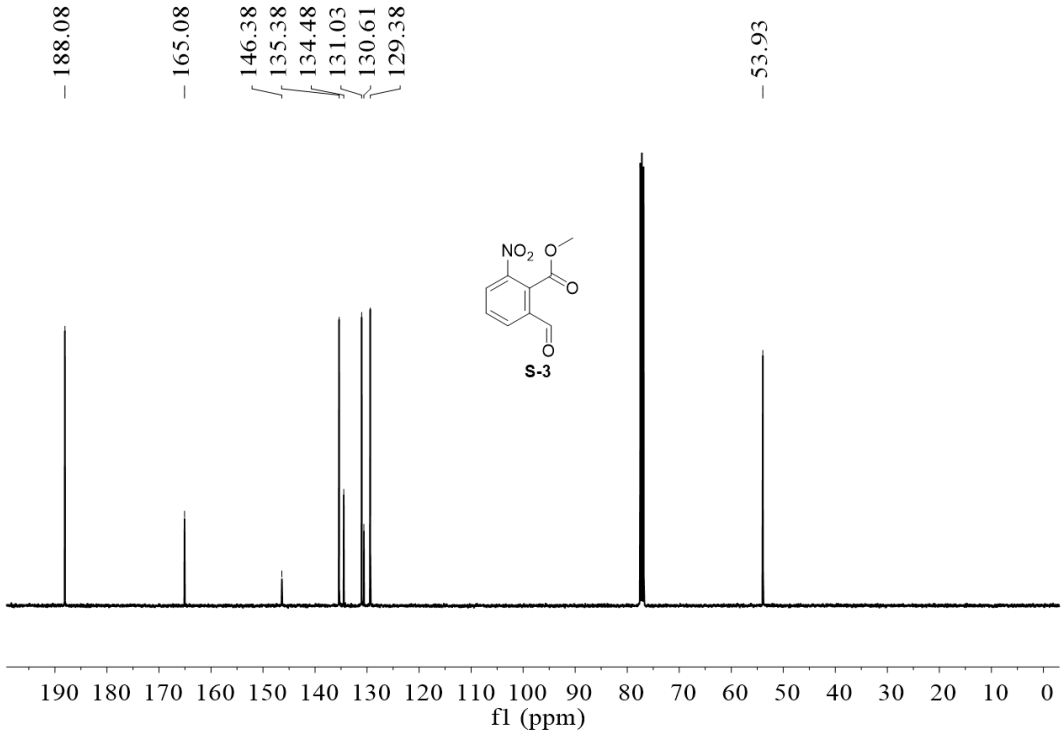

Figure S4. ^{13}C NMR spectrum (101 MHz) of **S-3** in $CDCl_3$.

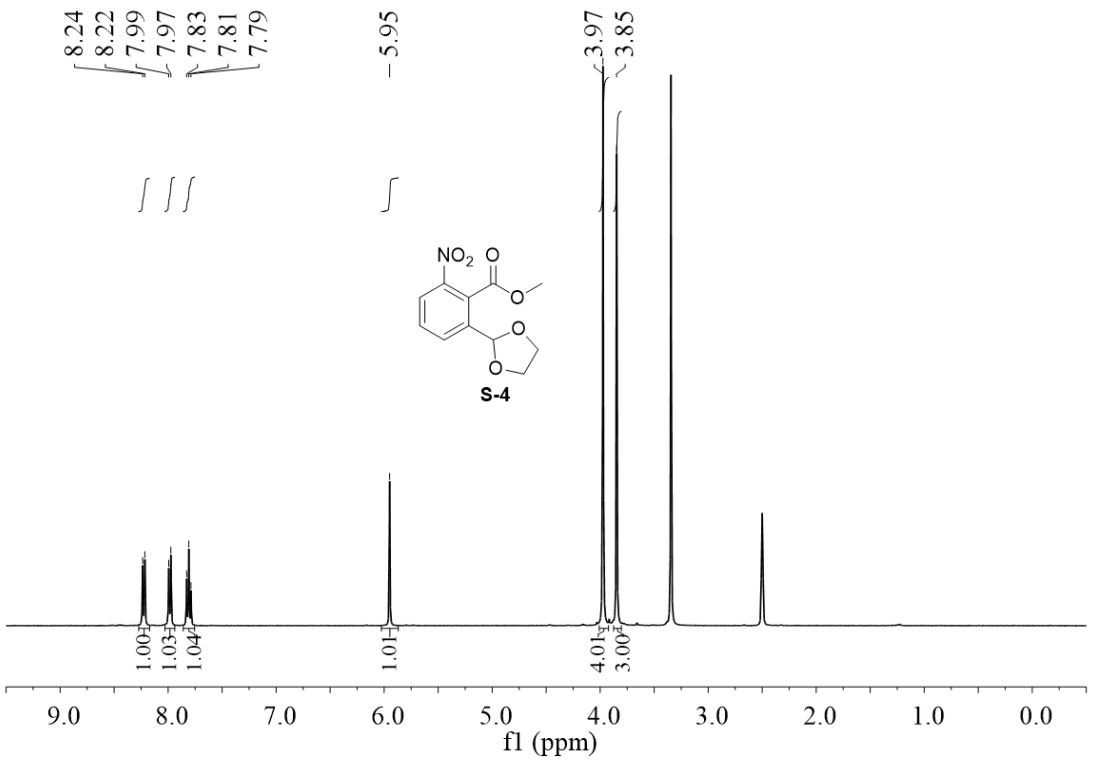

Figure S5. [1]H NMR spectrum (400 MHz) of **S-4** in DMSO-d_6.

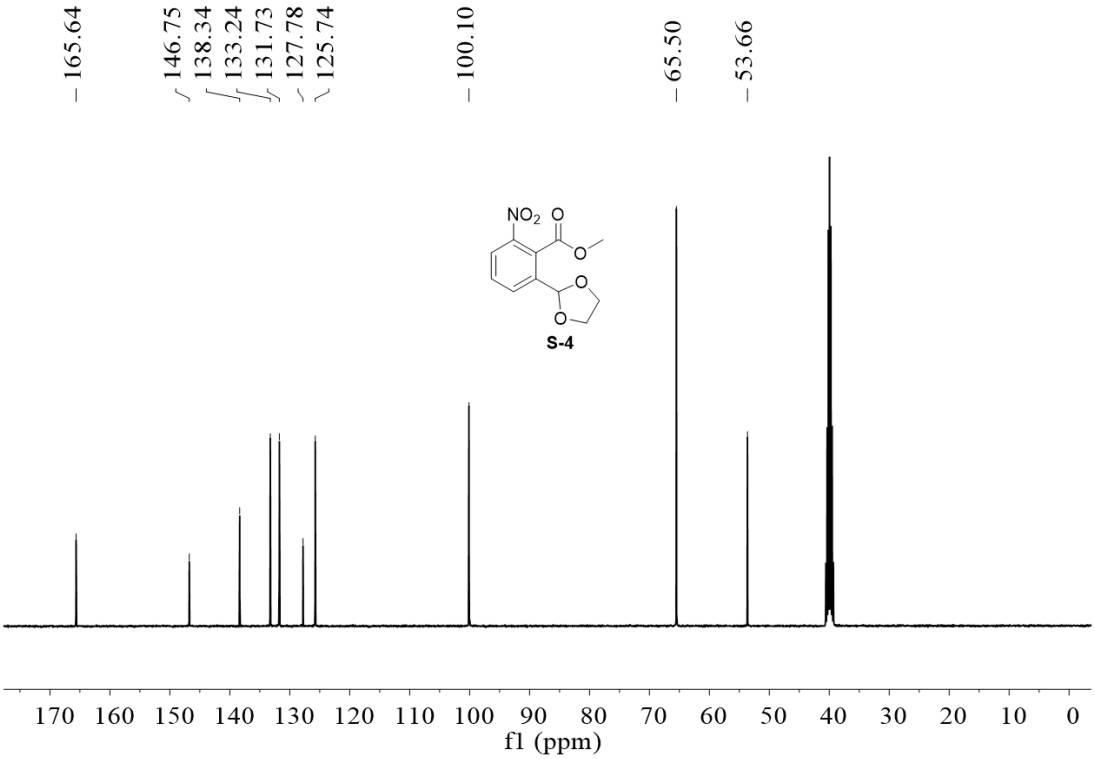

Figure S6. [13]C NMR spectrum (101 MHz) of S-**4** in DMSO-d_6.

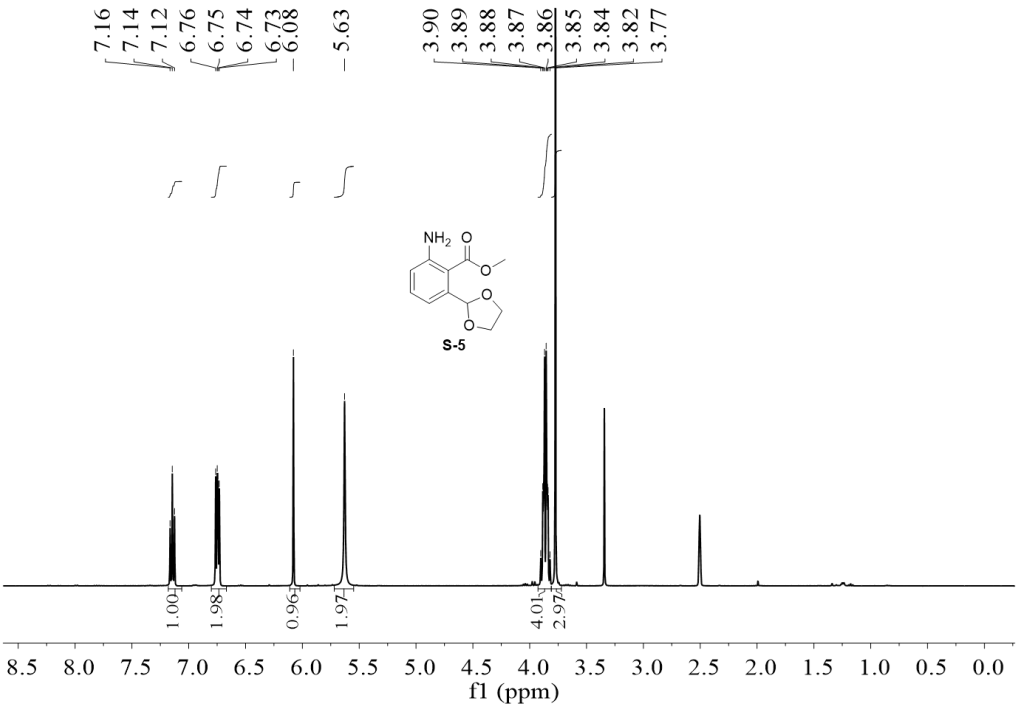

Figure S7. ^{1}H NMR spectrum (400 MHz) of **S-5** in DMSO-*d*$_6$.

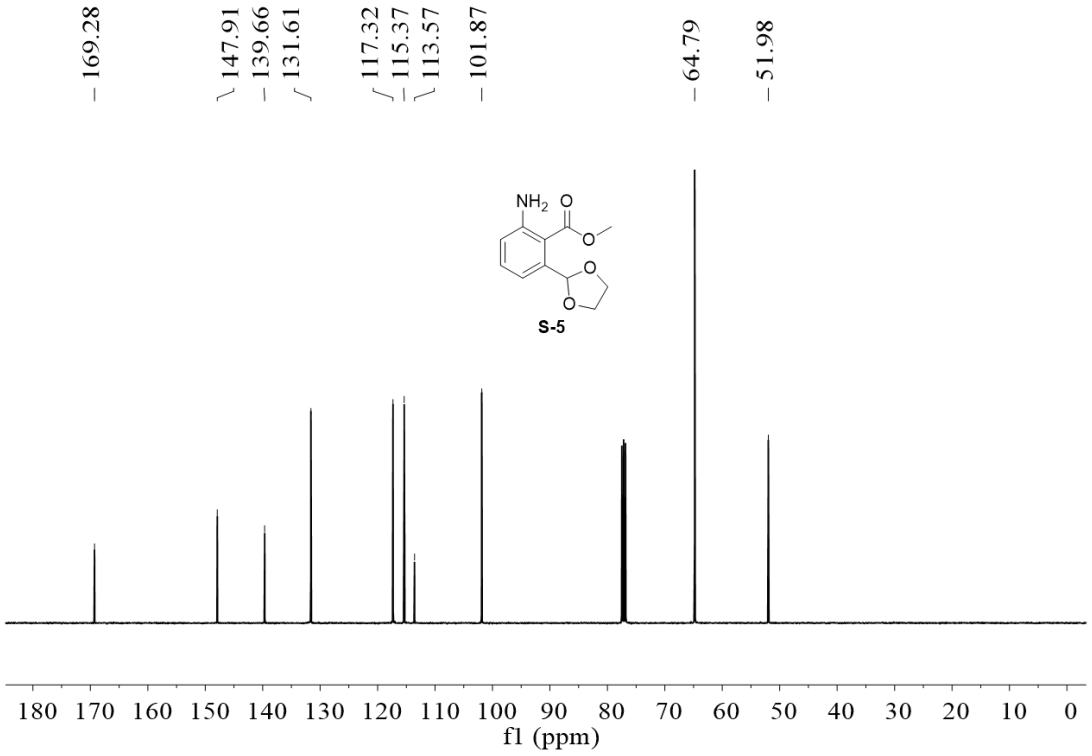

Figure S8. ^{13}C NMR spectrum (101 MHz) of S-**5** in $CDCl_3$.

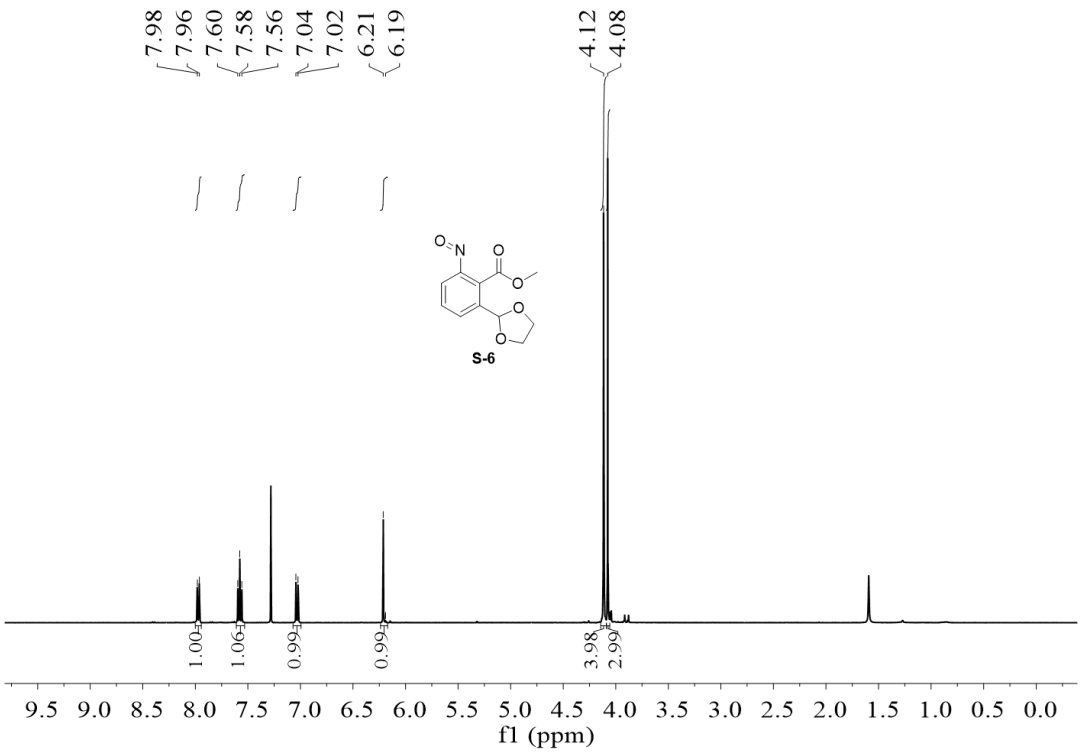

Figure S9. ^{1}H NMR spectrum (400 MHz) of **S-6** in $CDCl_3$.

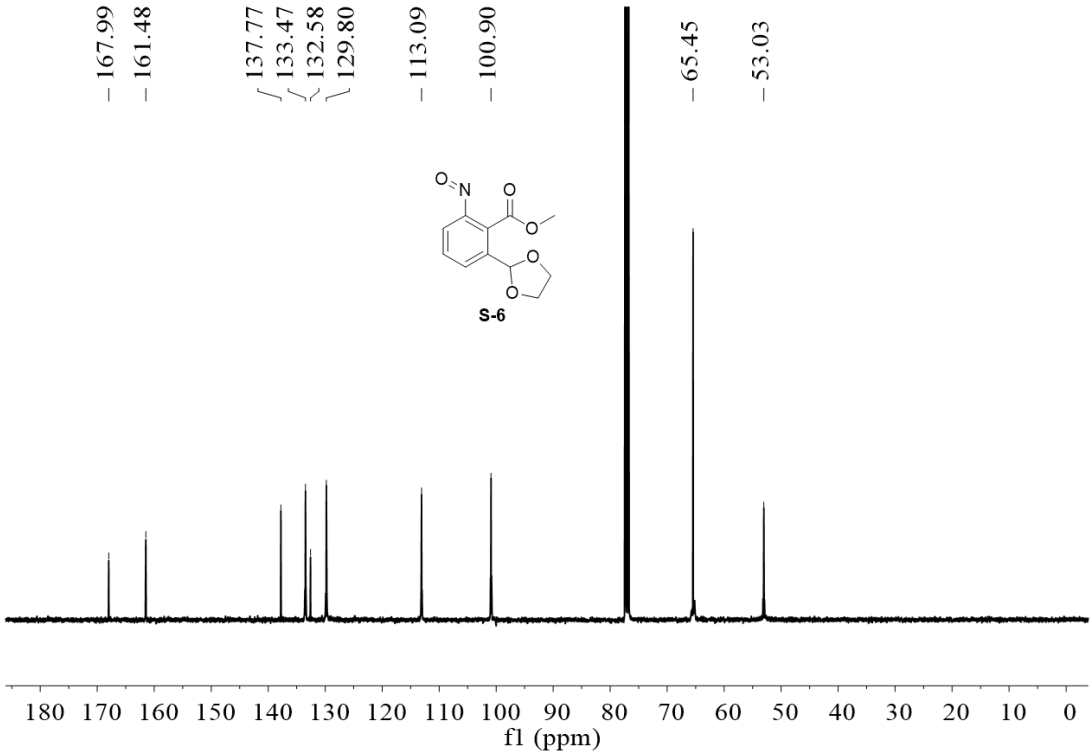

Figure S10. ^{13}C NMR spectrum (101 MHz) of S-**6** in $CDCl_3$.

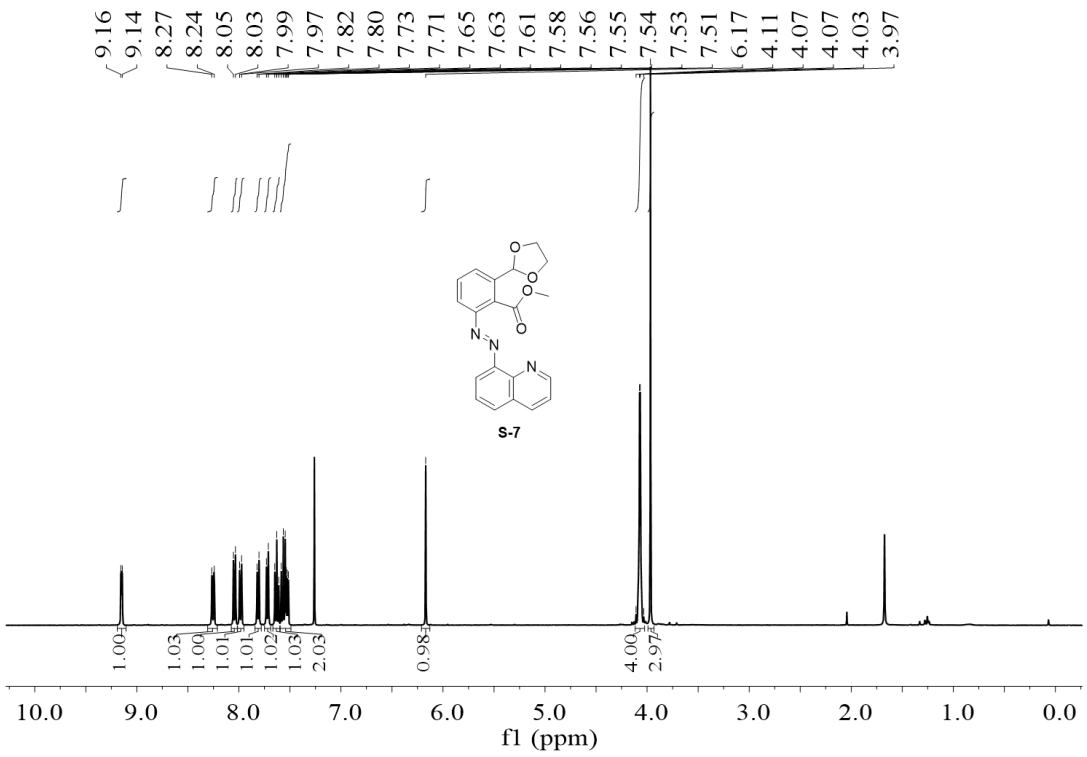

Figure S11. ^{1}H NMR spectrum (400 MHz) of **S-7** in $CDCl_3$.

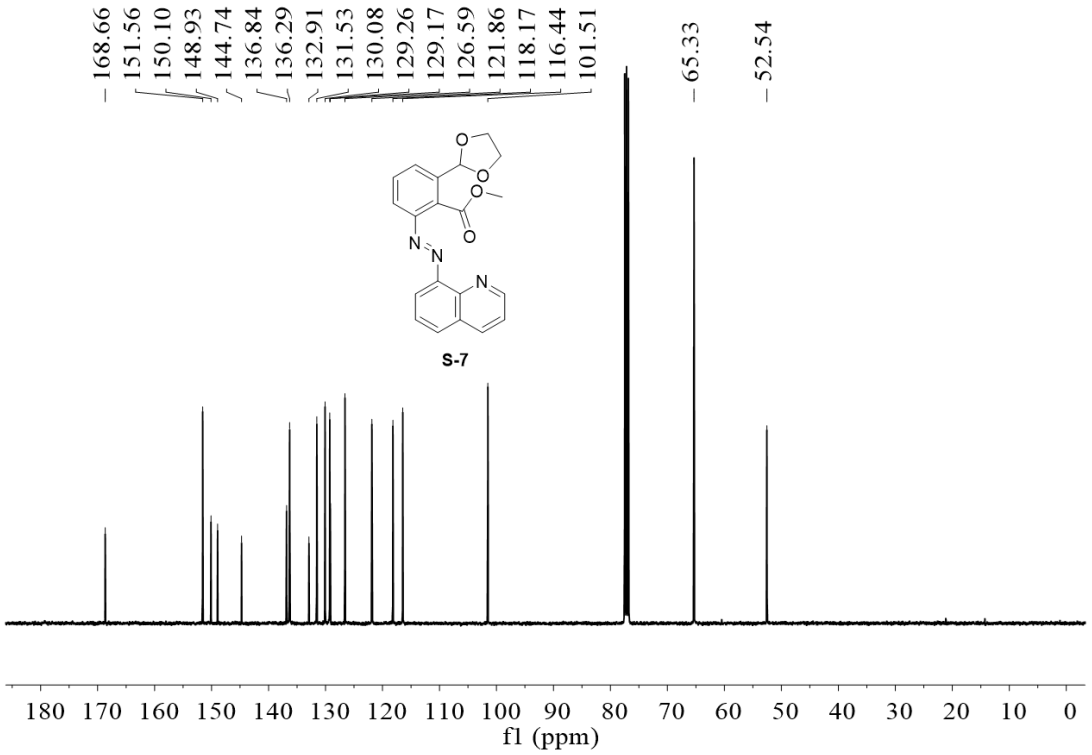

Figure S12. ^{13}C NMR spectrum (101 MHz) of **S-7** in $CDCl_3$.

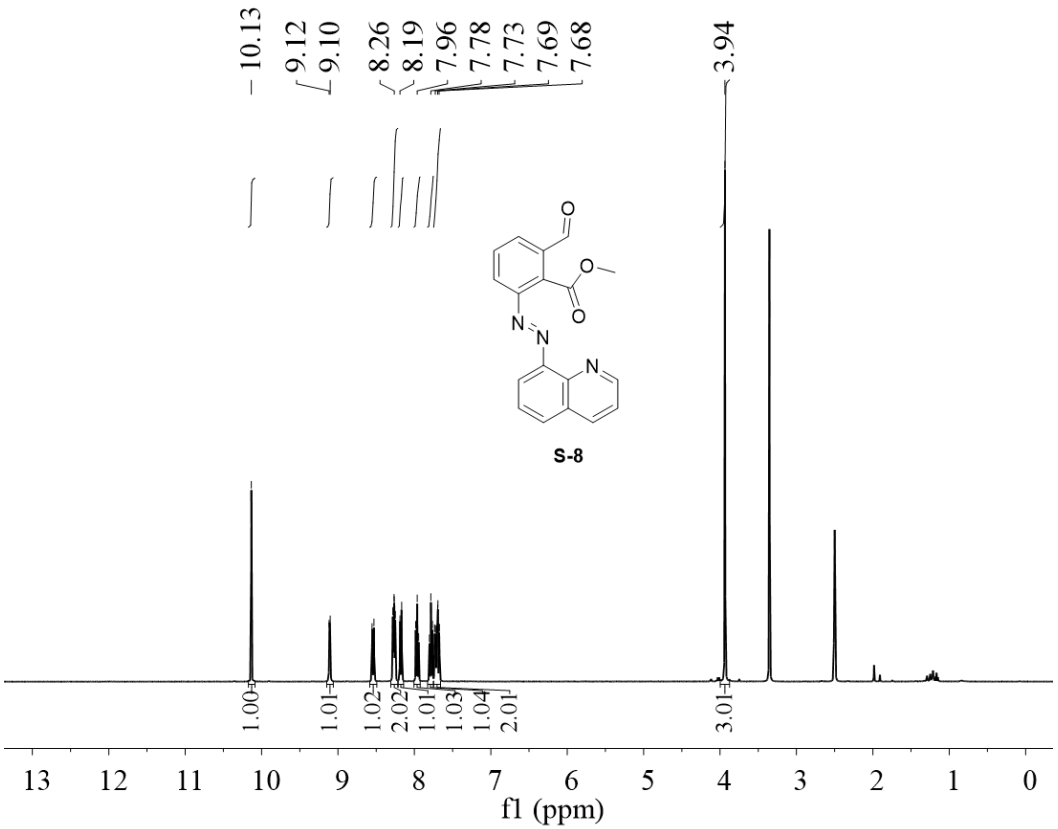

Figure S13. ^{1}H NMR spectrum (400 MHz) of **S-8** in DMSO-d_6.

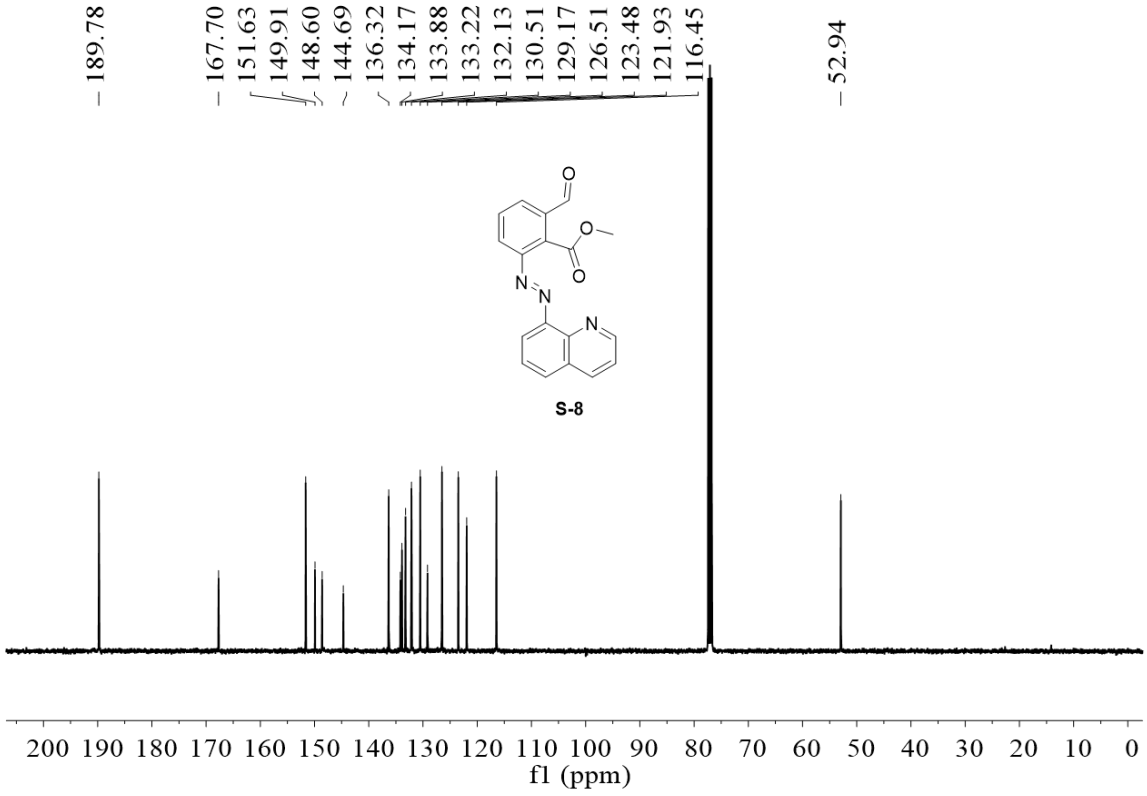

Figure S14. ^{13}C NMR spectrum (101 MHz) of S-**8** in $CDCl_3$.

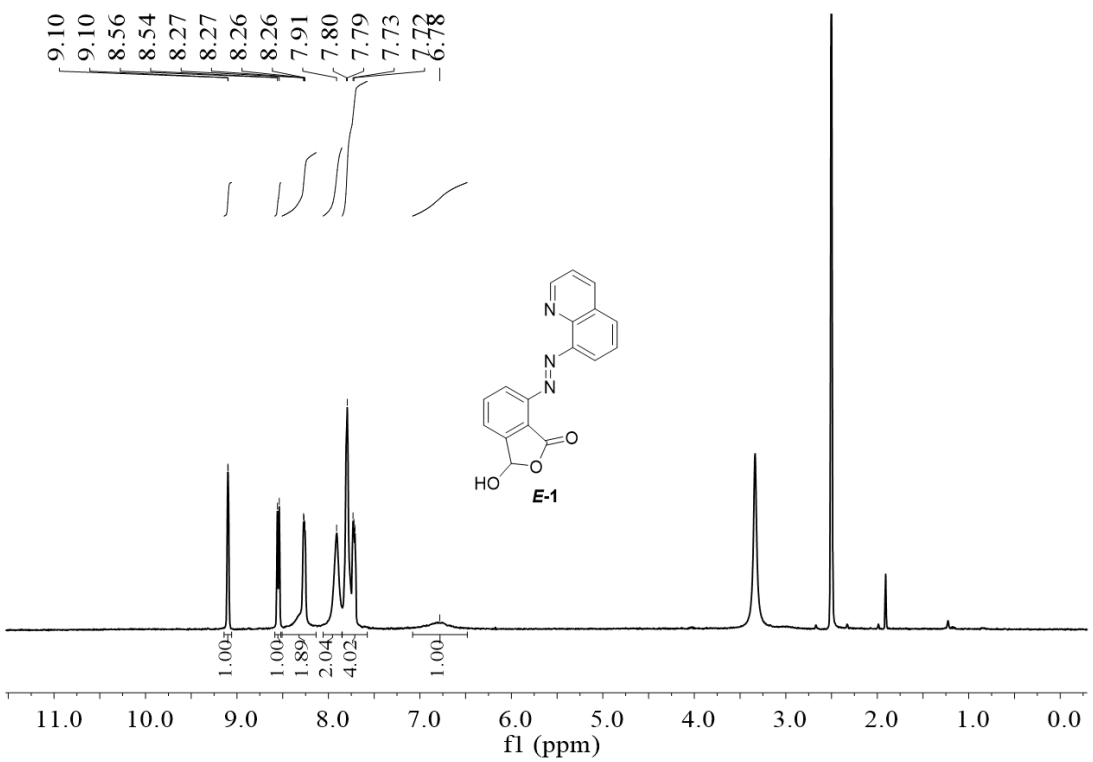

Figure S15. ^{1}H NMR spectrum (400 MHz) of *E*-**1** in DMSO-d_6.

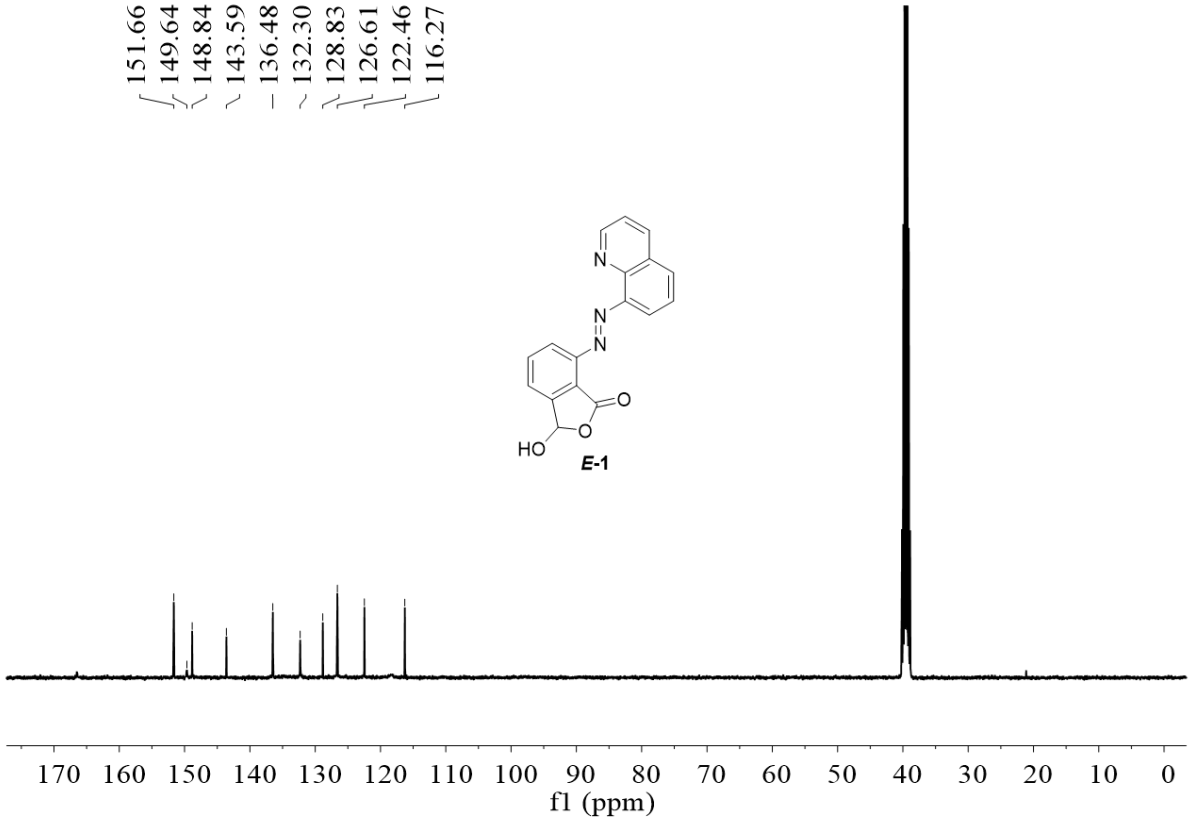

Figure S16. ^{13}C NMR spectrum (101 MHz) of *E*-**1** in DMSO-d_6.

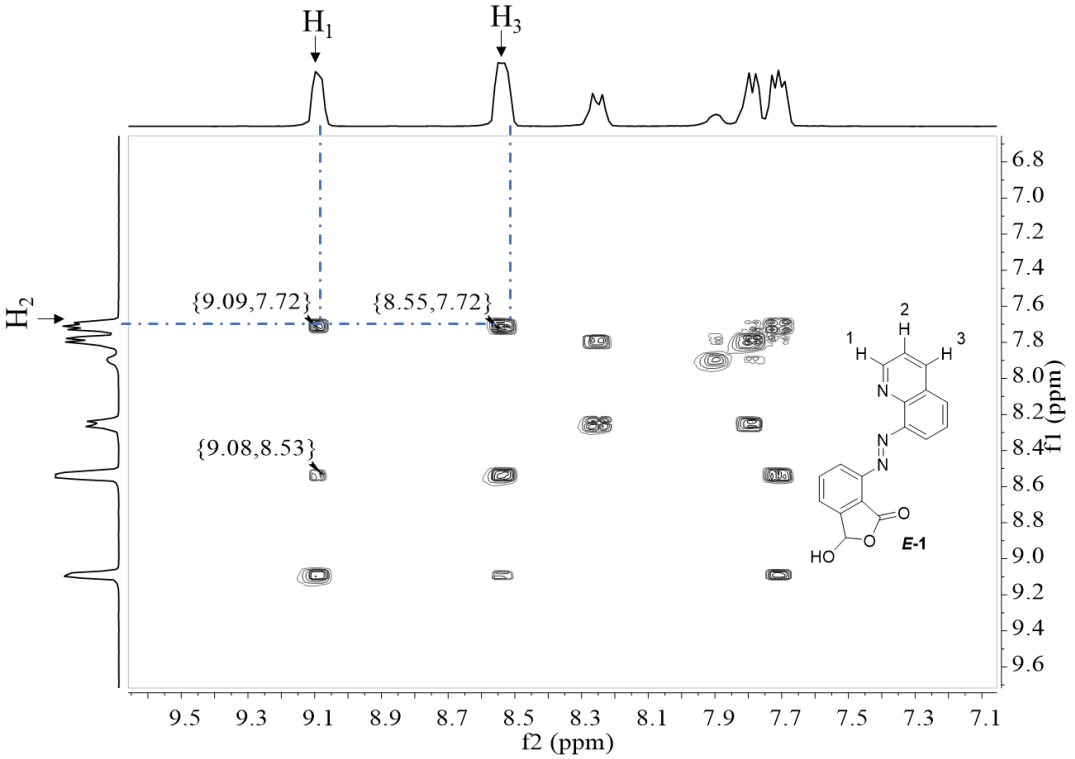

Figure S17. ^{1}H-^{1}H 2D-COSY spectrum (400 MHz) of *E*-**1** in DMSO-d_6.

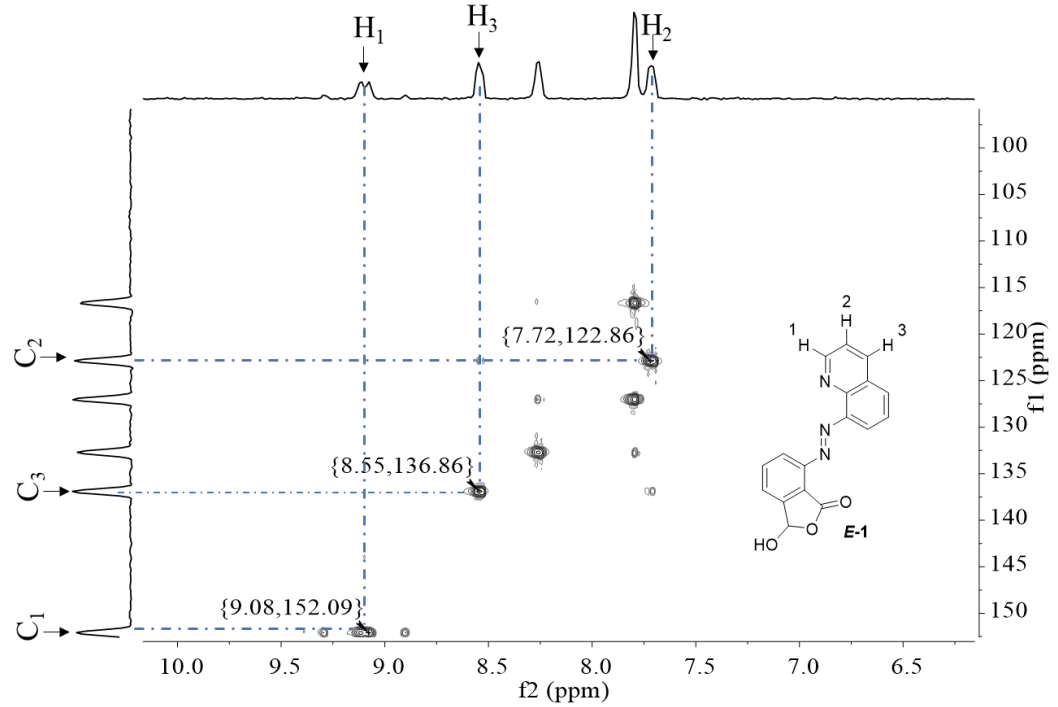

Figure S18. ^{1}H-^{13}C 2D-HMQC spectrum (400 MHz) of *E*-**1** in DMSO-d_6.

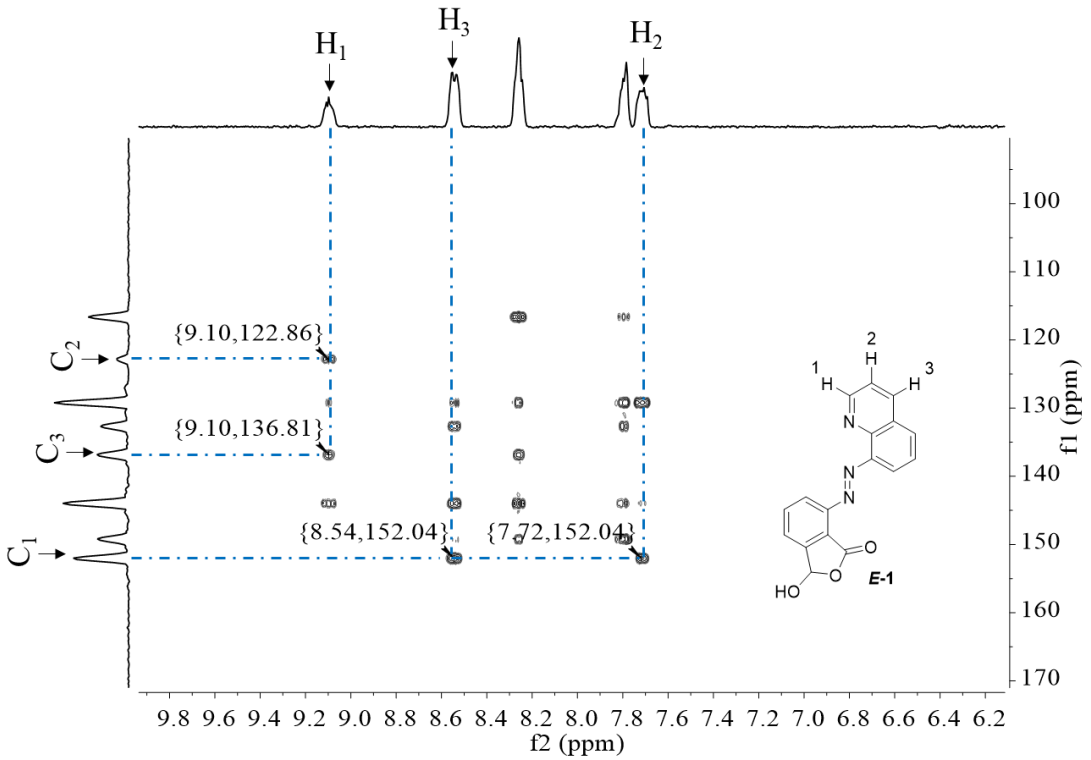

Figure S19. ^{1}H-^{13}C 2D-HMBC spectrum (400 MHz) of *E*-**1** in DMSO-d_6.

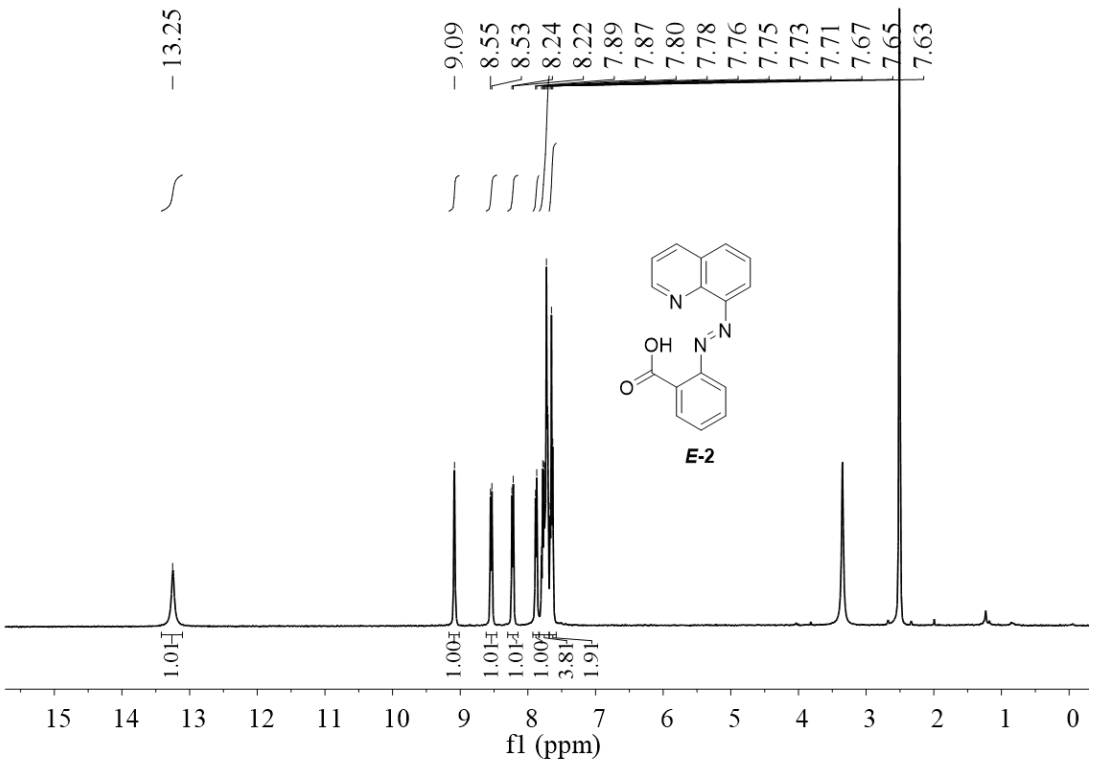

Figure S20. ^{1}H NMR spectrum (400 MHz) of *E*-**2** in DMSO-d_6.

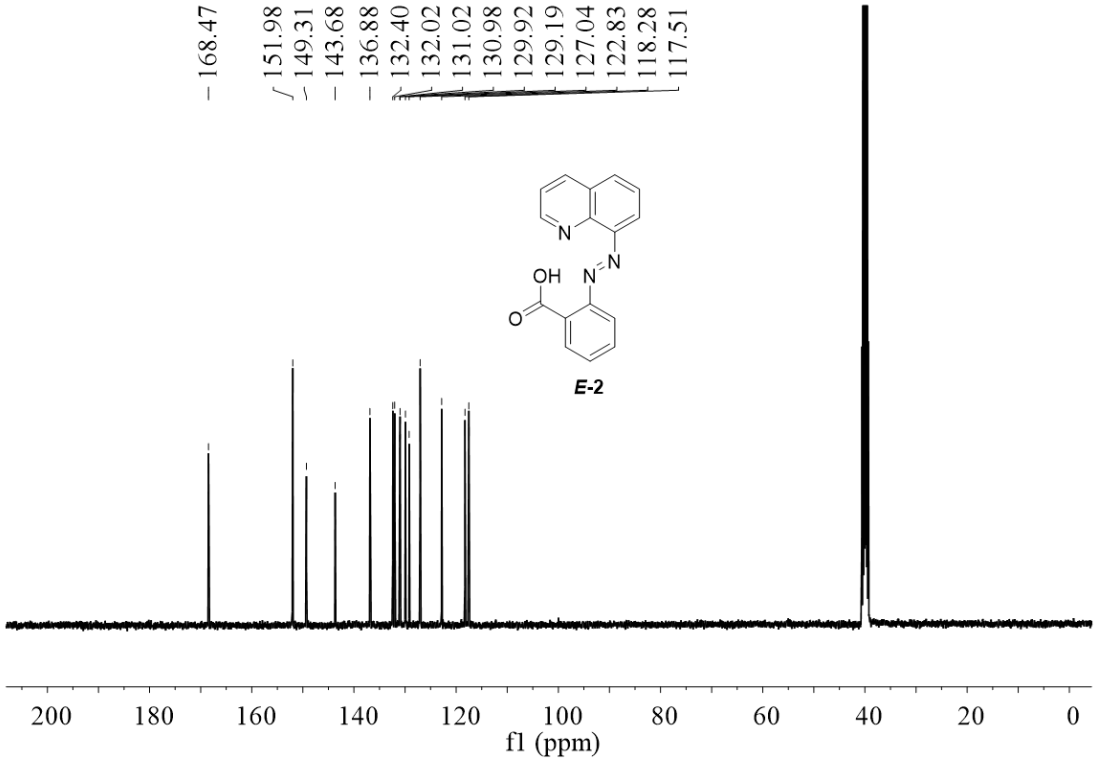

Figure S21. ^{13}C NMR spectrum (101 MHz) of *E*-**2** in DMSO-d_6.

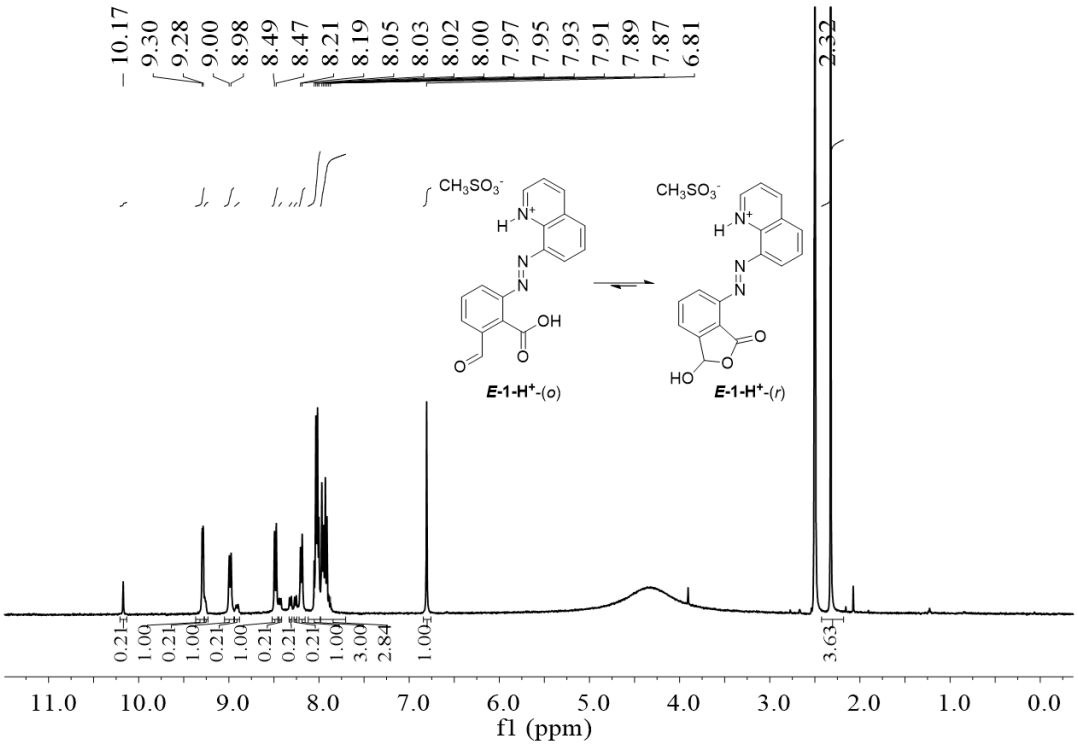

Figure S22. ^{1}H NMR spectrum (400 MHz) of *E*-**1**-H^{+} in DMSO-*d*$_6$.

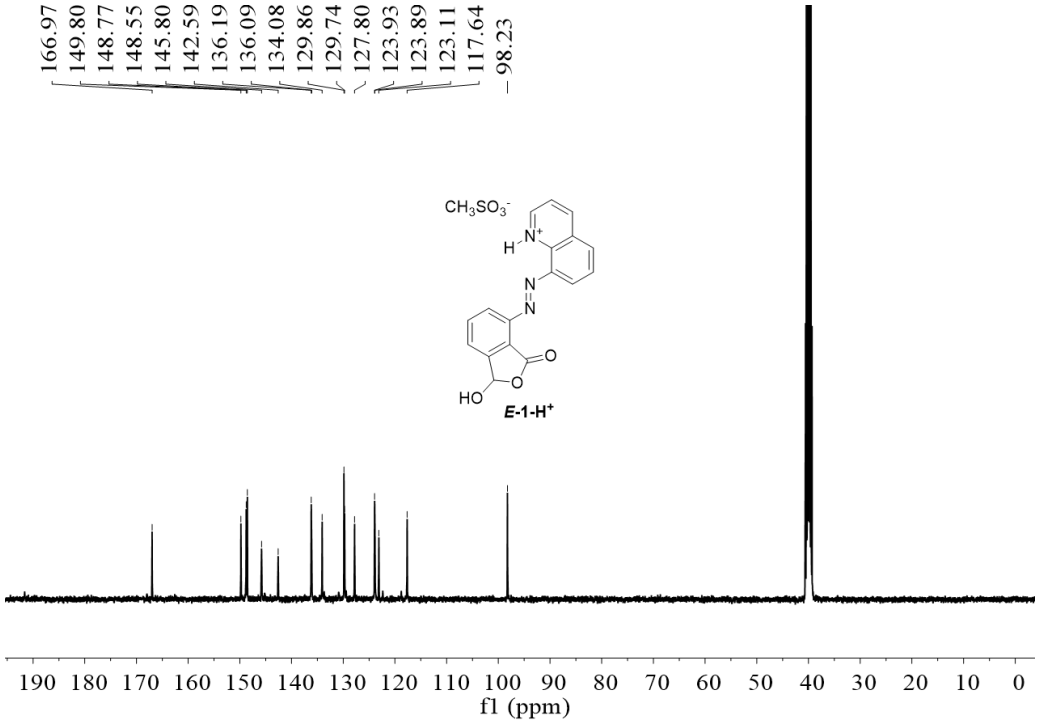

Figure S23. ^{13}C NMR spectrum (101 MHz) of *E*-**2** in DMSO-*d*$_6$.

X-ray Crystallography

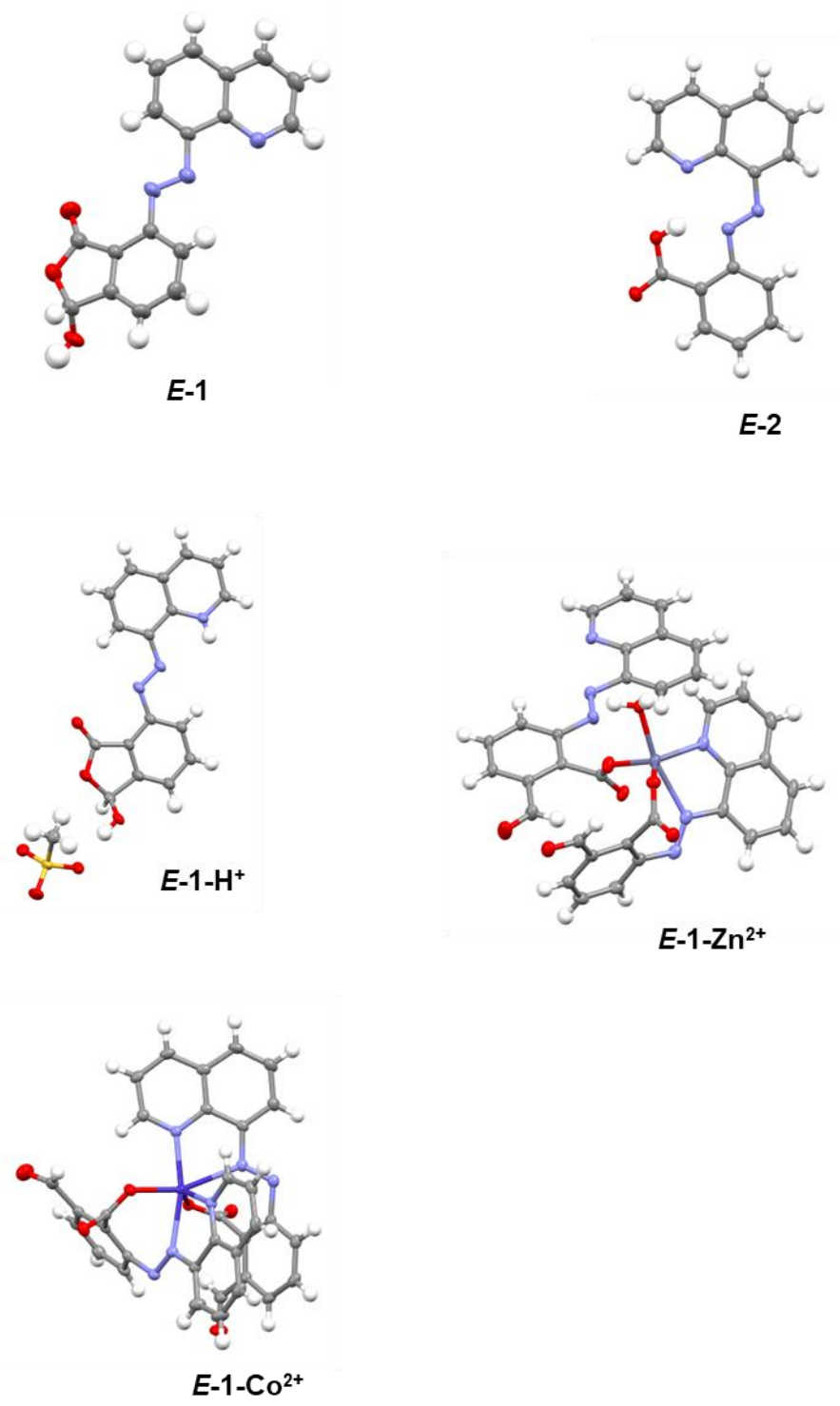

Figure S24. Crystal structures of *E*-**1**, *E*-**2**, *E*-**1**-H^+, *E*-**1**-Zn^{2+}, and *E*-**1**-Co^{2+}. The thermal ellipsoids were scaled to the 50% probability level for *E*-**1**, *E*-**2**, *E*-**1**-H^+, *E*-**1**-Zn^{2+}, and *E*-**1**-Co^{2+}.

Table S1. Summary of crystallographic data.

Compound	*E*-**1**	*E*-**2**	*E*-**1**-H^+	*E*-**1**-Zn^{2+}	*E*-**1**-Co^{2+}
Formula	$C_{17}H1_1N_3O_3$	$C_{16}H_{11}N_3O_2$	$C_{18}H_{15}N_3O_6S$	$C_{34}H_{24}N_6O_8Zn$	$C_{34}H_{22}CoN_6O_7$
Formula weight	305.29	277.28	401.39	709.96	685.50
T/*K*	293(2)	100.0(2)	100(2)	100.00(10)	100(2)
Crystallization solvent	DMSO/H_2O	DMSO/H_2O	DMSO/H_2O	DMSO/H_2O	DMSO/H_2O
Color	red	red	red	red	red
Crystal system	monoclinic	monoclinic	triclinic	triclinic	triclinic
Space group	$P2_1$	$P2_1/n$	P-1	P-1	P-1
a / Å	3.9819(3)	6.9630(6)	9.1825(5)	7.4257(2)	10.3354(4)
b / Å	14.7672(9)	12.2129(10)	9.2868(7)	13.6826(4)	10.6777(4)
c / Å	11.4435(8)	15.0009(12)	10.5049(8)	15.0095(5)	13.1615(3)
α / °	90	90	91.395(6)	80.434(3)	97.249(2)
β / °	94.161(7)	98.316(8)	104.674(6)	78.161(3)	95.452(2)
γ / °	90	90	99.577(5)	81.361(3)	92.065(3)
V/ Å^3	671.12(8)	1262.24(18)	852.44(11)	1461.12(8)	1432.65(8)
Z	2	4	2	2	2
*D*x / g cm^{-3}	1.511	1.459	1.564	1.614	1.589
μ / mm^{-1}	0.562	0.519	1.366	1.143	3.640
F(000)	316.0	576.0	416.0	728.0	702.0
θ range / °	6.734 to 122.242	8.15 to 121.072	7.582 to 119.652	5.282 to 120.556	5.916 to 120.75
GOF on F^2	1.006	1.077	1.073	1.064	1.084
R_1 [$I > 2\sigma(I)$]	0.0857	0.0657	0.1060	0.0567	0.0579
wR_2 (all data)	0.1783	0.1771	0.2205	0.1481	0.1356

3. Photoswitching Behaviors

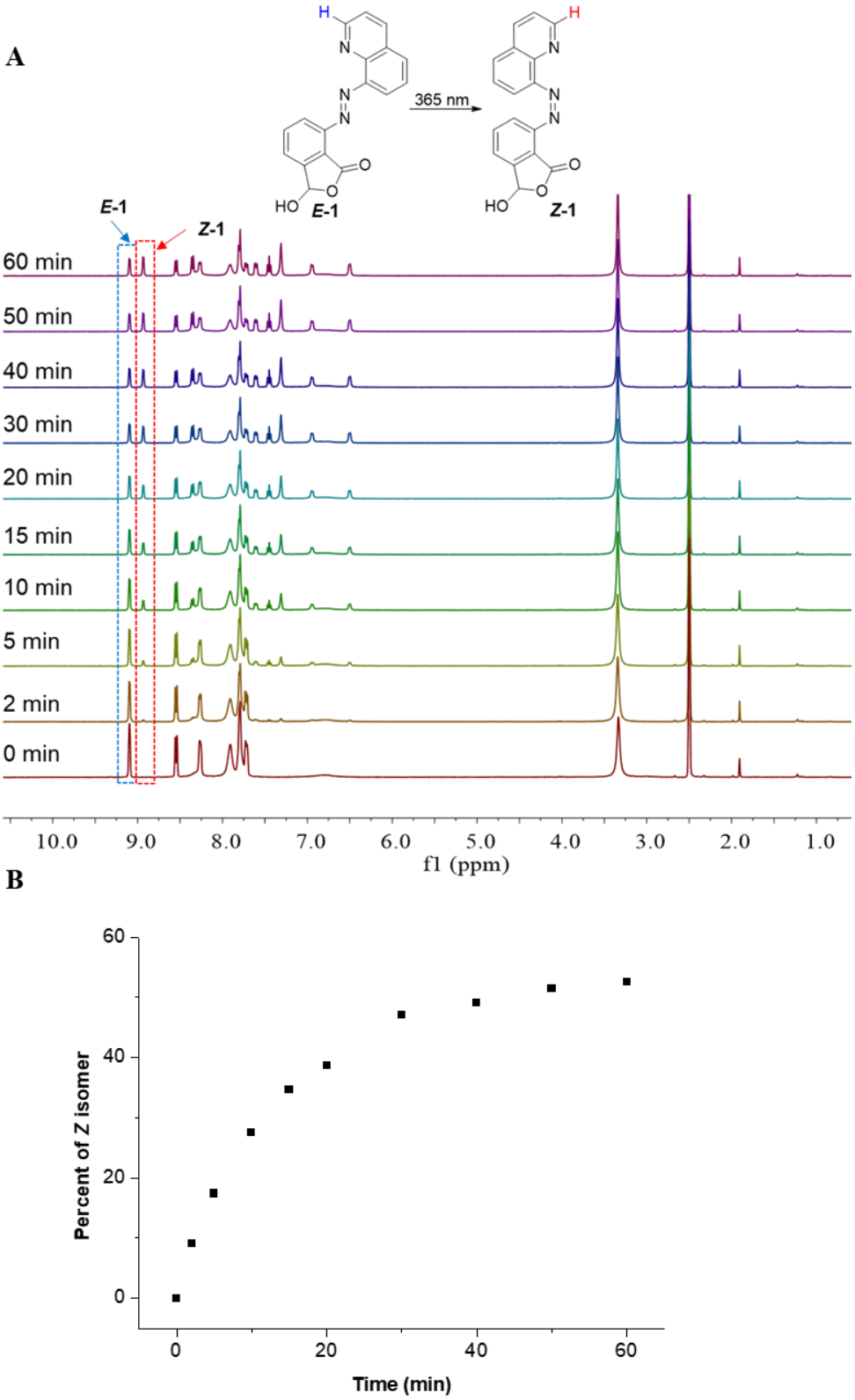

Figure S25. (A) Changes in ^{1}H NMR spectrum of *E*-**1** in DMSO-d_6 (10 mM) upon 365 nm light irradiation at varied time. (B) Photoisomerization kinetic curve of *E*-**1**. The percent of *Z*-**1** is 54% after irradiation for 1 h.

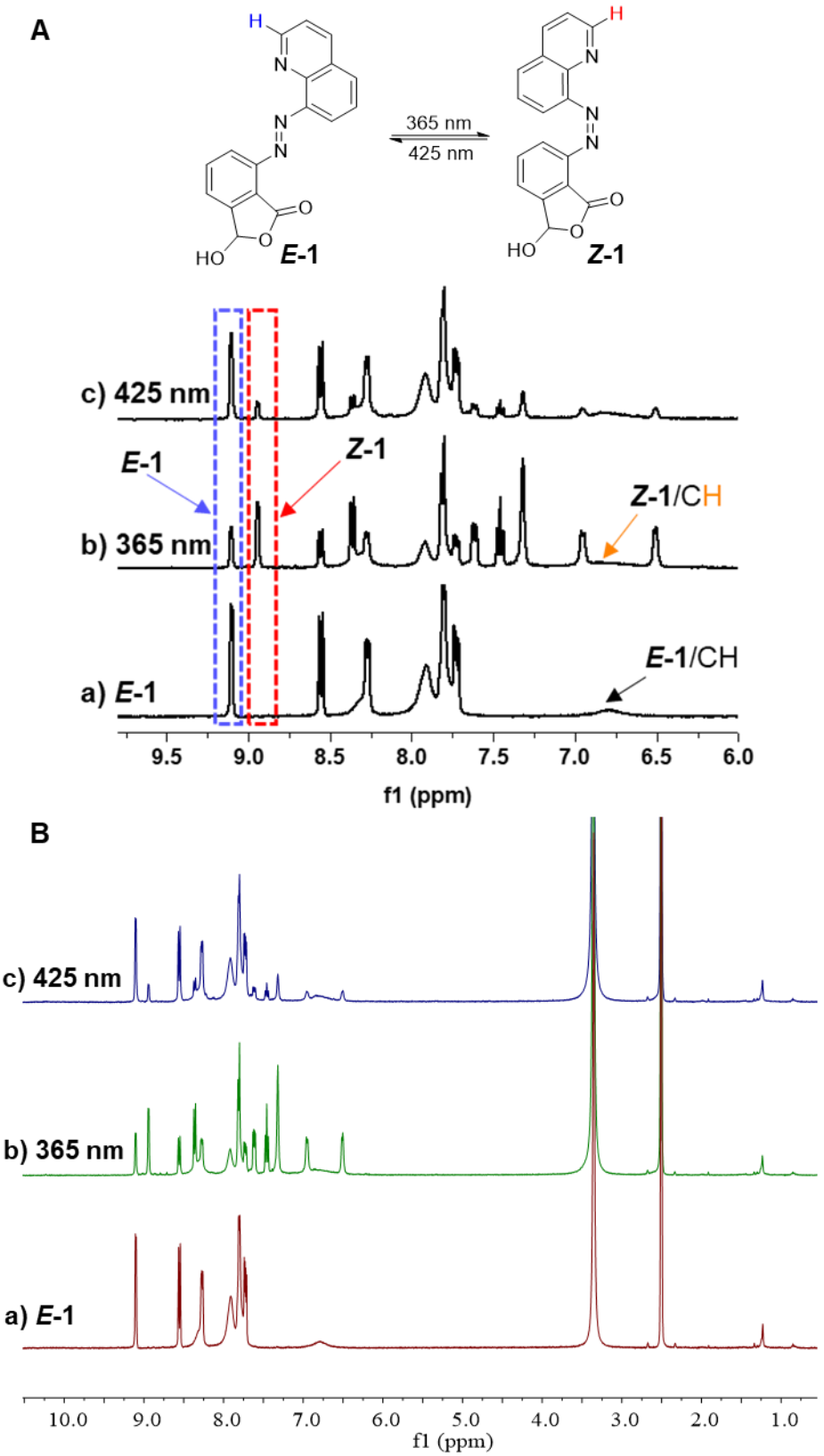

Figure S26. (A) (a) ^{1}H NMR spectrum of *E*-**1** in DMSO-d_6 (10 mM); (b) after irradiation for 1.5 h with 365 nm light (60% *Z*); (c) further irradiation for 0.5 h with 425 nm light (20% *Z*). (B) The full ^{1}H NMR spectra of panel A.

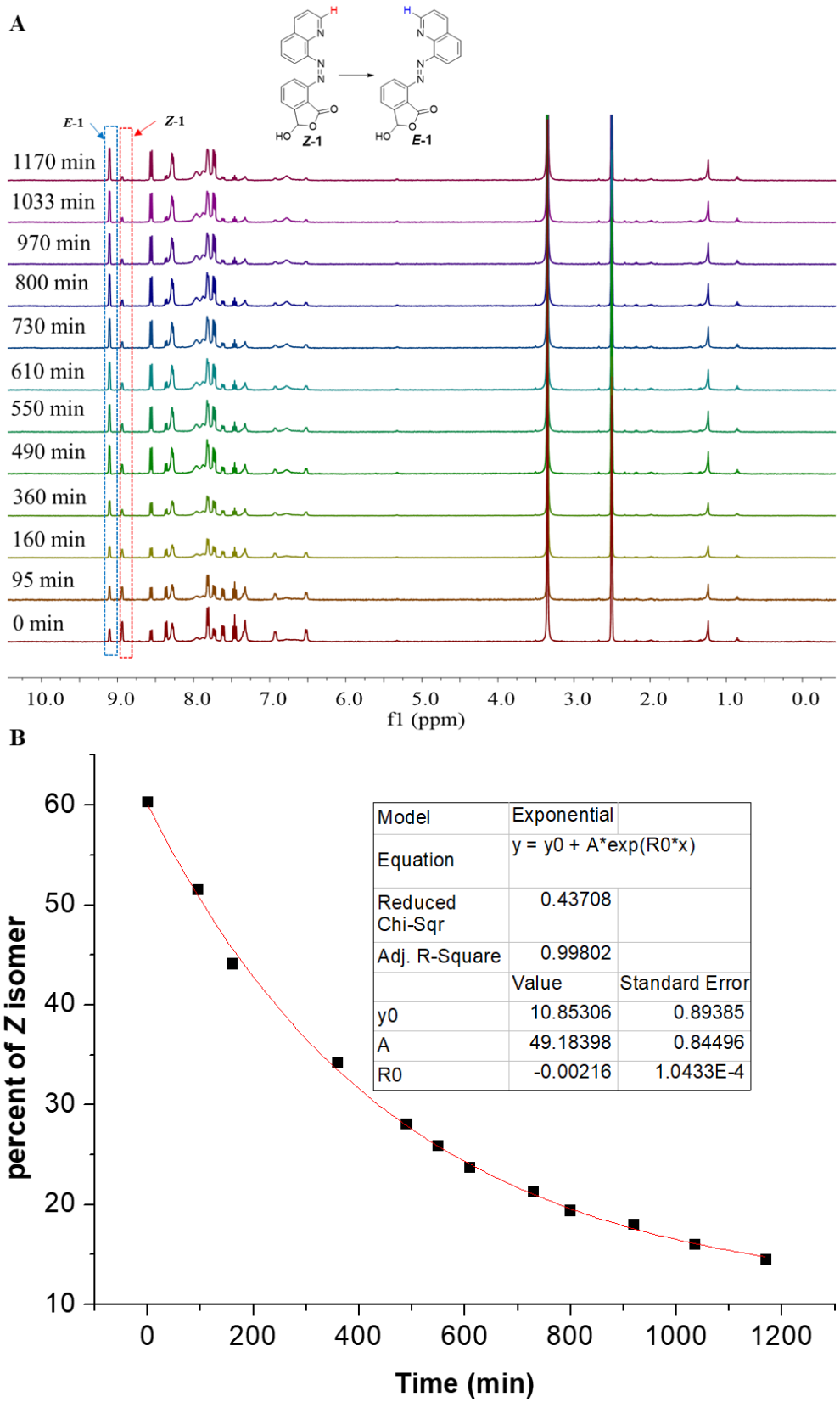

Figure S27. Changes in ^{1}H NMR spectrum (A) as well as thermal isomerization kinetic curve (B) after the irradiation of *E*-**1** in DMSO-d_6 (10 mM) for 1.5 h at 365 nm (0 min in A) and then waiting in the dark (25 ºC) at varied time. The half-life of *Z*-**1** was determined to be 5.4 h at 25 ºC.

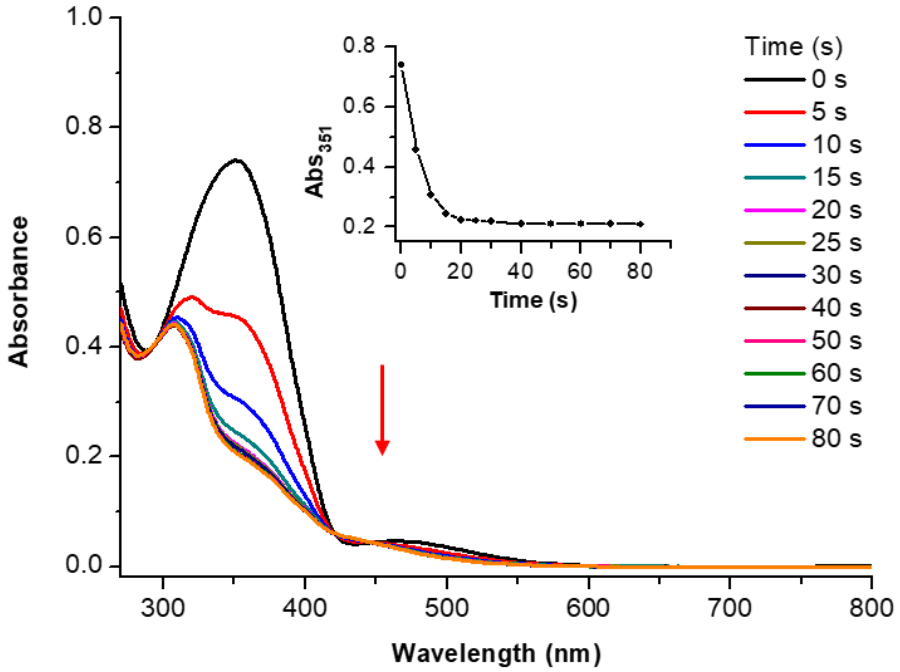

Figure S28. Photoisomerization of *E*-**1** to give *Z*-**1**: changes in absorption spectra upon irradiation of *E*-**1** (75 μM in DMSO) with 365 nm light. Inset: the photoisomerization kinetic curve of *E*-**1**, via monitoring the absorbance at 351 nm.

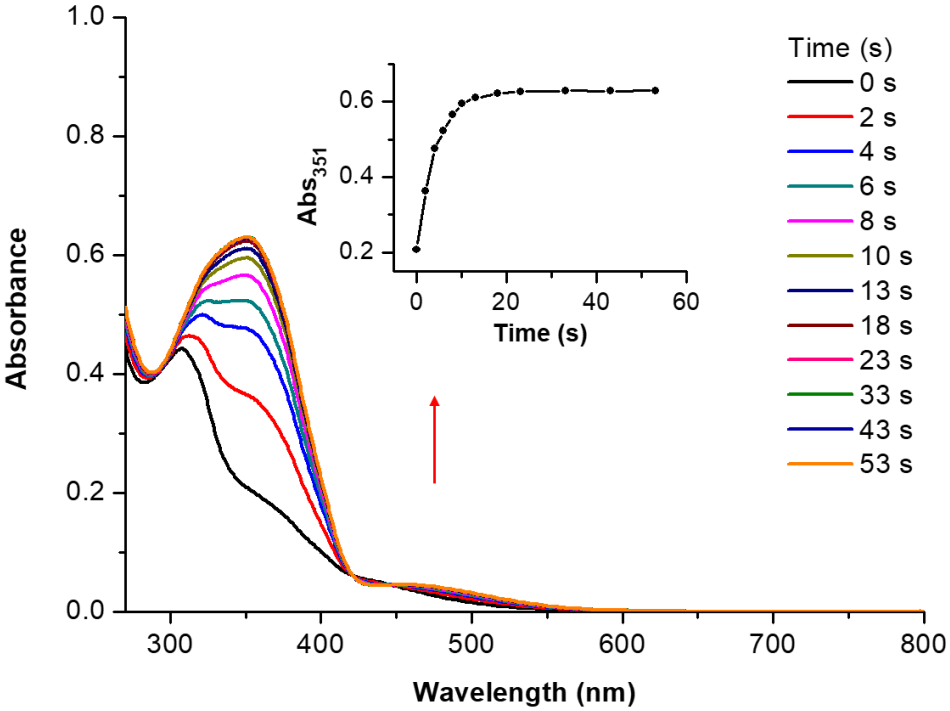

Figure S29. Photoisomerization of *Z*-**1** (created through irradiation of *E*-**1** at 365 nm) to give *E*-**1**: changes in absorption spectra upon irradiation of *Z*-**1** (75 μM in DMSO) with 425 nm light. Inset: the photoisomerization kinetic curve of *Z*-**1**, via monitoring the absorbance at 351 nm.

4. pH effects

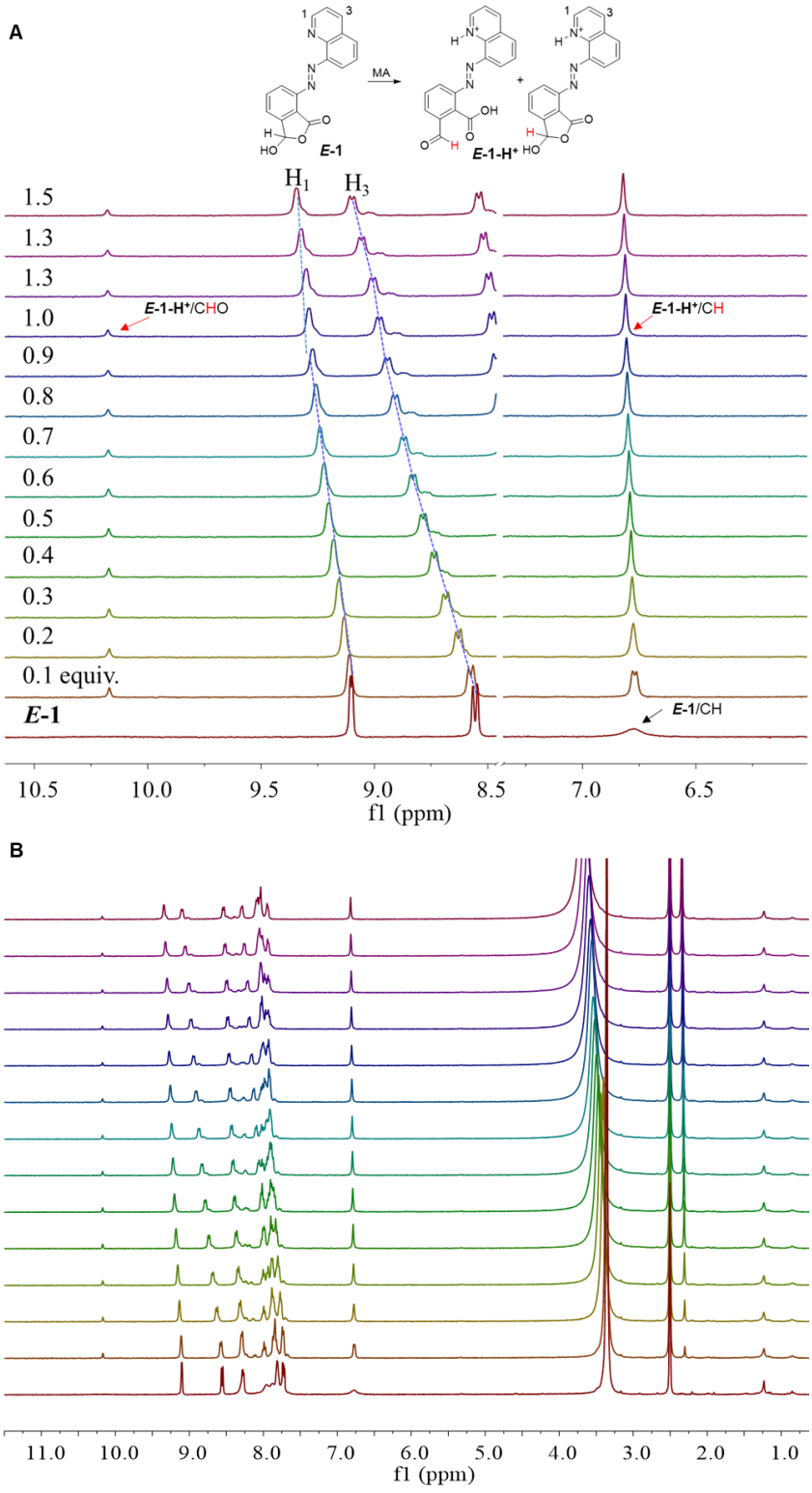

Figure S30. (A) Changes in ^{1}H NMR spectrum upon titration of *E*-**1** with methanesulfonic acid (MA) in DMSO-d_6 (10 mM). (B) The full ^{1}H NMR spectra of panel A. The titration of MA into *E*-**1** resulted in the protonation of quinoline to get *E*-**1**-H^{+}, and excess MA could induce the protonation of azo group.

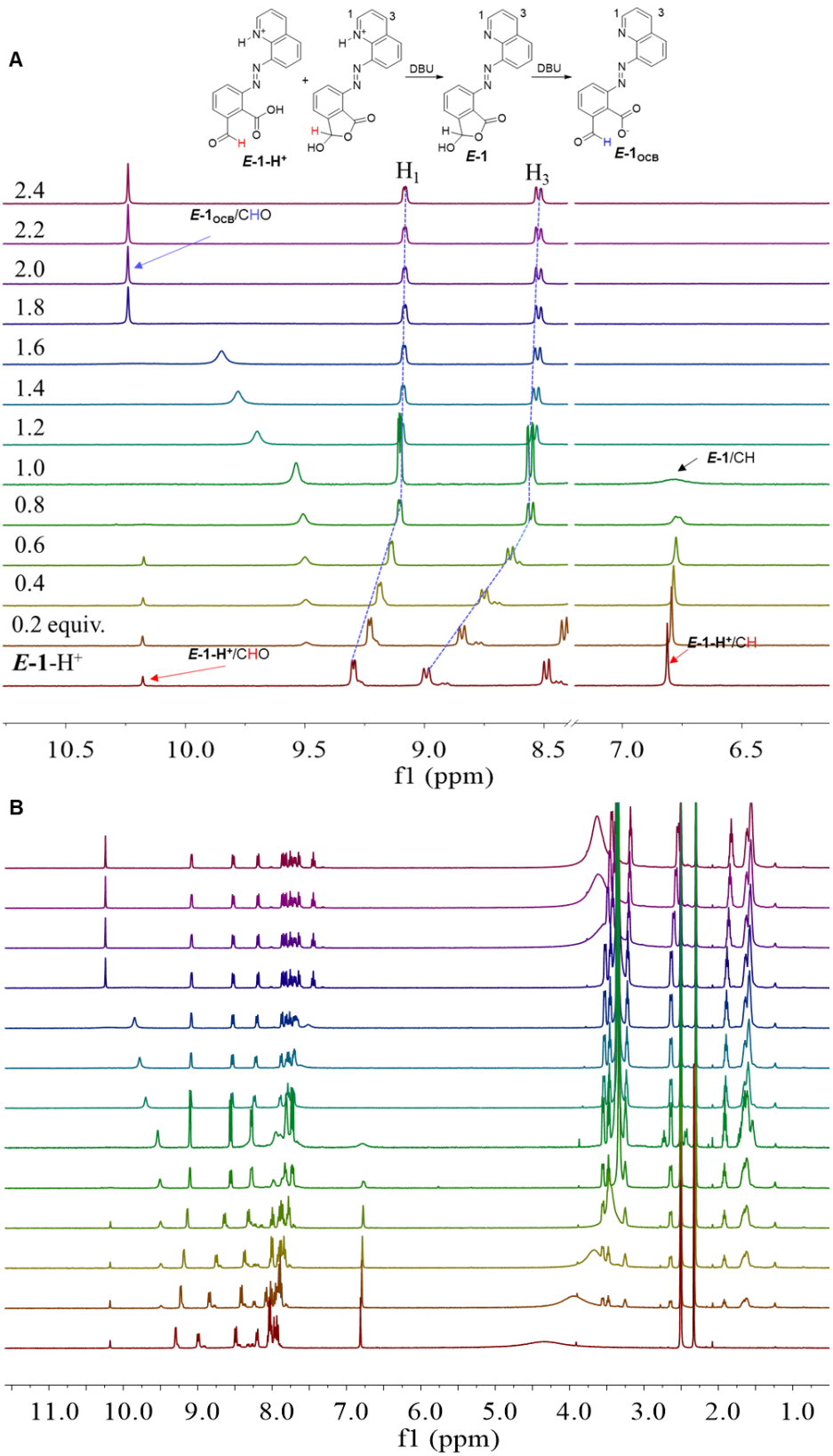

Figure S31. (A) Changes in ^{1}H NMR spectrum upon titration of *E*-**1**-H^{+} with DBU in DMSO-d_6 (10 mM). (B) The full ^{1}H NMR spectra of panel A. The titration of DBU into *E*-**1**-H^{+} induced the deprotonation of quinolinium to get *E*-**1** and then ring opening of cyclic hemiacetal to get *E*-**1**$_{OCB}$.

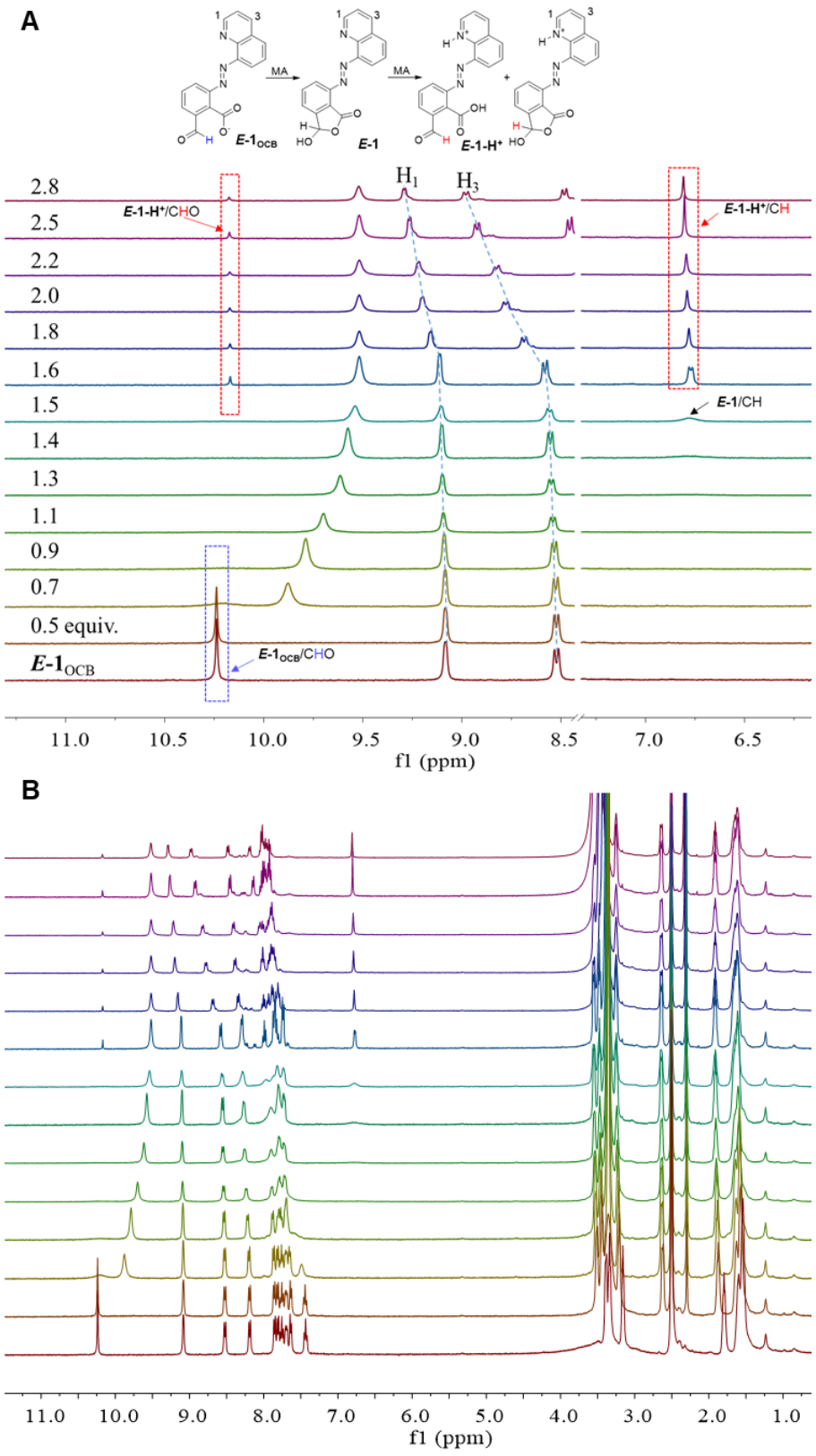

Figure S32. (A) Changes in ^{1}H NMR spectrum upon titration of *E*-**1**$_{OCB}$ with MA in DMSO-d_6 (10 mM). *E*-**1**$_{OCB}$ was prepared *in situ* through adding 1.5 equiv. DBU into *E*-**1**. (B) The full ^{1}H NMR spectra of panel A. The conversion of *E*-**1**$_{OCB}$ to *E*-**1** and then *E*-**1**-H^{+} was confirmed.

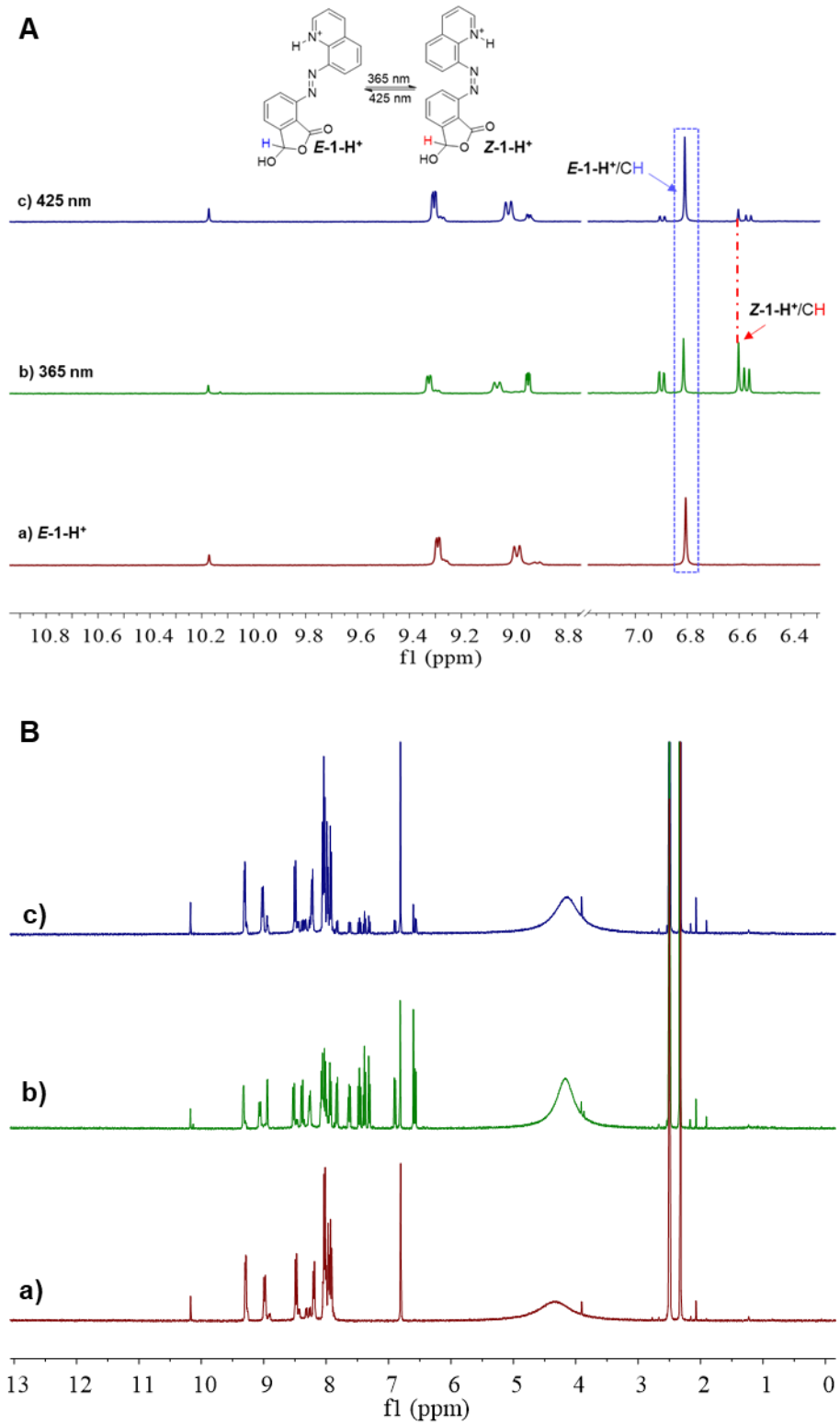

Figure S33. (A) (a) ^{1}H NMR spectrum of *E*-**1**-H^{+} in DMSO-d_6 (10 mM); (b) after irradiation for 1.5 h with 365 nm light (44% *Z*); (c) further irradiation for 0.5 h with 425 nm light (13% *Z*). (B) The full ^{1}H NMR spectra of panel A.

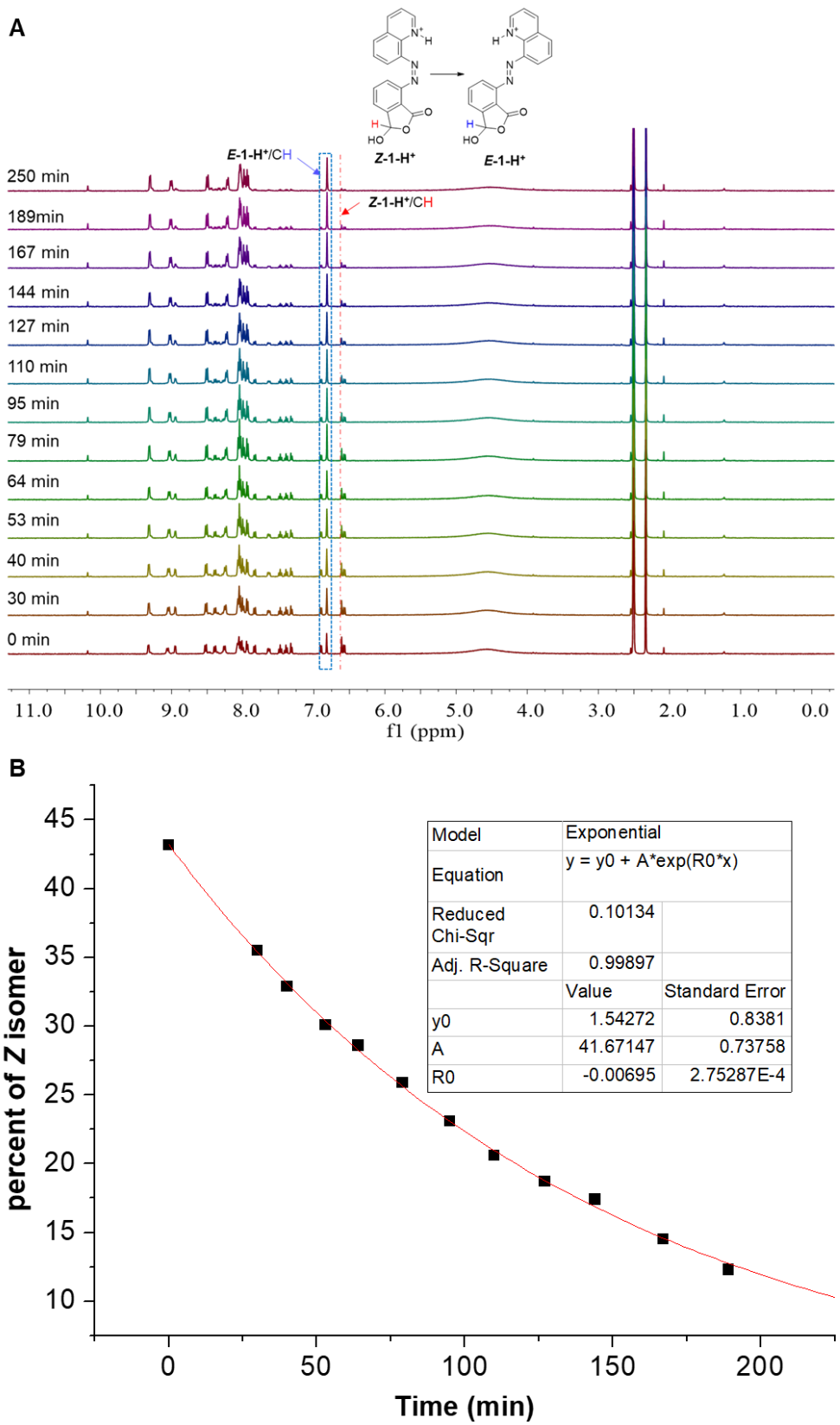

Figure S34. Changes in ^{1}H NMR spectrum (A) as well as thermal isomerization kinetic curve (B) after the irradiation of *E*-**1**-H^{+} in DMSO-d_6 (10 mM) for 1.5 h at 365 nm (0 min in A) and then waiting in the dark (25 ºC) at varied time. The half-life of *Z*-**1**-H^{+} was determined to be 100 min at 25 ºC.

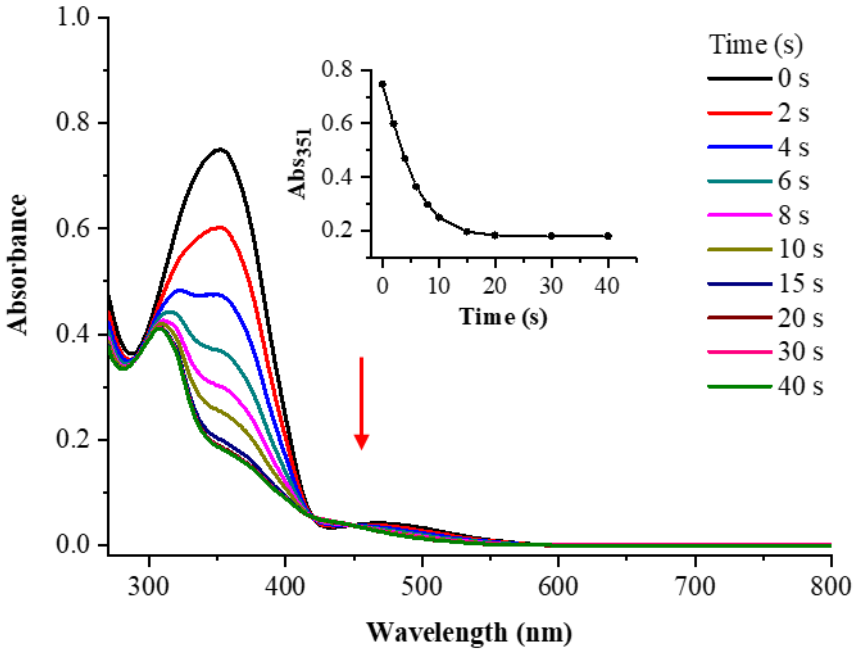

Figure S35. Photoisomerization of *E*-**1**-H$^+$ to give *Z*-**1**-H$^+$: changes in absorption spectra upon irradiation of *E*-**1**-H$^+$ (50 μM in DMSO) with 365 nm light. Inset: the photoisomerization kinetic curve of *E*-**1**-H$^+$, via monitoring the absorbance at 351 nm.

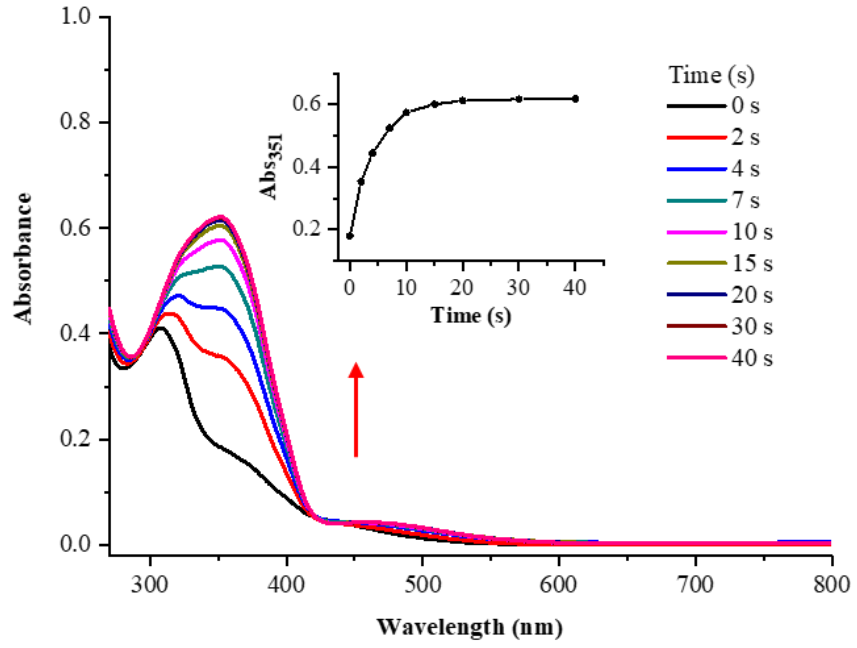

Figure S36. Photoisomerization of *Z*-**1**-H$^+$ (created through irradiation of *E*-**1**-H$^+$ at 365 nm) to give *E*-**1**-H$^+$: changes in absorption spectra upon irradiation of *Z*-**1**-H$^+$ (50 μM in DMSO) with 425 nm light. Inset: the photoisomerization kinetic curve of *Z*-**1**-H$^+$, via monitoring the absorbance at 351 nm.

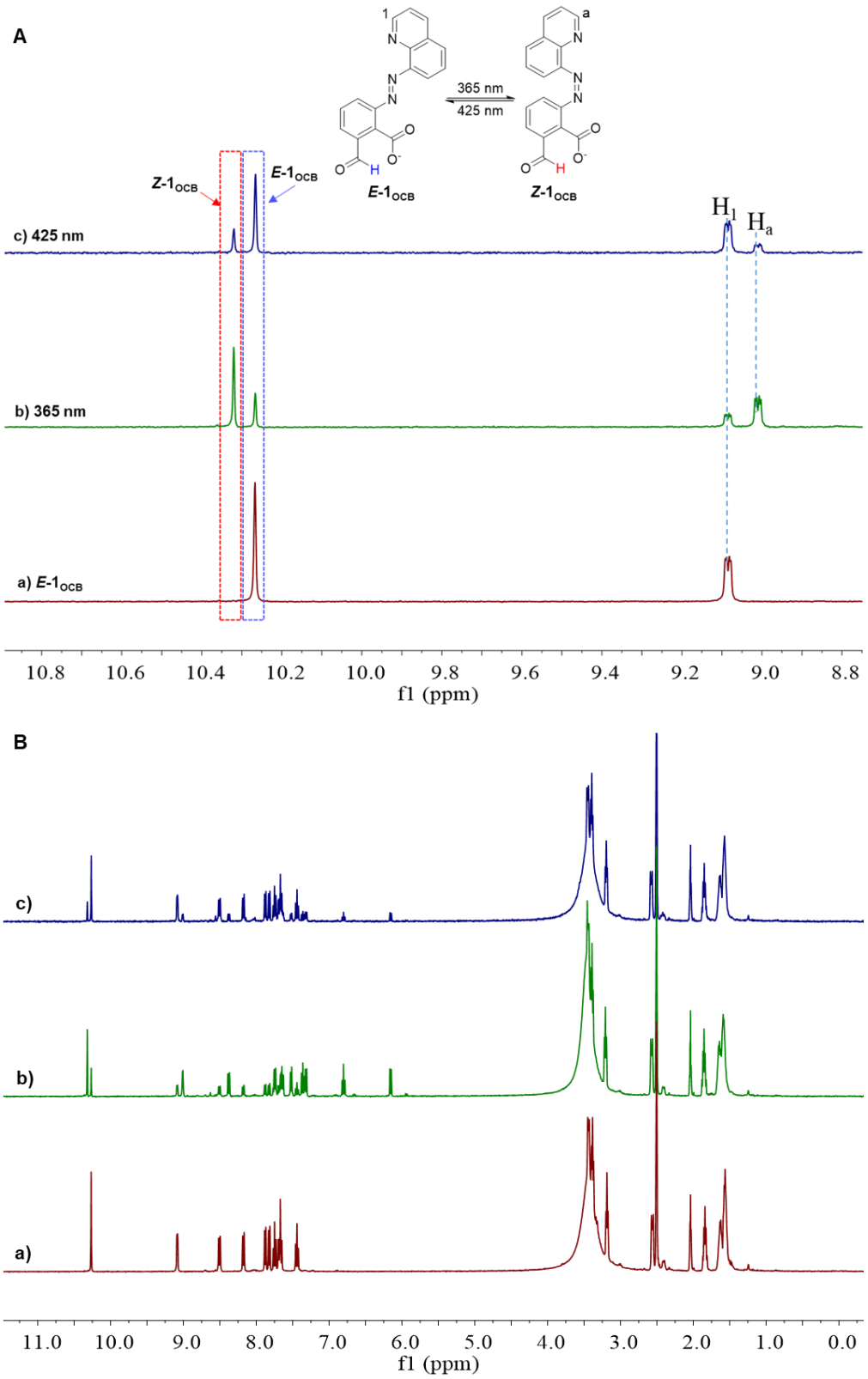

Figure S37. (A) (a) ^{1}H NMR spectrum of *E*-**1**$_{OCB}$ in DMSO-d_6 (10 mM); (b) after irradiation for 1.5 h with 365 nm light (69% *Z*); (c) further irradiation for 0.5 h with 425 nm light (24% *Z*). (B) The full ^{1}H NMR spectra of panel A.

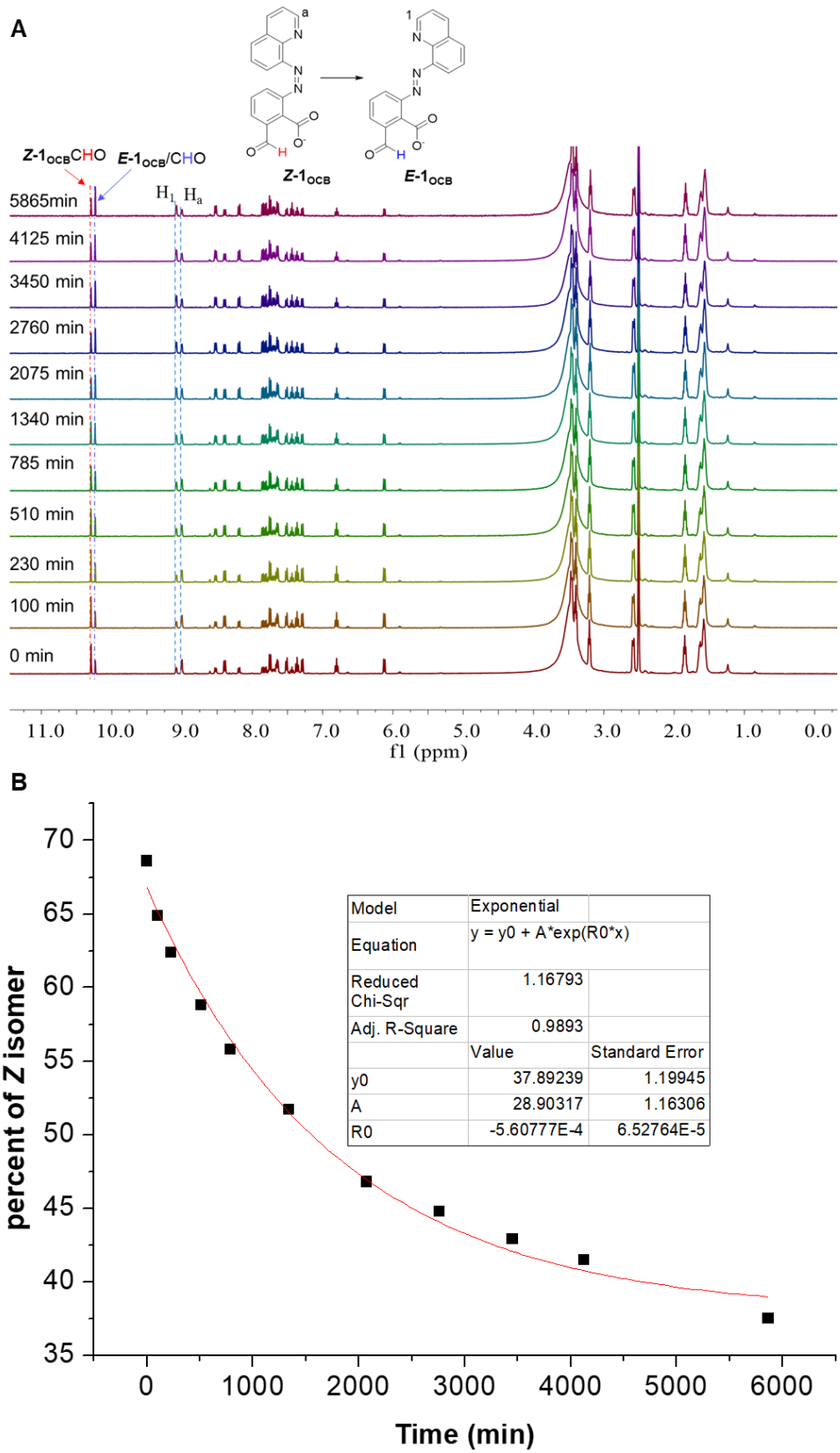

Figure S38. Changes in ^{1}H NMR spectrum (A) as well as thermal isomerization kinetic curve (B) after the irradiation of *E*-**1**$_{OCB}$ in DMSO-d_6 (10 mM) for 1.5 h at 365 nm (0 min in A) and then waiting in the dark (25 ºC) at varied time. The half-life of *Z*-**1**$_{OCB}$ was determined to 20.6 h at 25 ºC.

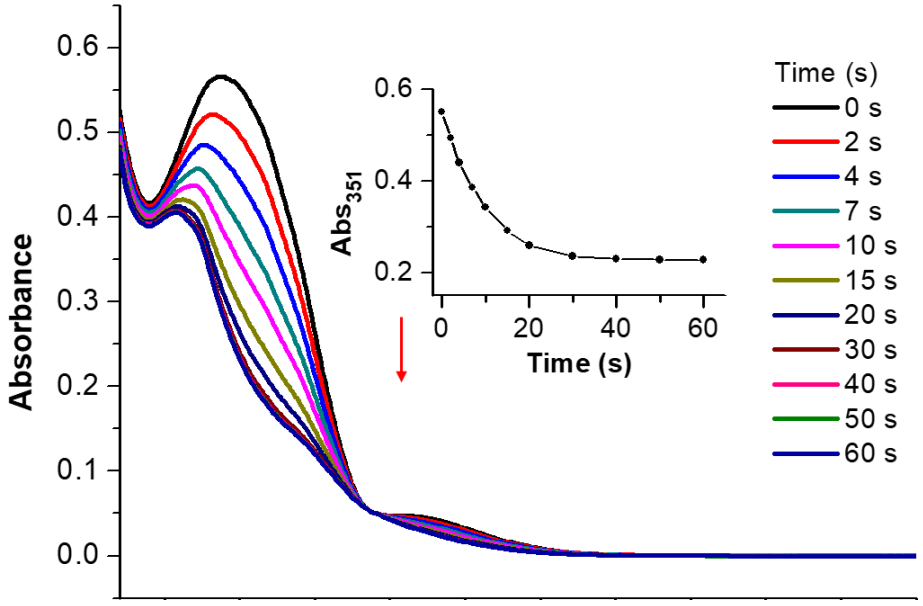

Figure S39. Photoisomerization of *E*-**1**$_{OCB}$ to give *Z*-**1**$_{OCB}$: changes in absorption spectra upon irradiation of *E*-**1**$_{OCB}$ (50 μM in DMSO) with 365 nm light. Inset: the photoisomerization kinetic curve of *E*-**1**$_{OCB}$, via monitoring the absorbance at 351 nm.

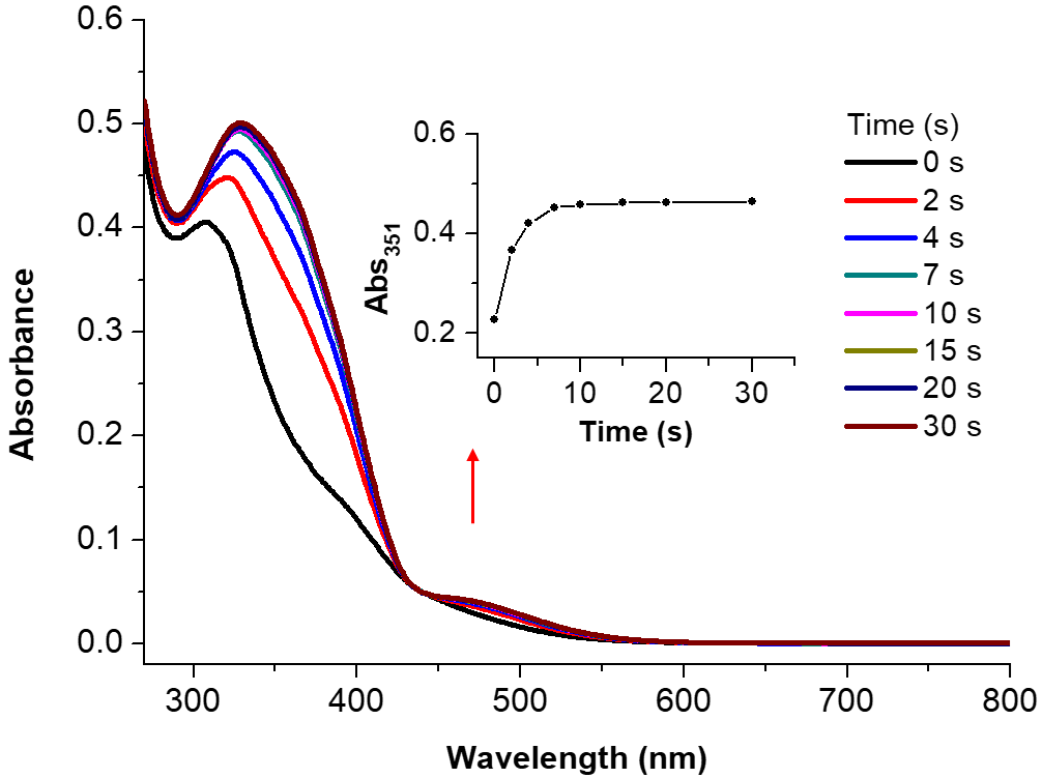

Figure S40. Photoisomerization of *Z*-**1**$_{OCB}$ (created through irradiation of *E*-**1**$_{OCB}$ at 365 nm) to give *E*-**1**$_{OCB}$: changes in absorption spectra upon irradiation of *Z*-**1**$_{OCB}$ (50 μM in DMSO) with 425 nm light. Inset: the photoisomerization kinetic curve of *Z*-**1**$_{OCB}$, via monitoring the absorbance at 351 nm.

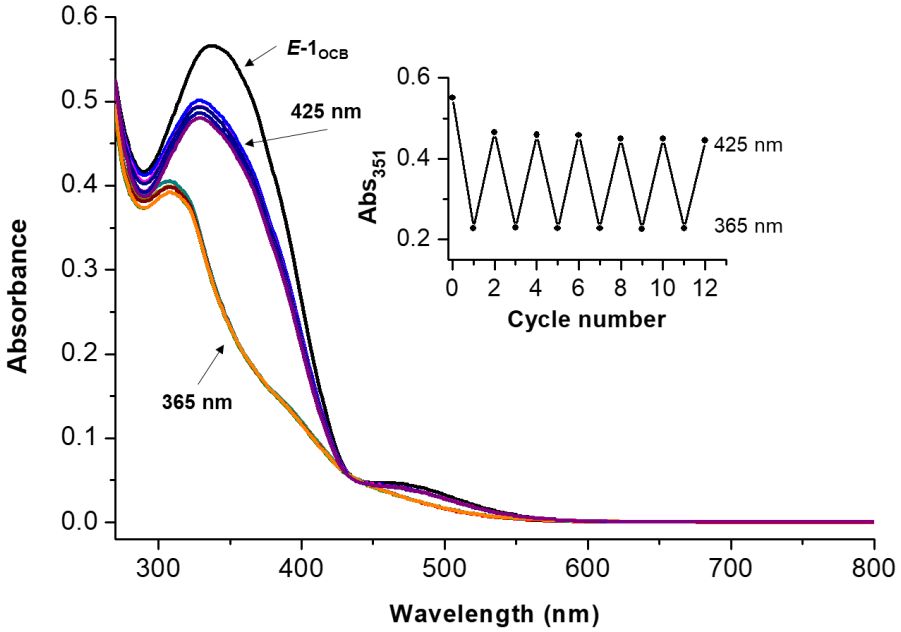

Figure S41. UV-vis spectra of *E*-**1**$_{OCB}$ (50 μM) in DMSO after alternative irradiation at 365 and 425 nm. The inset shows the multiple cycles of photoswitching in response to 365 and 425 nm light.

5. Coordination Effects

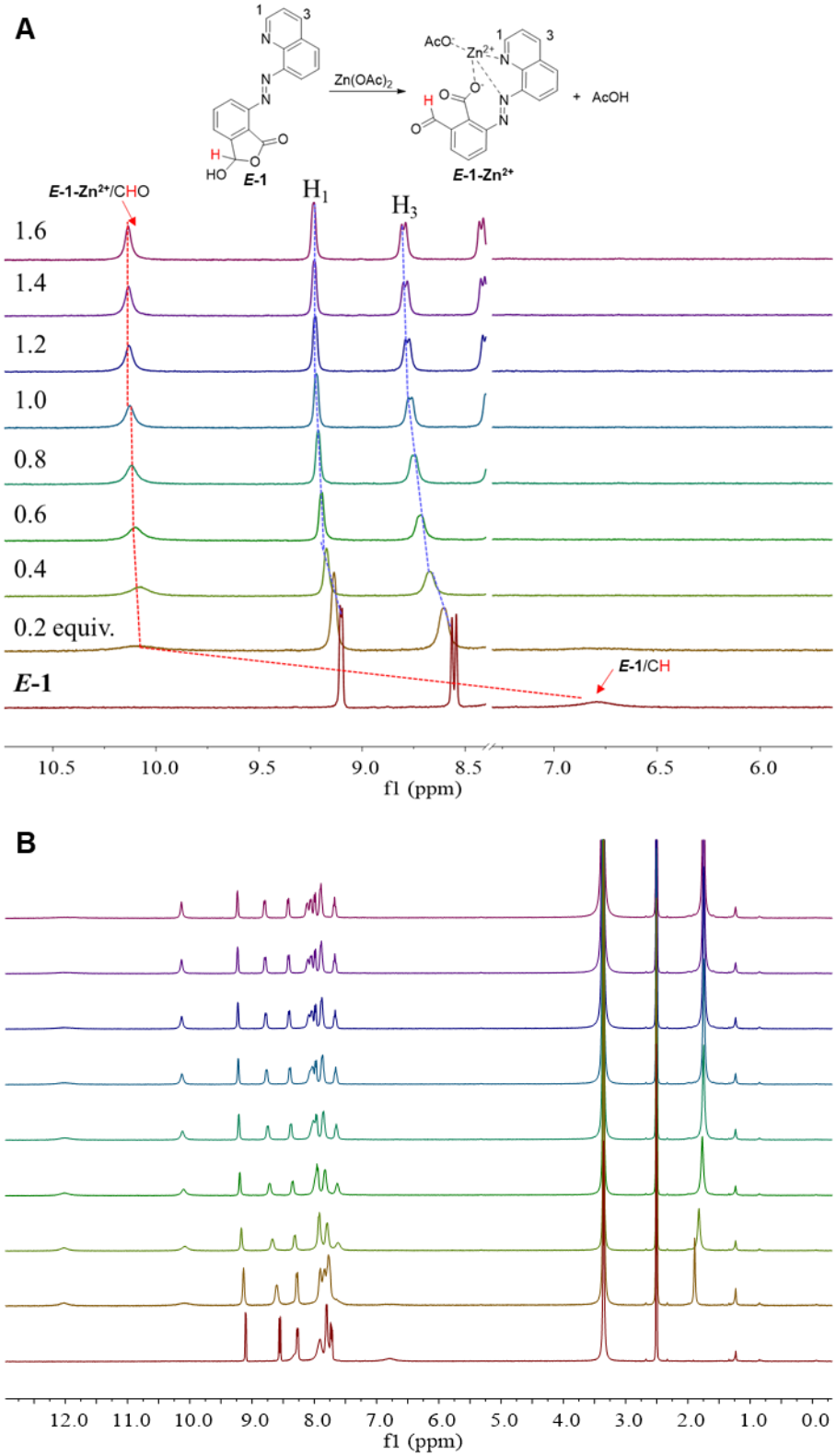

Figure S42. (A) Changes in ^{1}H NMR spectrum upon titration of *E*-**1** with $Zn(OAc)_2 \cdot 2H_2O$ in DMSO-d_6 (10 mM). (B) The full ^{1}H NMR spectra of panel A. The titration result indicated that the stoichiometry of the complexation is 1:1.

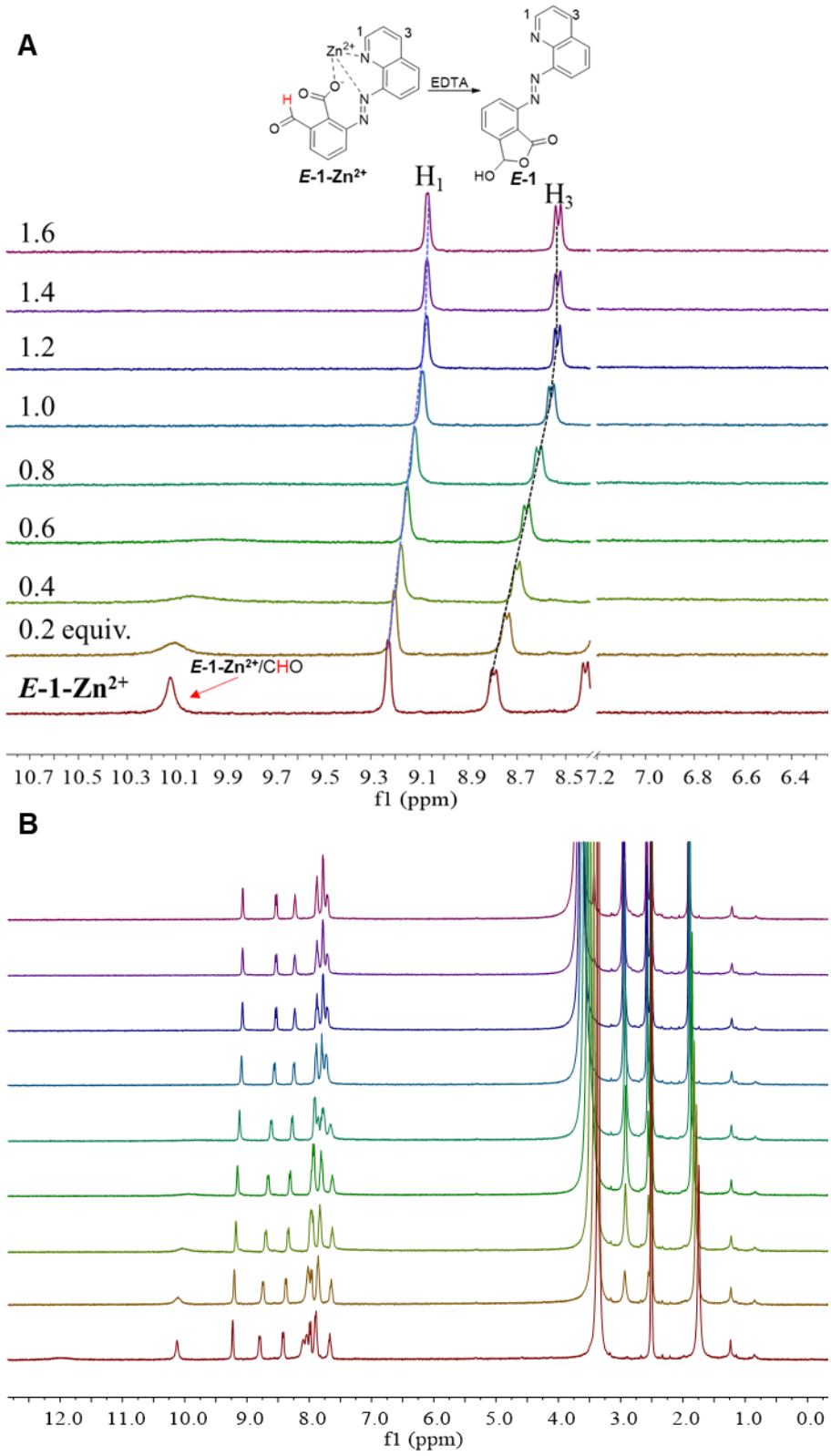

Figure S43. (A) Changes in ^{1}H NMR spectrum upon titration of *E*-**1**-Zn^{2+} with EDTA in DMSO-d_6 (10 mM). (B) The full ^{1}H NMR spectra of panel A. The titration result indicated that EDTA can chelate with Zn^{2+} in *E*-**1**-Zn^{2+} to give *E*-**1**. Both -CHO and -CH peaks in ^{1}H NMR spectrum were not observed, likely due to the fast conversion of ring-chain equilibrium.

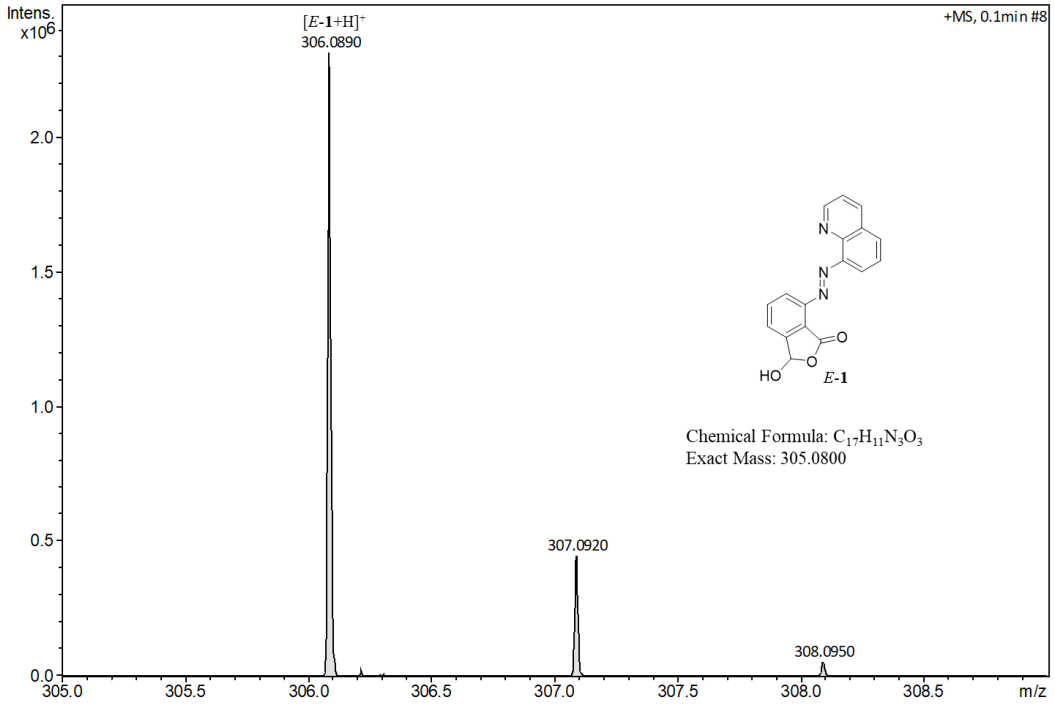

Figure S44. ESI mass spectrum of the mixture of *E*-**1**-Zn^{2+} and EDTA (1.0 equiv.) in DMSO-d_6 (10 mM). Mass spectrum further validated that *E*-**1** was created after addition of EDTA.

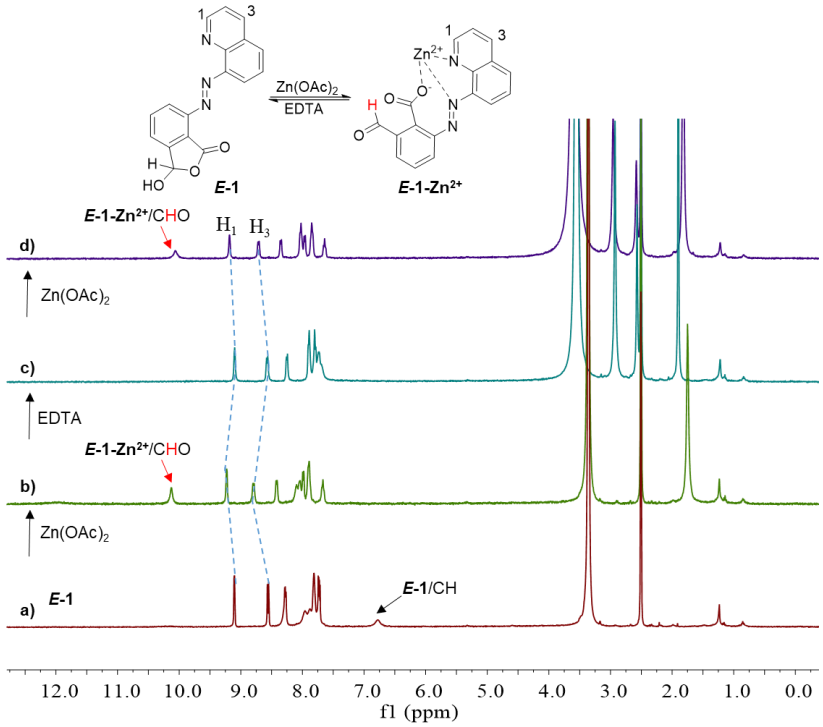

Figure S45. Control over the ring-chain tautomerization with $Zn(OAc)_2$/EDTA. (a) ^1H NMR spectrum of *E*-**1** in DMSO-d_6 (10 mM); (b) its mixture with $Zn(OAc)_2 \cdot 2H_2O$ (1.0 equiv.); (c) the addition of EDTA (1.0 equiv.); (d) further addition of $Zn(OAc)_2 \cdot 2H_2O$ (1.0 equiv.).

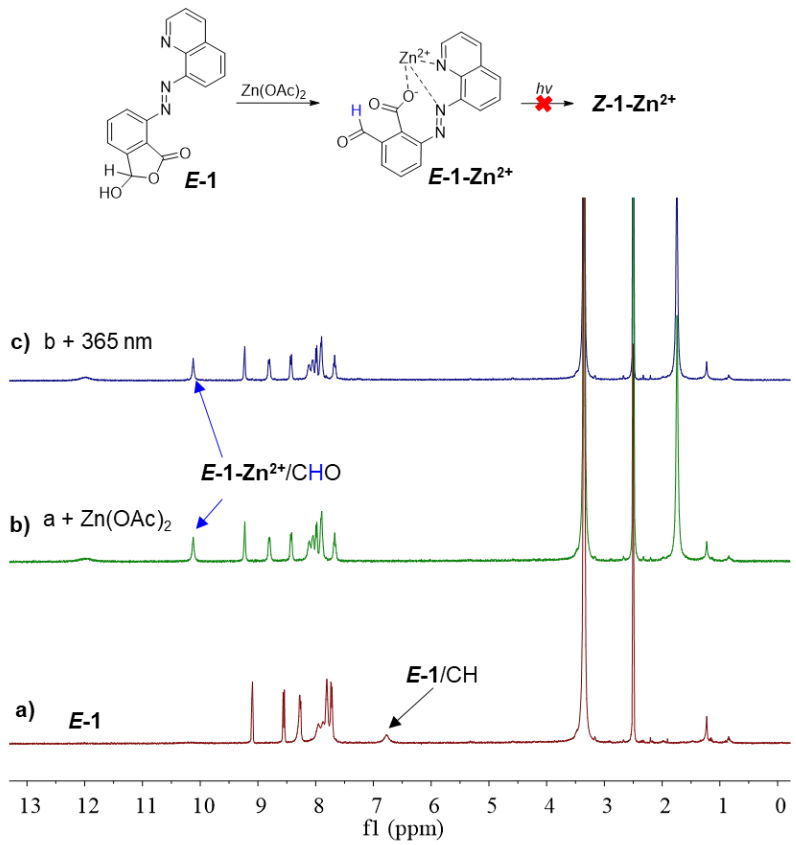

Figure S46. (a) ^{1}H NMR spectrum of *E*-**1** in DMSO-d_6 (10 mM); (b) its mixture with $Zn(OAc)_2 \cdot 2H_2O$ (1.5 equiv.); (c) after irradiation for 1.5 h at 365 nm. Photoisomerization of *E*-**1**-Zn^{2+} was not found.

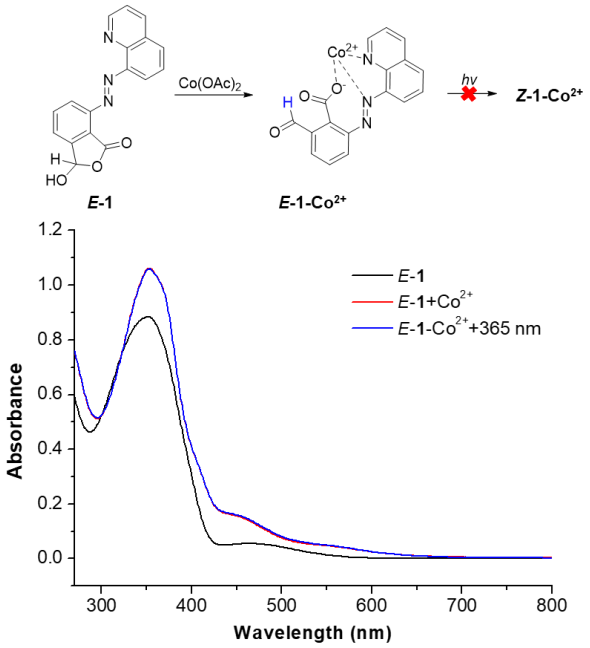

Figure S47. Changes in absorption spectra upon coordination of *E*-**1** with $Co(OAc)_2$ (1.5 equiv.) to give *E*-**1**-Co^{2+}, followed by irradiation for 1 min at 365 nm. Photoisomerization of *E*-**1**-Co^{2+} was not found.

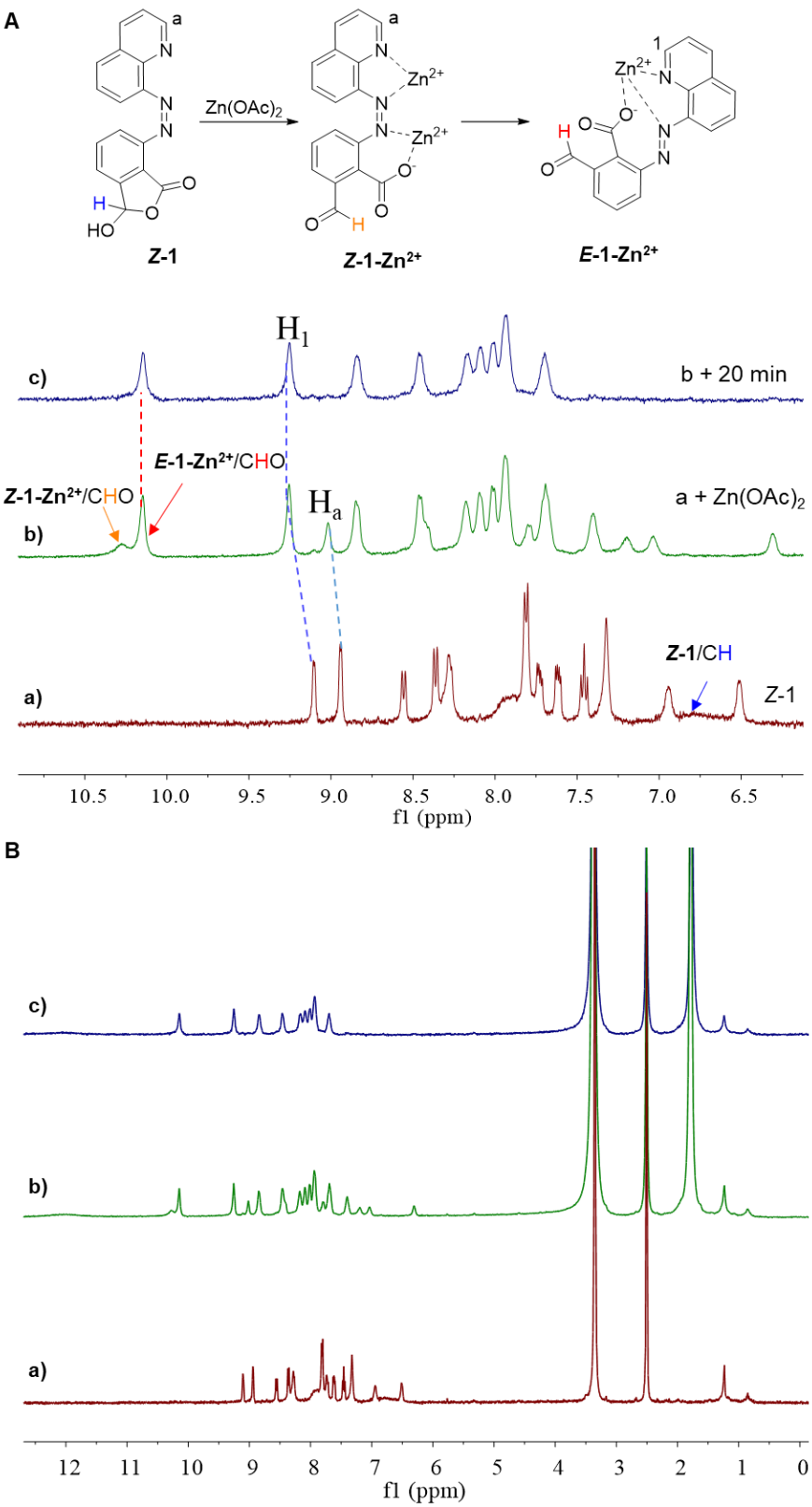

Figure S48. (A) (a) ^{1}H NMR spectrum of *Z*-enriched solution of **1** by irradiation of *E*-**1** for 1.5 h at 365 nm in DMSO-d_6 (10 mM); (b) its mixture with $Zn(OAc)_2 \cdot 2H_2O$ (2.5 equiv.); (c) after 20 min. (B) The full ^{1}H NMR spectra of panel A. *Z*-**1**-Zn^{2+} appeared and then converted to *E*-**1**-Zn^{2+} after 20 min.

6. Dynamic Covalent Chemistry

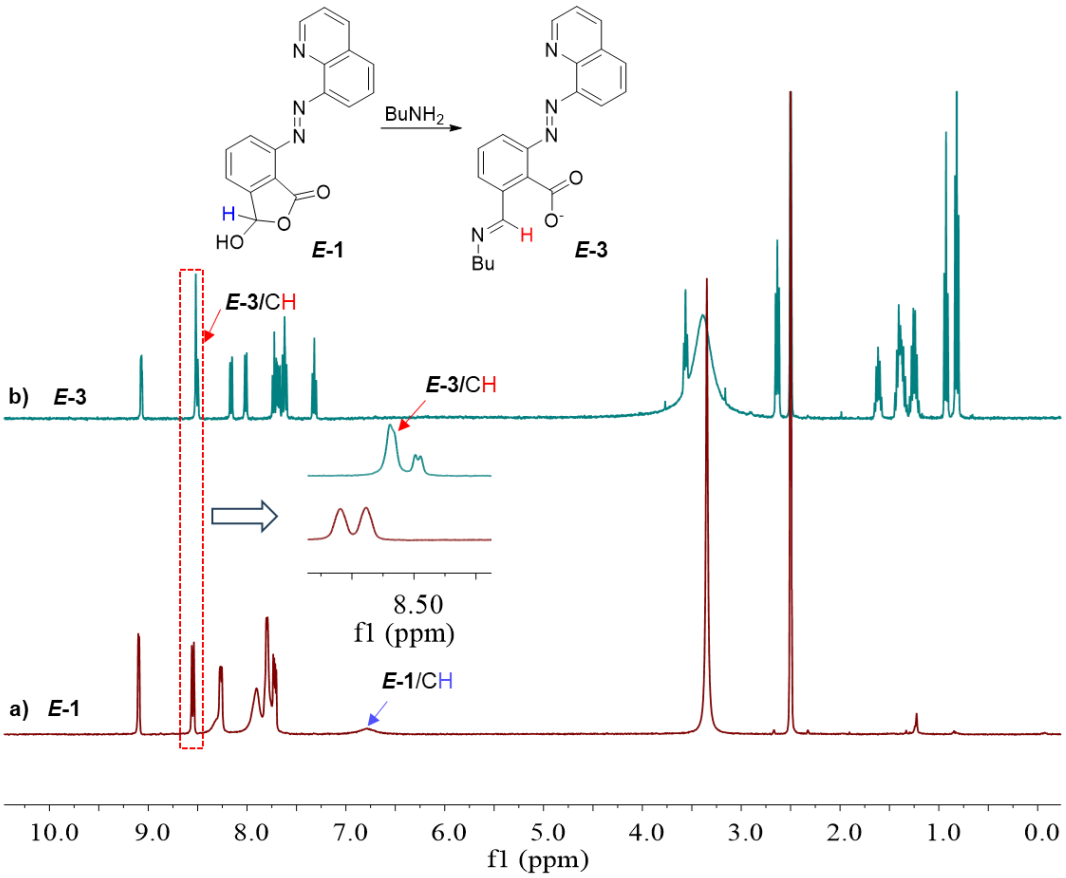

Figure S49. (a) ^{1}H NMR spectrum of *E*-**1** in DMSO-d_6 (10 mM); (b) its reaction with 1-butylamine (3 equiv.) after 15 min. The reaction *E*-**1** with amine afforded *E*-**3** quantitatively.

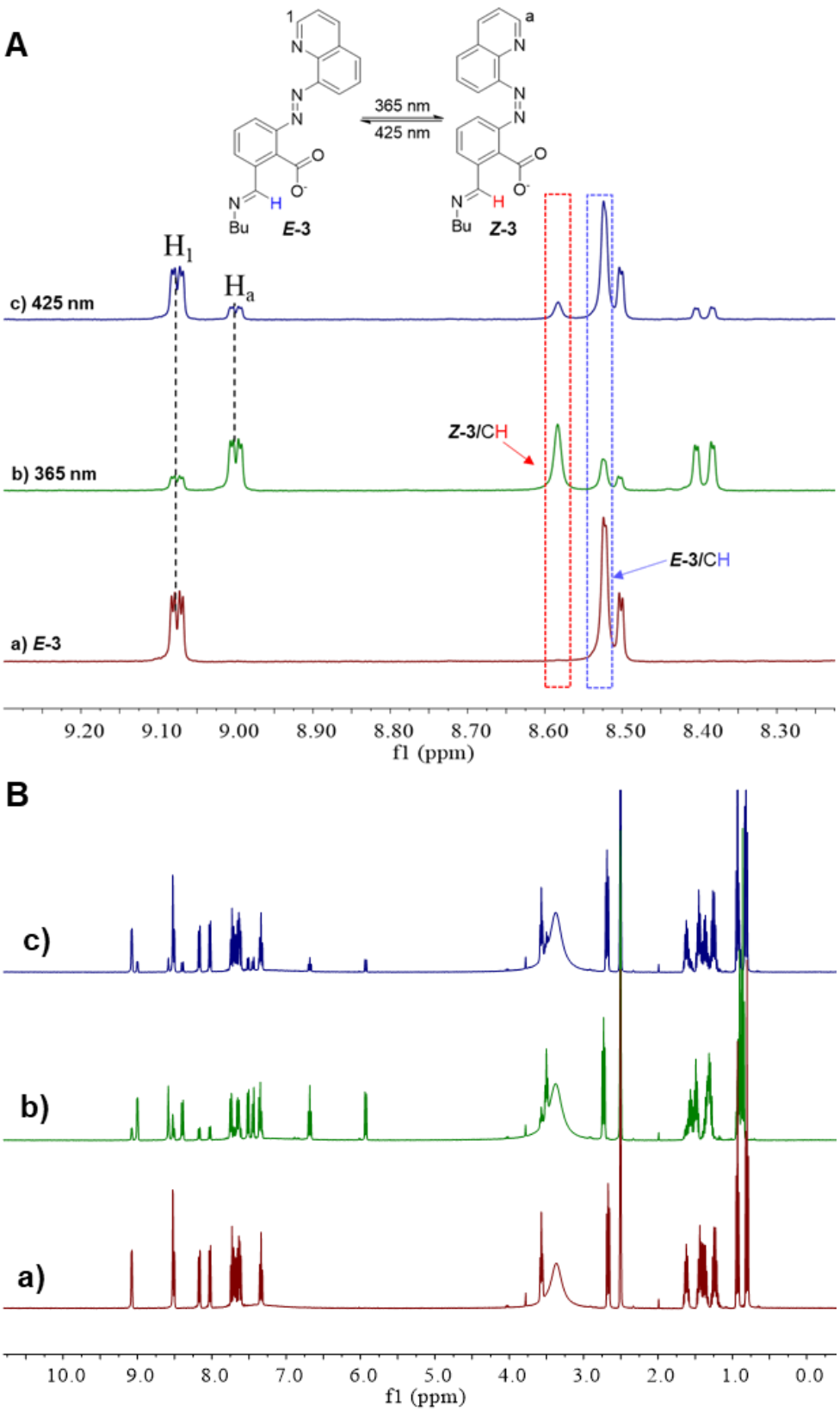

Figure S50. (A) (a) ^{1}H NMR spectrum of *E*-**3** in DMSO-d_6 (10 mM); (b) after irradiation for 1.5 h with 365 nm light (78% *Z*); (c) further irradiation for 0.5 h with 425 nm light (19% *Z*). (B) The full ^{1}H NMR spectra of panel A.

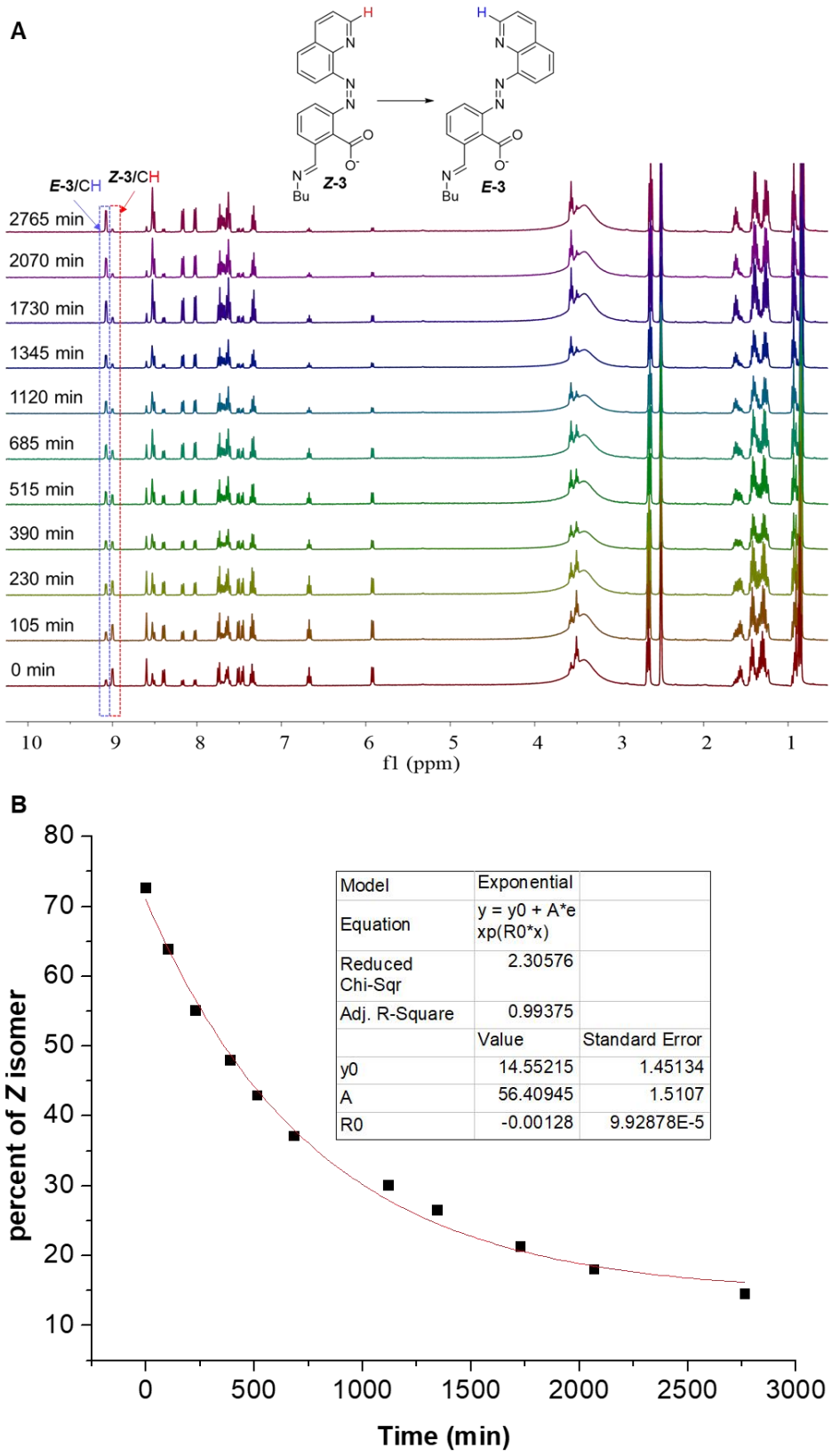

Figure S51. Changes in ^{1}H NMR spectrum (A) as well as thermal isomerization kinetic curve (B) after the irradiation of *E*-**3** in DMSO-d_6 (10 mM) for 1.5 h at 365 nm (0 min in A) and then waiting in the dark (25 ºC) at varied time. The half-life of *Z*-**3** was determined to be 9.0 h at 25 ºC.

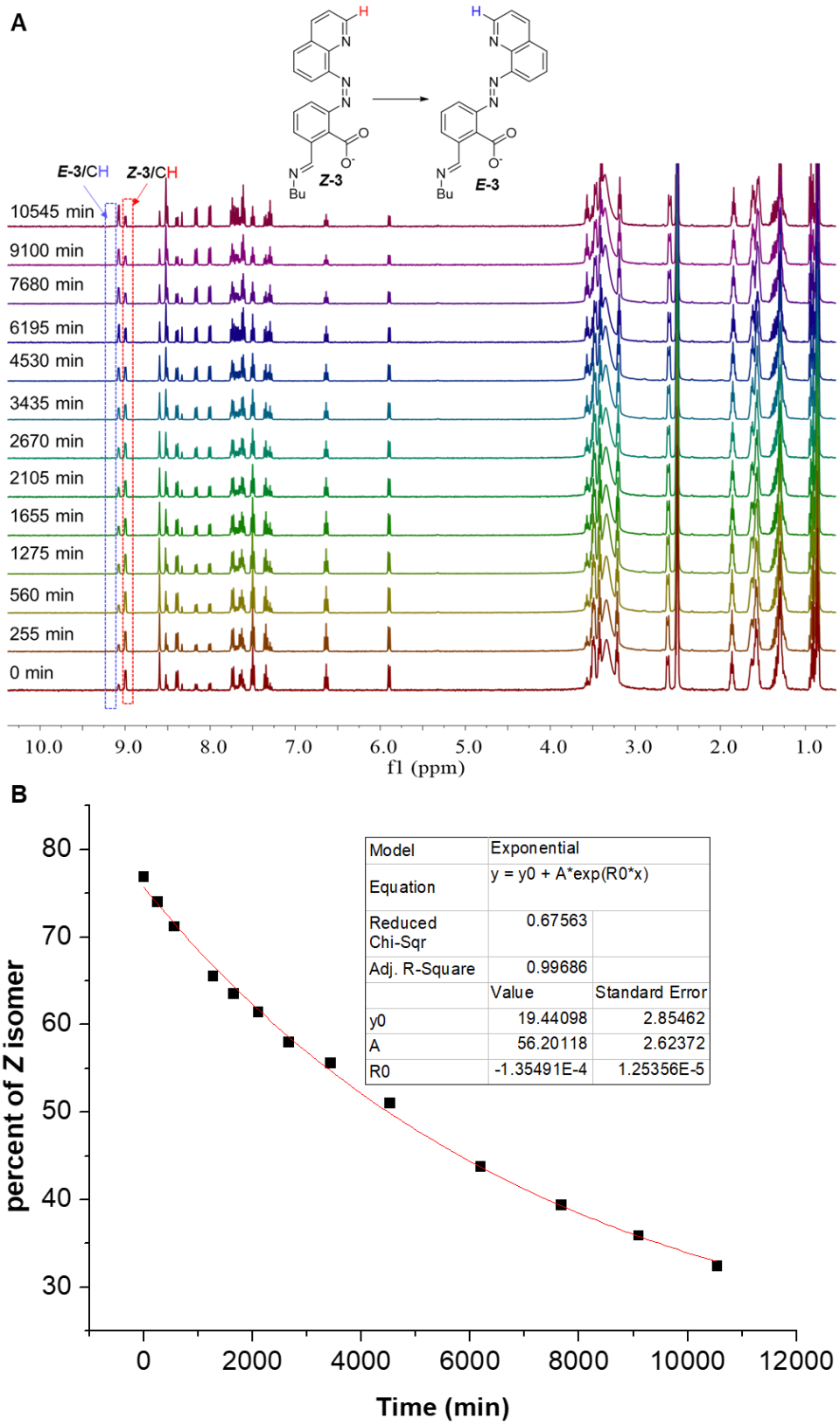

Figure S52. Changes in ^{1}H NMR spectrum (A) as well as thermal isomerization kinetic curve (B) after the irradiation of *E*-**3** (in the presence of 1 equiv. DBU) in DMSO-d_6 (10 mM) for 1.5 h at 365 nm (0 min in A) and then waiting in the dark (25 ºC) at varied time. The half-life of *Z*-**3** in the presence of DBU was determined to be 85.6 h at 25 ºC.

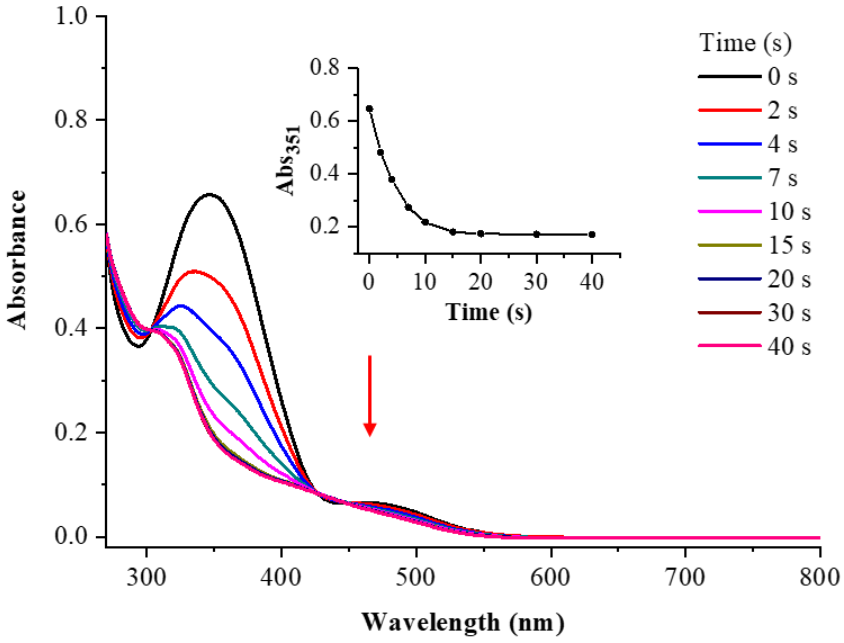

Figure S53. Photoisomerization of *E*-**3** to give *Z*-**3**: changes in absorption spectra upon irradiation of *E*-**3** (50 μM in DMSO) with 365 nm light. Inset: the photoisomerization kinetic curve of *E*-**3**, via monitoring the absorbance at 351 nm.

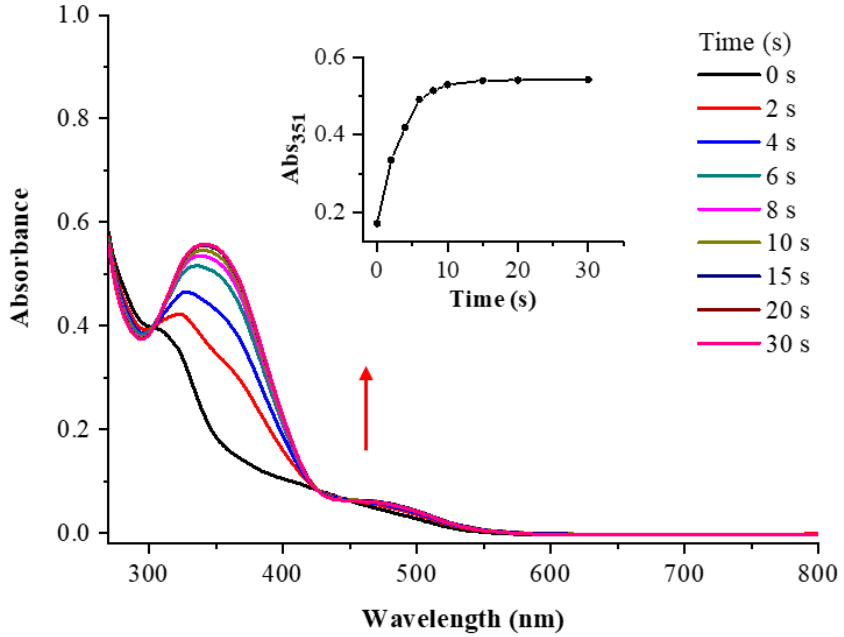

Figure S54. Photoisomerization of *Z*-**3** (created through irradiation of *E*-**3** at 365 nm) to give *E*-**3**: changes in absorption spectra upon irradiation of *Z*-**3** (50 μM in DMSO) with 425 nm light. Inset: the photoisomerization kinetic curve of *Z*-**3**, via monitoring the absorbance at 351 nm.

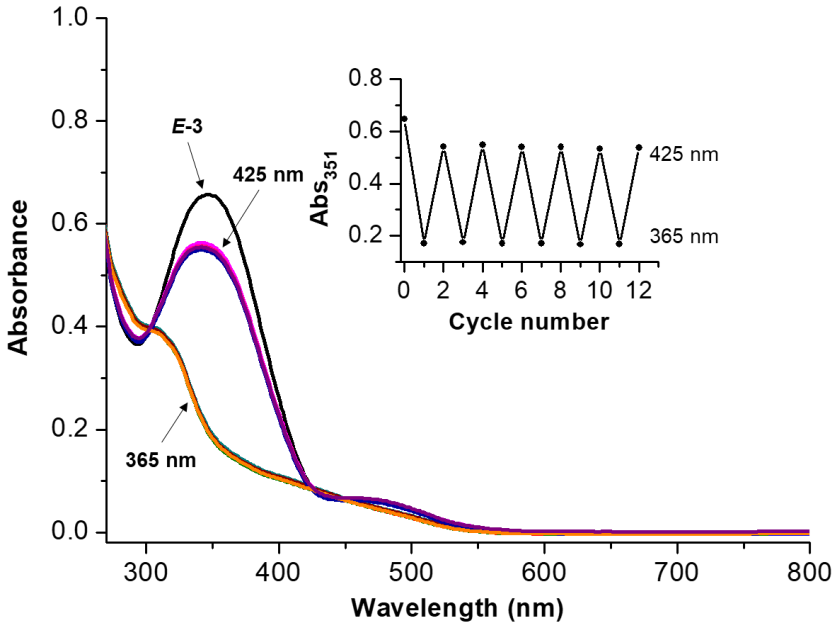

Figure S55. UV-vis spectra of *E*-**3** (50 μM) after alternative irradiation at 365 and 425 nm. The inset shows the multiple cycles of photoswitching in response to 365 and 425 nm light.

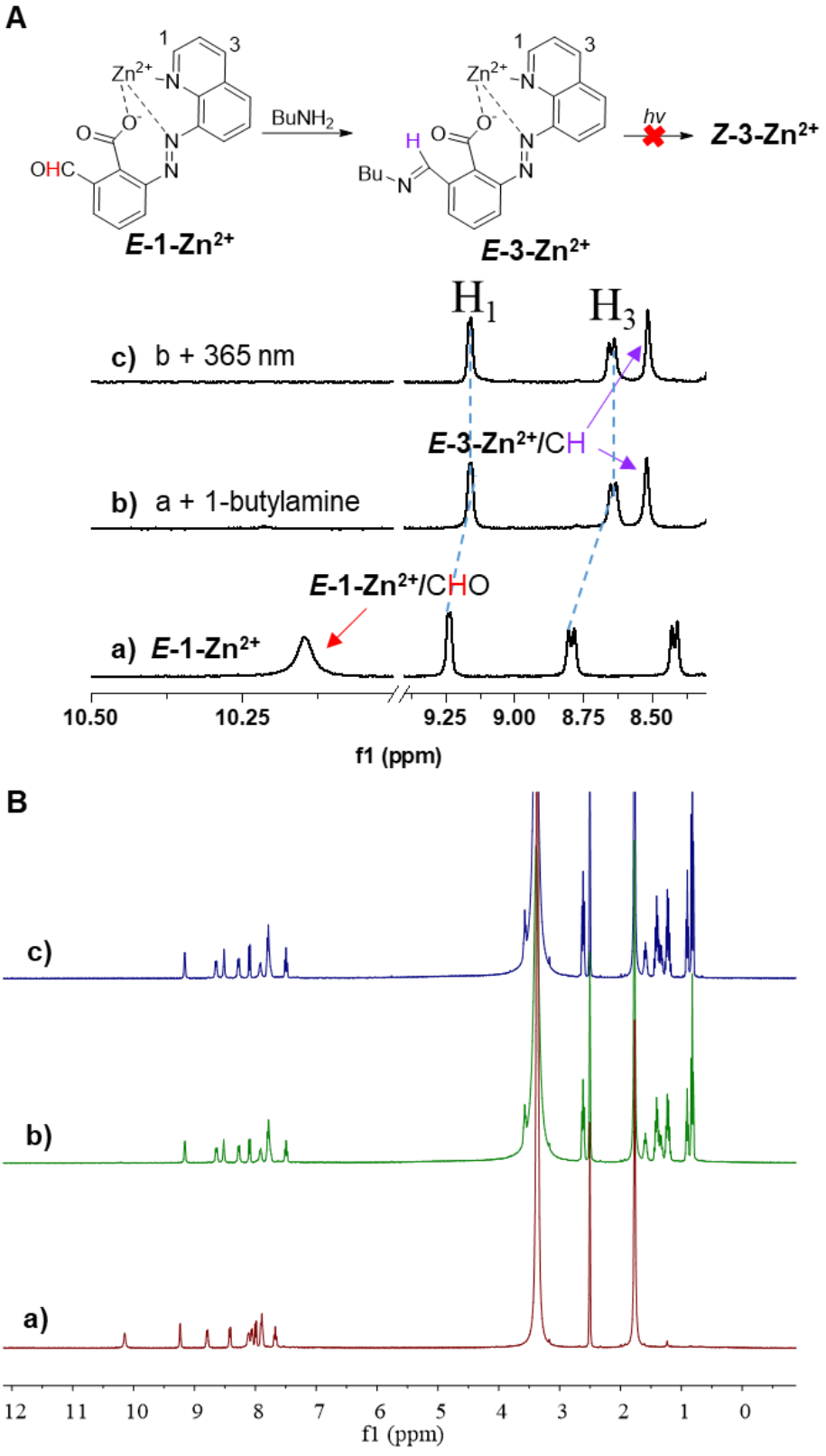

Figure S56. (A) (a) ^{1}H NMR spectrum of *E*-**1**-Zn^{2+} in DMSO-d_6 (10 mM); (b) its reaction with 1-butylamine (3 equiv.) after 15 min; (c) after irradiation for 1.5 h at 365 nm. (B) The full ^{1}H NMR spectra of panel A. Photoisomerization of *E*-**3**-Zn^{2+} was not observed.

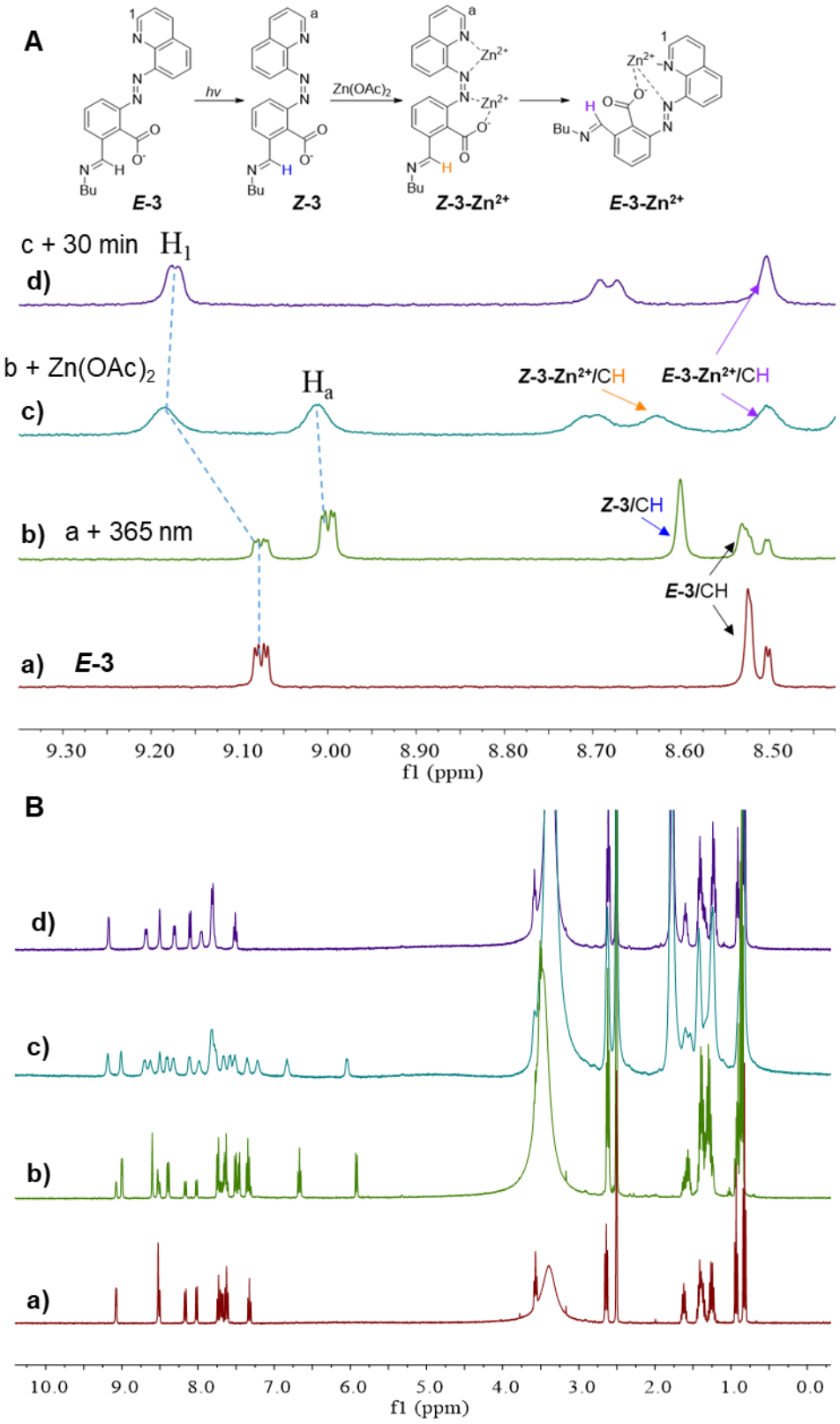

Figure S57. (A) (a) ^{1}H NMR spectrum of *E*-**3** in DMSO-d_6 (10 mM); (b) after irradiation for 1.5 h at 365 nm; (c) its mixture with $Zn(OAc)_2 \cdot 2H_2O$ (2.5 equiv.); (d) after 30 min in the dark. (B) The full ^{1}H NMR spectra of panel A. *Z*-**3**-Zn^{2+} appeared and then converted to *E*-**3**-Zn^{2+} after 30 min.

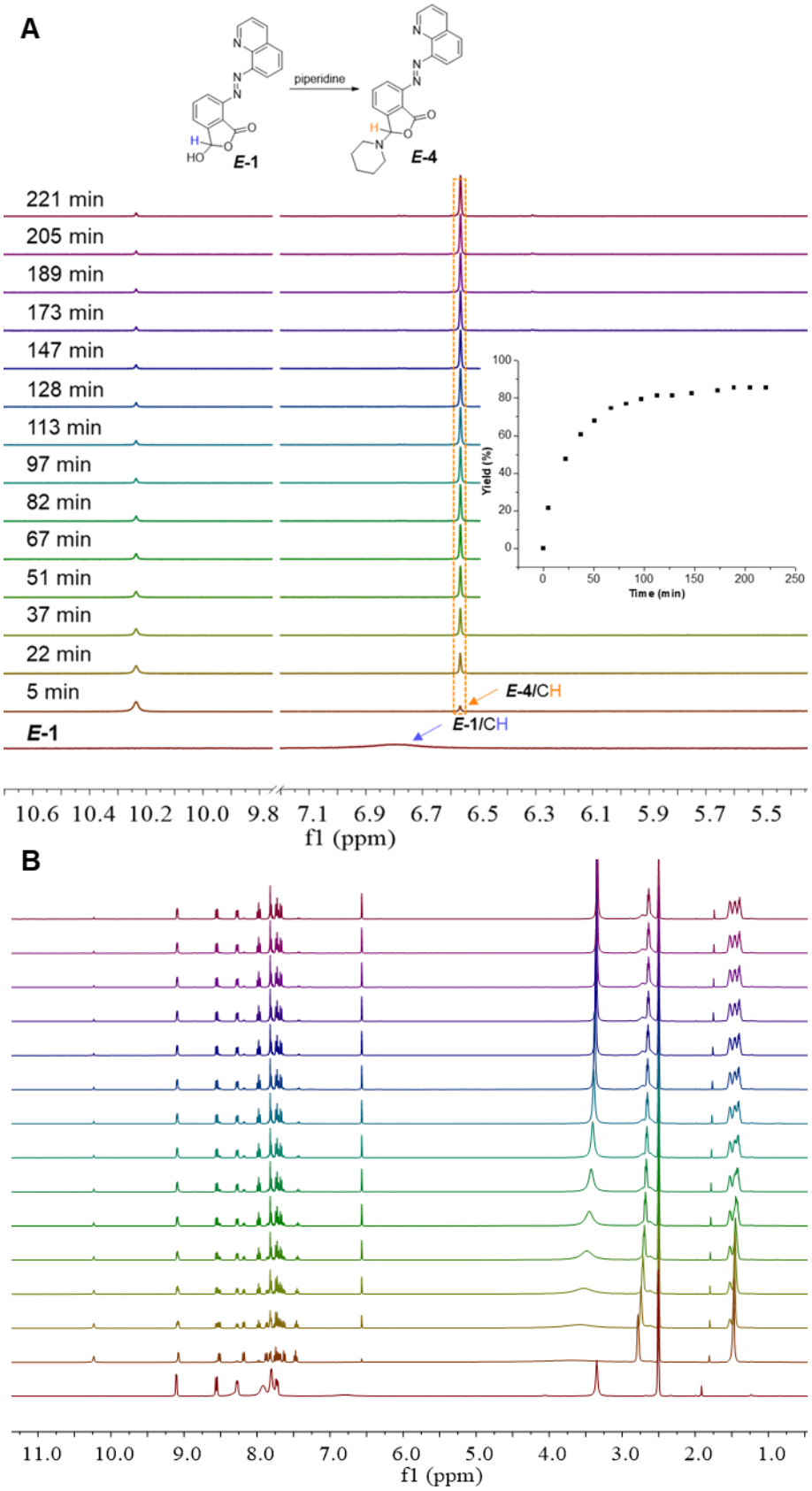

Figure S58. (A) Changes in ^{1}H NMR spectrum of *E*-**1** upon the reaction with piperidine (1.5 equiv.) in DMSO-d_6 (10 mM). The inset shows the kinetic curve of the reaction. (B) The full ^{1}H NMR spectra of panel A. The yield of *E*-**4** is 85%.

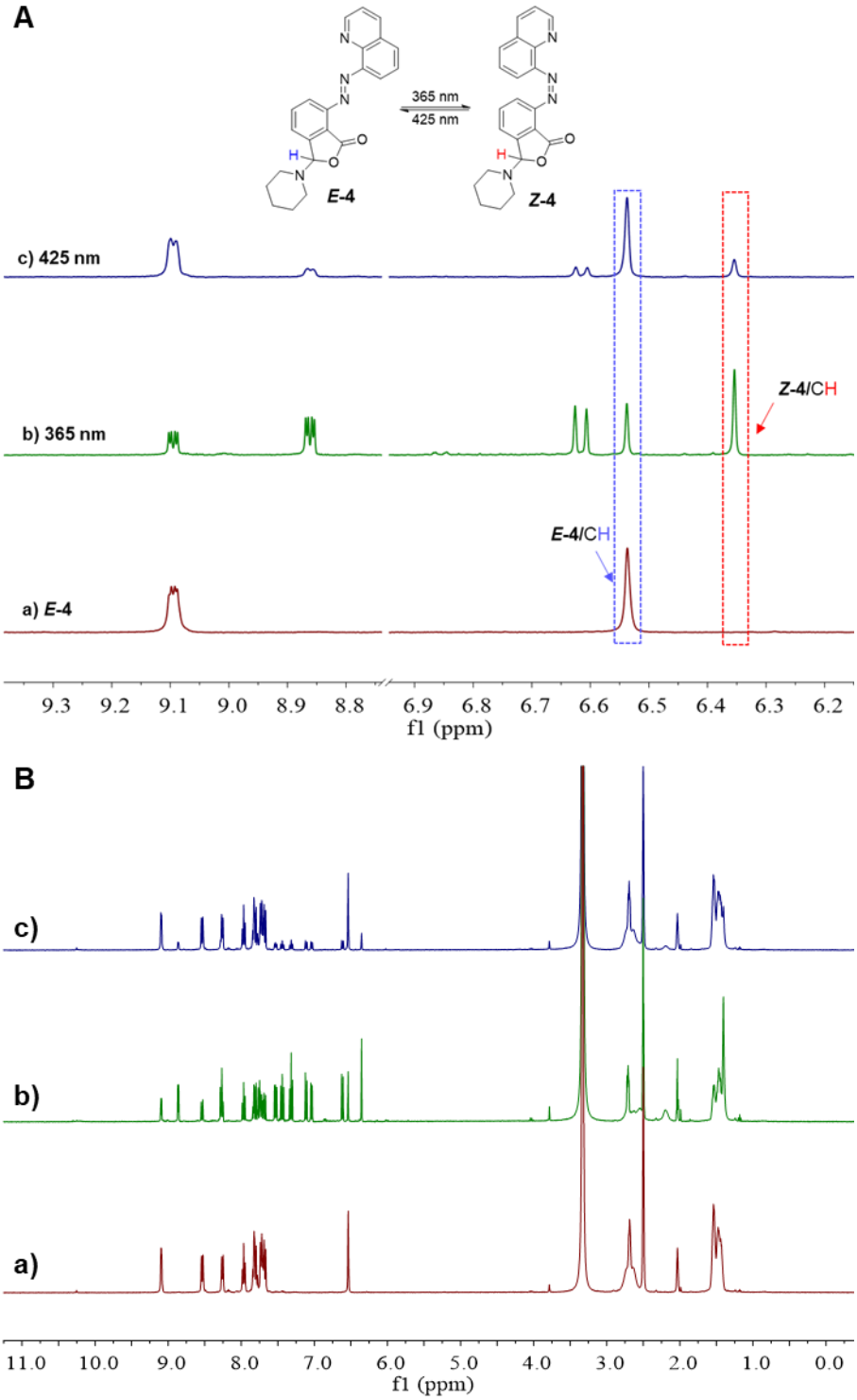

Figure S59. (A) (a) ^{1}H NMR spectrum of *E*-**4** in 5:1 DMSO-d_6:CD_3CN (10 mM); (b) after irradiation for 1.5 h with 365 nm light (60% *Z*); (c) further irradiation for 0.5 h with 425 nm light (20% *Z*). (B) The full ^{1}H NMR spectra of panel A.

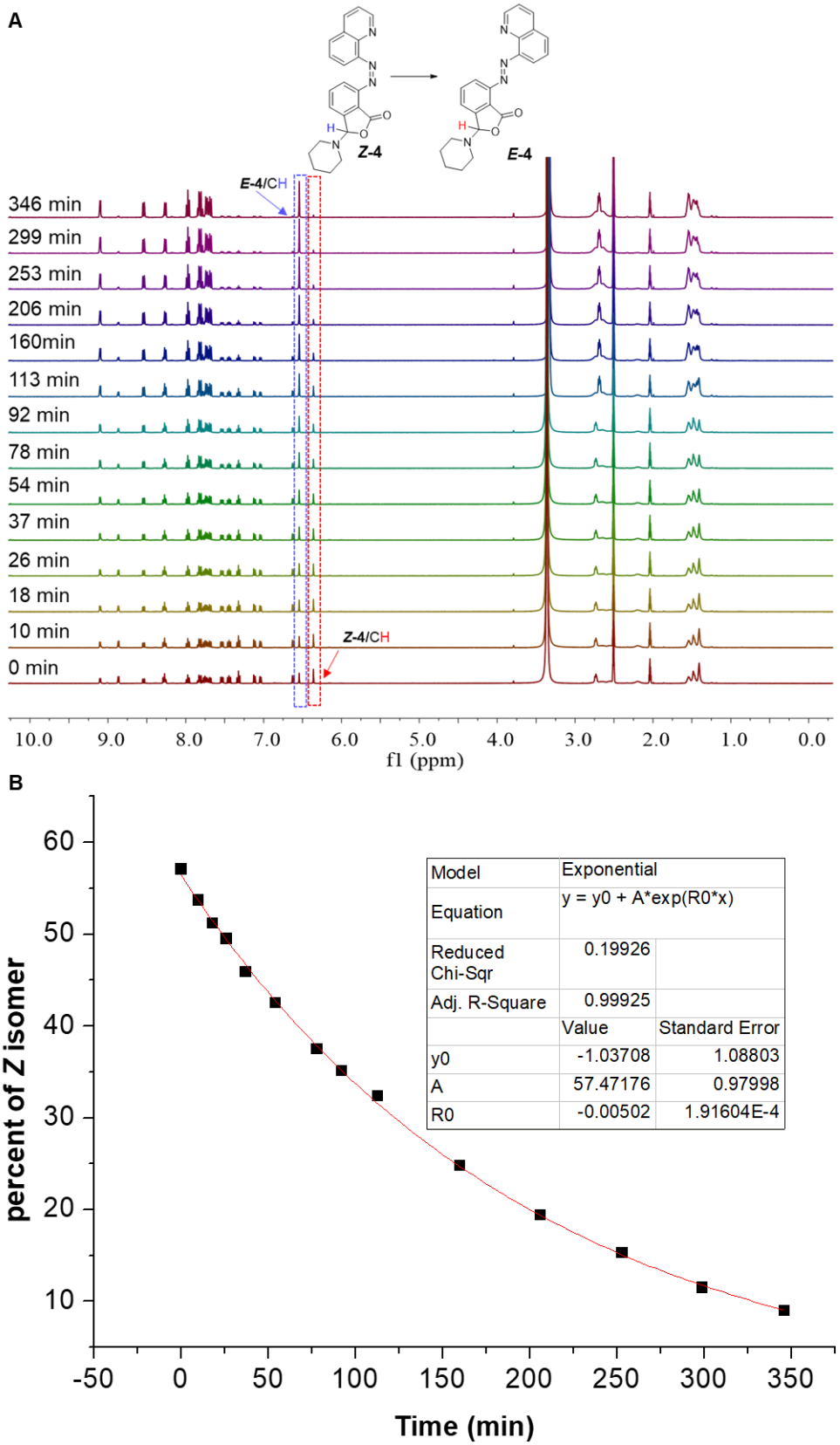

Figure S60. Changes in ^{1}H NMR spectrum (A) as well as thermal isomerization kinetic curve (B) after the irradiation of *E*-**4** in DMSO-d_6 (10 mM) for 1.5 h at 365 nm (0 min in A) and then waiting in the dark (25 ºC) at varied time. The half-life of *Z*-**4** was determined to be 2.3 h at 25 ºC.

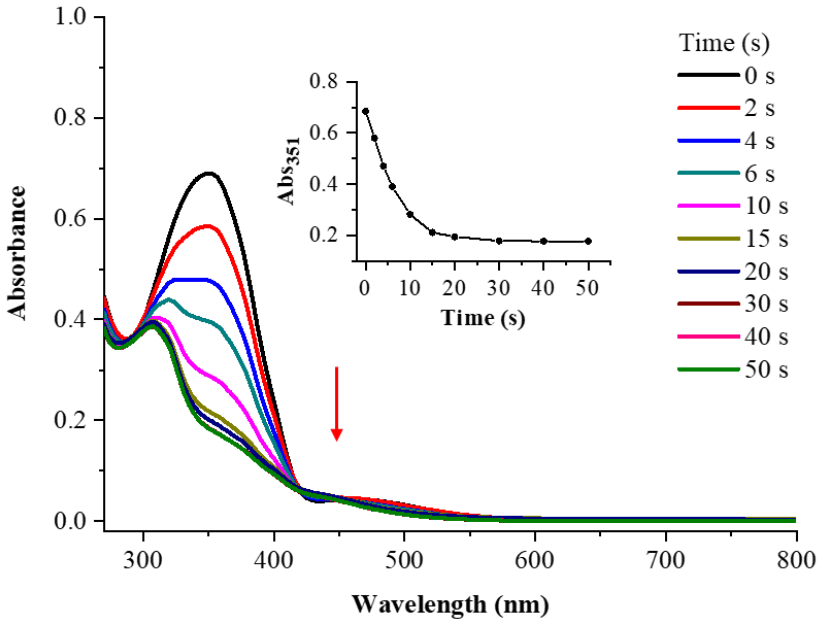

Figure S61. Photoisomerization of *E*-**4** to give *Z*-**4**: changes in absorption spectra upon irradiation of *E*-**4** (50 μM in DMSO) with 365 nm light. Inset: the photoisomerization kinetic curve of *E*-**4**, via monitoring the absorbance at 351 nm.

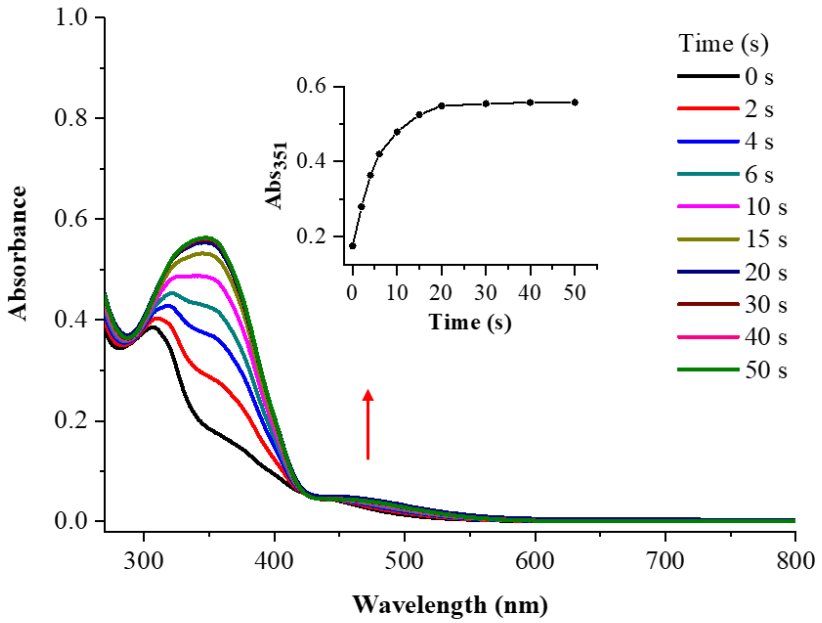

Figure S62. Photoisomerization of *Z*-**4** (created through irradiation of *E*-**4** at 365 nm) to give *E*-**4**: changes in absorption spectra upon irradiation of *Z*-**4** (50 μM in DMSO) with 425 nm light. Inset: the photoisomerization kinetic curve of *Z*-**4**, via monitoring the absorbance at 351 nm.

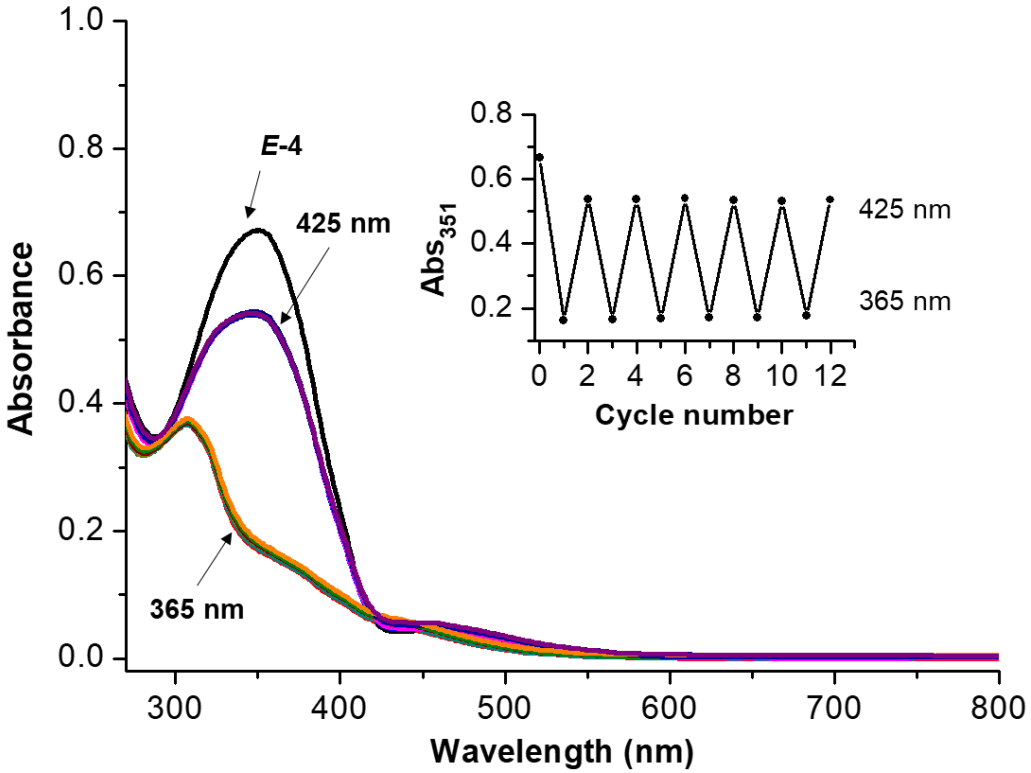

Figure S63. UV-vis spectra of *E*-**4** (50 μM) after alternative irradiation at 365 and 425 nm. The inset shows the multiple cycles of photoswitching in response to 365 and 425 nm light.

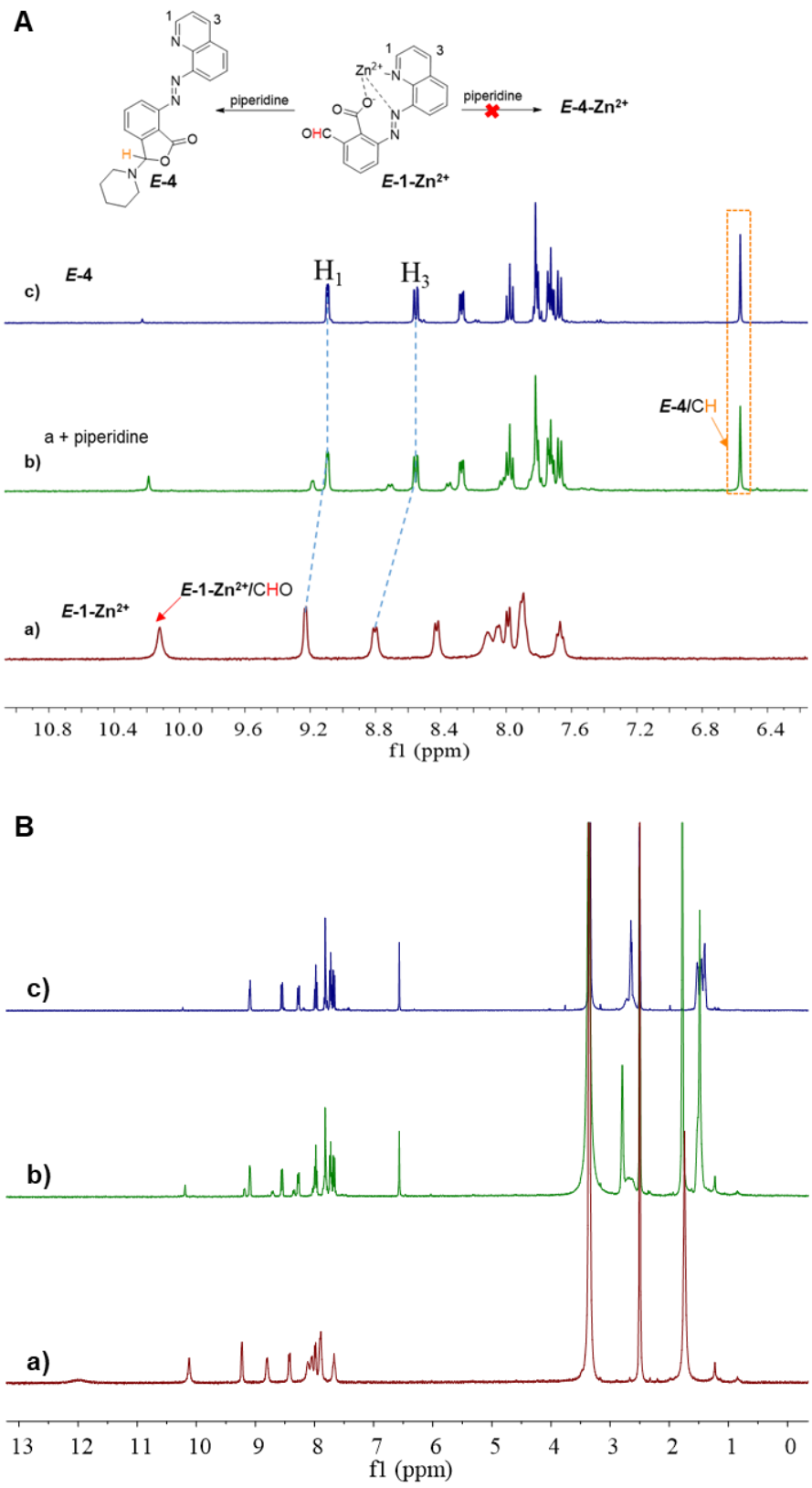

Figure S64. (A) (a) ^{1}H NMR spectrum of *E*-**1**-Zn^{2+} in DMSO-d_6 (10 mM); (b) its reaction with piperidine (1.5 equiv.); (c) ^{1}H NMR spectrum of *E*-**4** in DMSO-d_6 (10 mM) as control. (B) The full ^{1}H NMR spectra of panel A. The reaction of *E*-**1**-Zn^{2+} with piperidine afforded *E*-**4** in 75% yield.

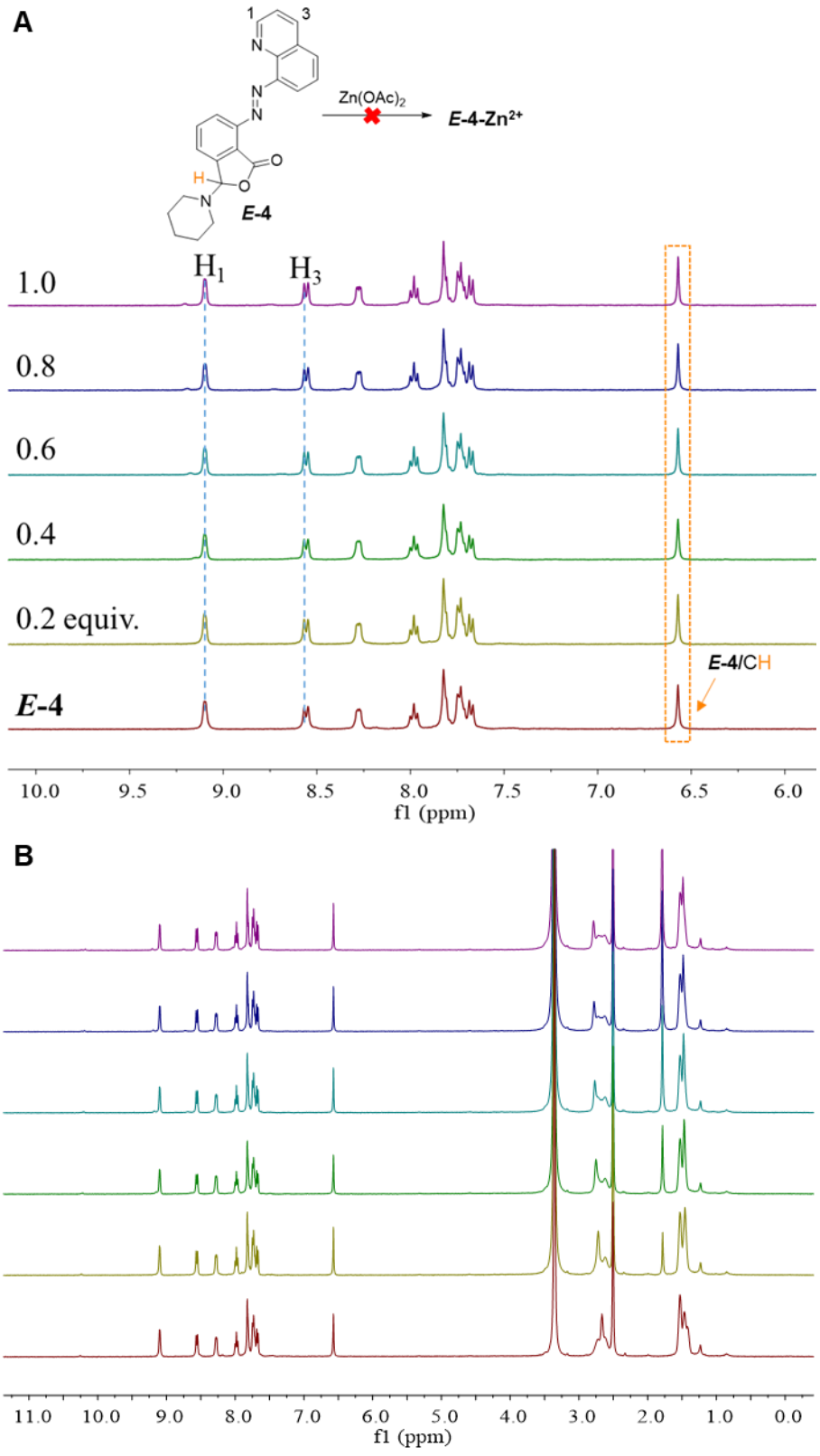

Figure S65. (A) Changes in ^{1}H NMR spectrum upon titration of *E*-**4** with $Zn(OAc)_2 \cdot 2H_2O$ in DMSO-d_6 (10 mM). (B) The full ^{1}H NMR spectra of panel A. The chelation of *E*-**4** with Zn^{2+} was not found.

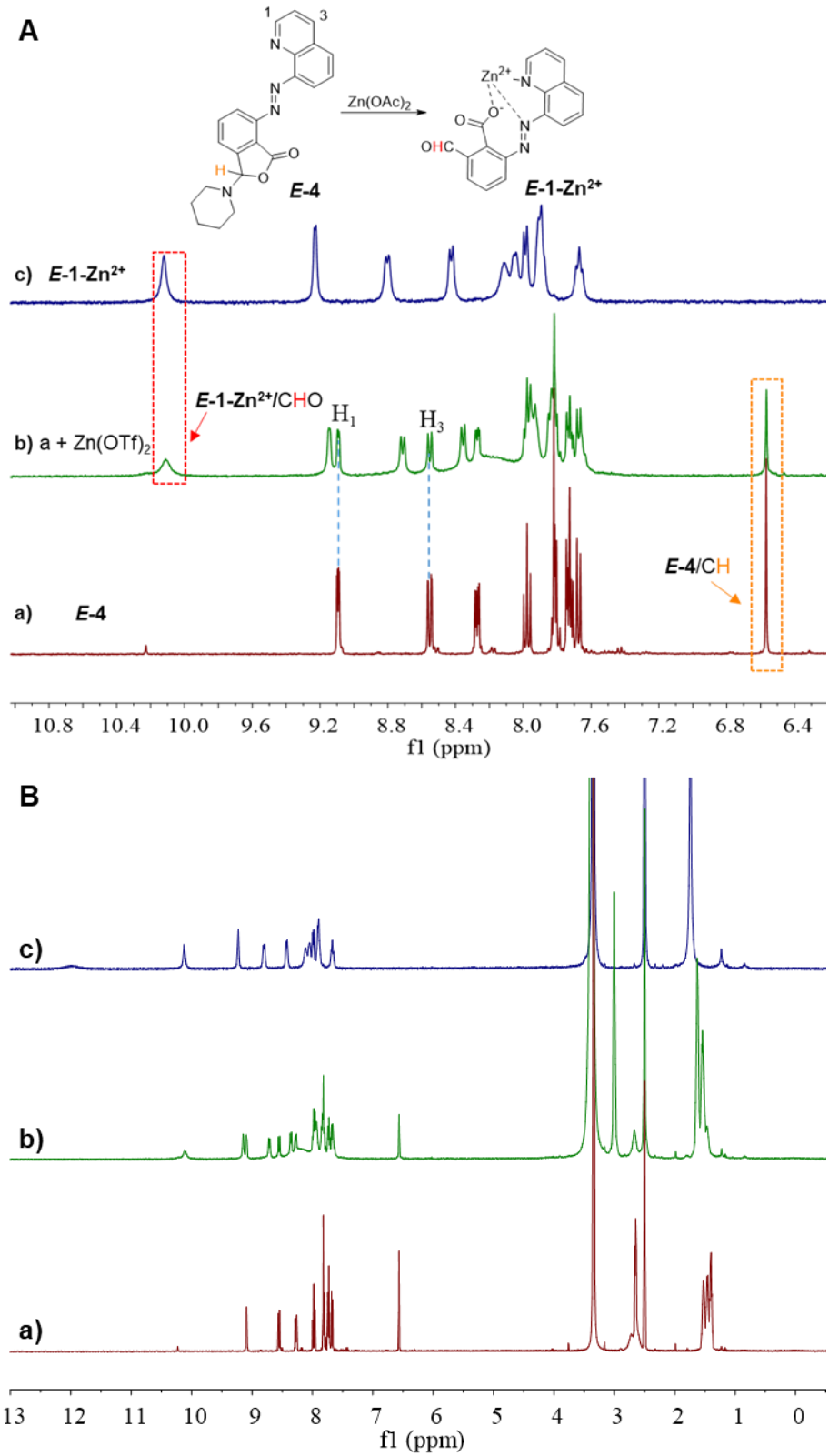

Figure S66. (a) ^{1}H NMR spectrum of *E*-**4** in DMSO-d_6 (10 mM); (b) its reaction with $Zn(OTf)_2$ (3.0 equiv.); (c) ^{1}H NMR spectrum of *E*-**1**-Zn^{2+} in DMSO-d_6 (10 mM) as control. (B) The full ^{1}H NMR spectra of panel A. The reaction of *E*-**4** with $Zn(OTf)_2$ afforded *E*-**1**-Zn^{2+} in 58% yield.

7. Photoisomerisation quantum yields

Determination of molar photon flux. Photon flux was calculated according to the literature method.[S3] 2 mL (V_1) of potassium ferrioxalate (30 mM in 0.1 M H_2SO_4) is irradiated with 365 nm LED strip light. An aliquot of the irradiated volume (V_2, 0.5 mL) together with buffer (1.2 M NaOAc + 0.36 M H_2SO_4, 1 mL), and phenanthroline (6 mM, 2 mL) is diluted to 20 mL (V_3) and left to react for 1 h. Whereafter, the absorbance of the tris-phenanthroline complex is recorded at 510 nm. This procedure is repeated using different irradiation times to create a plot of absorbance as a function of irradiation time, and the slope is used to calculate the molar photon flux (q_{in}) through Equation 1:

$$q_{in} = slope \frac{V_1 V_3}{V_2 \varepsilon_{510nm} \phi l} \quad (1)$$

Where ε_{510nm} is 11100 $M^{-1} \cdot cm^{-1}$, l is the path length of the cuvette, and ϕ is the photochemical quantum yield at the used irradiation wavelength (1.21 for 365 nm).

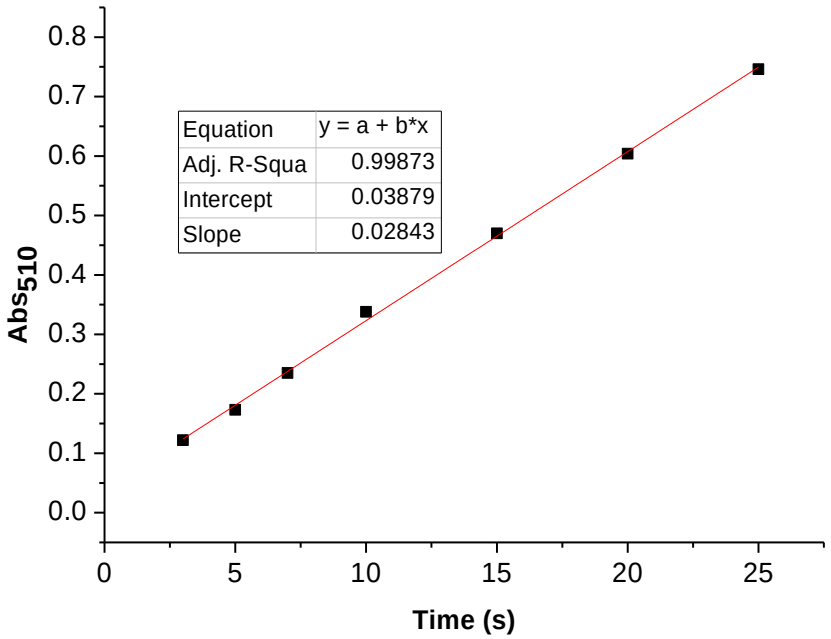

Figure S67. Absorbance of the tris-phenanthroline iron (II) complex as a function of irradiation time of potassium ferrioxalate. The photon flux of used 365 nm LED strip light was determined to be $1.692 \cdot 10^{-7}$ $mol \cdot s^{-1}$.

Determination of quantum yields. In a typical quantum yield experiment, 2.7 mL of azoarene solution in DMSO (20 µM) were irradiated with 365 nm LED strip light for different time periods. After every period the absorbance between 260 nm and 650 nm was recorded, respectively.

The quantum yields were calculated according to the literature method.[S4]

The rate of a unidirectional photochemical reaction initiated with monochromatic light is given by:

$$r_{A\to B} = \frac{q_{in}\phi_{A\to B}}{V}(1 - 10^{-\varepsilon_A[A]l}) \qquad (2)$$

When the absorbance is much less than 0.43, Taylor expansion of the exponential and truncation at the linear term gives an approximate first-order rate equation (3) from which an expression relating the quantum yield to an observed first-order rate constant, photon flux and measurable properties of the sample can be derived (4):

$$r_{A\to B} = \frac{q_{in}\phi_{A\to B}\varepsilon_A l}{V}[A] \qquad (3)$$

$$\phi_{A\to B} = \frac{kV}{q_{in}\varepsilon_A l \ln 10} \qquad (4)$$

where ϕ is quantum yield; k is rate constant (obtained from the exponential fit of a graph of A vs. time); V is sample volume; ε_A is molar extinction coefficient (obtained from the linear fit of a graph of A vs. concentration); l is pathlength; and q_{in} is molar photon flux.

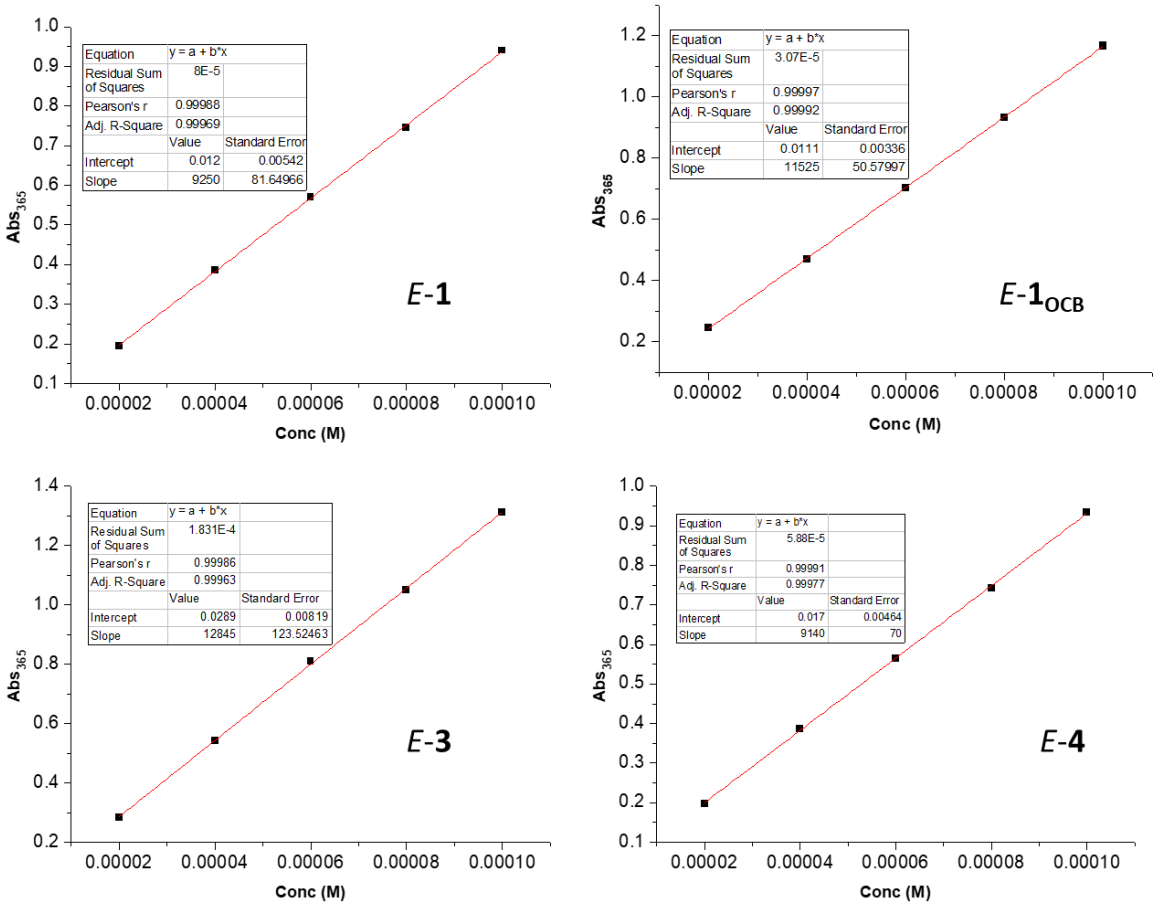

Figure S68. Determination of molar extinction coefficient at 365 nm.

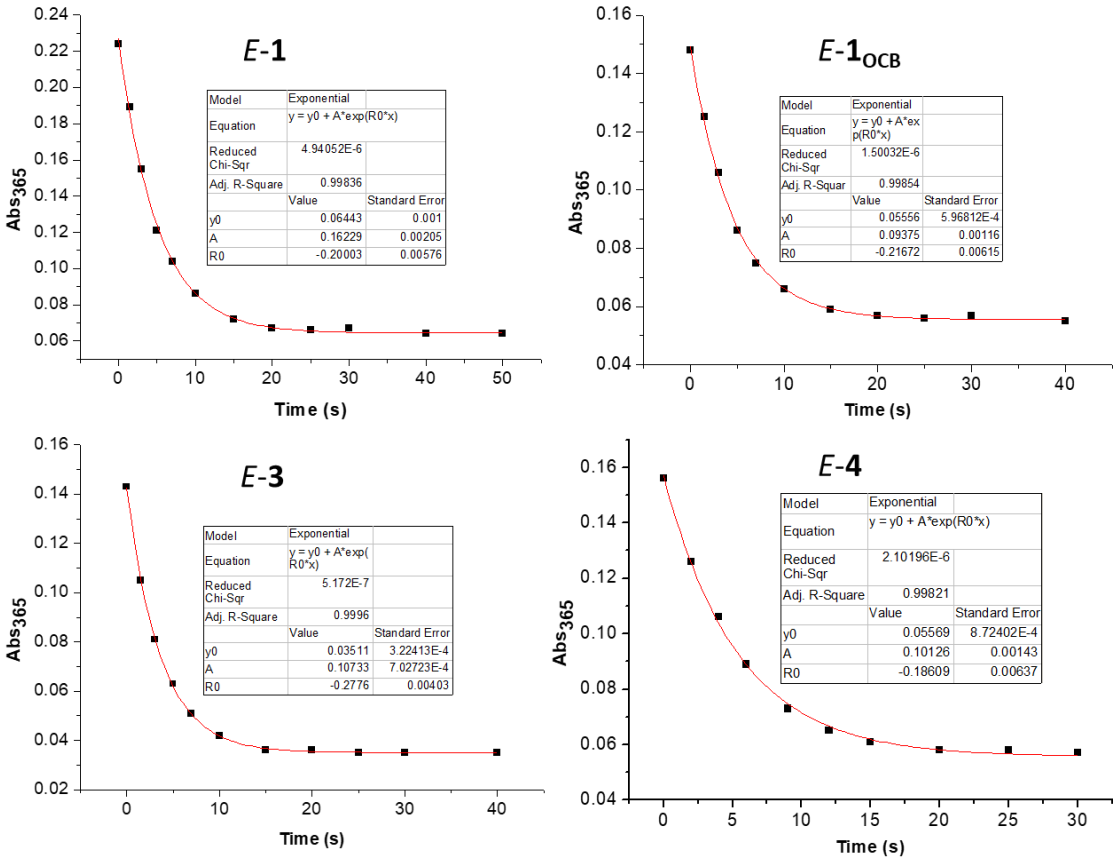

Figure S69. UV-vis spectroscopic studies for the kinetic curves of forward *E*-*Z* photoisomerization at 365 nm irradiation.

Table S2. Estimation of the quantum yield of forward *E*-*Z* photoisomerization of azoquinolines under 365 nm LED strip light irradiation.

Compound	Extinction coefficient ε ($M^{-1}\cdot cm^{-1}$)	Rate constant k (s^{-1})	Quantum yield ϕ
E-**1**	9250	0.200	0.15
E-**1**$_{OCB}$	11525	0.217	0.13
E-**3**	12845	0.278	0.15
E-**4**	9140	0.186	0.14

8. References

S1. H. Y. Zhang, S. L. Zhang, L. Liu, G. S. Luo, W. H. Duan and W. Wang, Synthesis of Chiral 3-Substituted Phthalides by a Sequential Organocatalytic Enantioselective Aldol-Lactonization Reaction. Three-Step Synthesis of (S)-(-)-3-Butylphthalide, *J. Org. Chem.*, 2010, **75**, 368-374.

S2. V. Chandrasekaran, E. Johannes, H. Kobarg, F. D. Sönnichsen and T. K. Lindhorst, Synthesis and Photochromic Properties of Configurationally Varied Azobenzene Glycosides, *Chemistryopen*, 2014, **3**, 99-108.

S3. K. Stranius and K. Börjesson, Determining the Photoisomerization Quantum Yield of Photoswitchable Molecules in Solution and in the Solid State, *Sci. Rep.*, 2017, **7**, 41145.

S4. C. E. Weston, R. D. Richardson, P. R. Haycock, A. J. P. White and M. J. Fuchter, Arylazopyrazoles: Azoheteroarene Photoswitches Offering Quantitative Isomerization and Long Thermal Half-Lives, *J. Am. Chem. Soc.*, 2014, **136**, 11878-11881.